

# D1.1. Requirements Baseline (RB) Document

Version-1.1, January 8, 2025

Deliverable 1.1 of ESA contract n° 4000144916/24/I-EF EO4BK

Authors:

Philippe Ciais, Antoine Lefebvre, Lan Anh Dinh, Ronny Lauerwald, Daniel Goll, Ana Bastos, Dominic Schierbaum, Stephen Sitch, Scott Barningham, Thais Rosan, Yang Su, Arthur Fendrich, Thomas Gasser.

For the attention of:	Plummer (Stephen.Plummer@esa.int)
For information to:	Frigot (Emma.Frigot@esa.int)

## Table of Contents

<b>Table of Contents .....</b>	<b>1</b>
<b>1. Goals of this document .....</b>	<b>2</b>
<b>2. Review of EO-based methods for mapping crop types and management practices, and EO data use in carbon models.....</b>	<b>2</b>
2.1. Review of methods used for crop types classification based on EO data.....	2
2.2. Review of methods to characterise crop phenology based on EO data.....	5
2.3. Review of methods to map agricultural management practices based on EO data.....	8
<b>3. Proposed methodologies to deliver EO-based maps of crop types, phenology, and agricultural cultivation practices for WP3 .....</b>	<b>11</b>
3.1 Proposed method to classify crop types at 10 m resolution from Sentinel data, Europe and Brazil.....	11
3.2. Proposed nomenclature for crop types .....	12
3.3 Reference data on crop types and management practices for training models. ....	15
3.4 Proposed method to derive phenology from Sentinel 1 and Sentinel 2 remote-sensing indices.....	16
3.5 Proposed methods to classify cropland management practices. ....	17
<b>4. Definition of performances metrics for crop types and cultivation practices maps &amp; existing reference maps as input to WP3 .....</b>	<b>35</b>
4.1. Performance metrics upon which the proposed methods and EO datasets produced in the project will be benchmarked.   35	
4.2 Reference crop types maps / datasets upon which the results of the methods proposed in section 3 can be benchmarked.   35	
4.3 Reference maps / datasets upon which the results of the methods proposed in section 3 can be benchmarked for management practices. ....	41
<b>5. Definition of modelling protocols that will be used in WP5 to estimate the impact of EO information on the BK approach.....</b>	<b>42</b>
5.1. Protocol for simulations with the land surface model ORCHIDEE to provide additional data to the BK model, as a backstop or extend the model's parameterizations. ....	42
5.2. Synthesis of knowledge on the effects of cropland management on soil carbon stocks changes .....	45
5.3. Transient carbon densities and turnover times calibration for the bookkeeping model.....	46
5.4. Protocol for BK simulations, including comparison to parameterizations of established BK models (OSCAR), to other land use and land cover datasets (LUH2 and HILDA+), and to idealised cases in which the C3/C4 and/or crop management distinctions are absent.....	47
5.5. Protocol for benchmarking LULCC fluxes from BK model against response functions of SOC and biomass C stocks for land use change transitions .....	48
5.6. Benchmarking against existing estimates of cropland C budgets including land use change .....	51
<b>7. First elements on threshold and target scientific and technical requirements to include EO data in carbon budgets that will inform the roadmap in WP6.....</b>	<b>55</b>

## 1. Goals of this document

As an outcome of the dialogue with national GHG agencies in that project, it became clear that there is high interest in the use of EO for improved estimates of LULCC fluxes by both communities. The potential is especially high for countries where the monitoring infrastructure is not fully established and with limited capacity to support time-consuming and cost-intensive inventories. EO4BK addresses key recommendations from that earlier dialogue:

- Provide high-resolution remote-sensing data (10-30 m) of LULCC and biomass for quantifying land use change fluxes in a spatiotemporally explicit and globally consistent manner and in a cost-effective way.
- Use EO-based datasets to constrain processes and parameters in Dynamic Global Vegetation Models (DGVMs) and Bookkeeping (BK) models, thus contributing to reducing uncertainties on land use change fluxes

The main objective of the EO4BK project is to improve understanding and quantification of changes in land use-related carbon pools and fluxes, by incorporating EO information in BK models. This project will pave the way for a new generation of BK models that are fully driven by EO data, allowing them to run at much higher resolution than is the case nowadays (currently: 25 km to country level).

This document reports the results of the literature and previous projects analysis carried out in WP1 to elaborate the baseline science requirements for high resolution land use and land use change data that will be generated in the EO4BK project. It includes:

- Review of EO-based methods for mapping crop types and management practices, and use of this type of EO data in carbon models (section 2)
- Definition of the methodologies proposed to deliver new EO-based maps of crop types and agricultural cultivation practices in Europe and Brazil for WP3 (section 3)
- Definition of benchmarking of the products expected from EO4BK against existing maps of crop types and cultivation practices, as input to WP3 (section 4)
- Definition of modelling protocols to estimate the impact of EO information produced in the project on the bookkeeping land management and land use change carbon modelling (BK) approach, as input to WP5 (section 5)
- Definition of benchmarking of the BK models developed in EO4BK against existing estimates of cropland carbon budgets including land use change, as input to WP5 (section 6)
- First elements on threshold and target scientific and technical requirements to include EO data in carbon budgets, that will inform the roadmap in WP6 (section 7)

## 2. Review of EO-based methods for mapping crop types and management practices, and EO data use in carbon models

### 2.1. Review of methods used for crop types classification based on EO data

Classifying crop types using moderate and high-resolution satellite data has been addressed using a variety of methods, each with its own strengths and challenges. High resolution is here defined as higher than 20 m, thus covering Sentinel 1 and 2 data (d'Andrimont et al., 2021a, 2021b). The crop classification methods generally fall into three categories: traditional machine learning techniques, deep learning approaches, and time series analysis. Classifying crop types using satellite data involves the choice of methods suited to different scales and types of data. Traditional machine learning methods like Random Forest and Support Vector Machines (SVMs) are robust and widely used, while deep learning methods such as Convolution Neural Networks (CNNs) and Long Short-Term Memories (LSTMs) offer state-of-the-art performance, especially with high-resolution imagery and time series data. The choice of a method depends on the specific requirements and science goals of the

study, such as the spatial and temporal resolution of the data, the complexity of the landscape, and computational resources, as summarised below.

Moderate Resolution Imaging Spectroradiometer (MODIS) data were used for large-scale crop classification by Zhu and Woodcock (2012). The main limitation of MODIS data is the coarse resolution that does not allow to separate crop types in complex agricultural landscapes with small field sizes such as in Europe. Using Sentinel-2 data provided by high-resolution imagery useful for detailed crop classification has been proposed by Gumma et al. (2020). Landsat data have been used in the US and Brazil due to their long-time coverage and moderate resolution, still sufficient in countries with large field sizes. Landsat is rather widely used for both moderate and high-resolution crop mapping (Wardlow & Egbert, 2008).

- **Key references:**

- d’Andrimont, R., Verhegghen, A., Lemoine, G., Kemperneers, K., Meroni, M., & Van Der Velde, M. (2021a). From parcel to continental scale – A first European crop type map based on Sentinel-1 and LUCAS Copernicus in-situ observations. *Remote Sensing of Environment*, 266, 112708. <https://doi.org/10.1016/j.rse.2021.112708>.
- d’Andrimont, R., Verhegghen, A., Meroni, M., Lemoine, G., Strobl, P., Eiselt, B., Yordanov, M., Martinez Sanchez, L., & Van Der Velde, M. (2021b). LUCAS Copernicus 2018: Earth-observation-relevant in situ data on land cover and use throughout the European Union. *Earth System Science Data*, 13(3), 1119–1133. <https://doi.org/10.5194/essd-13-1119-2021>.
- Zhu, Z., & Woodcock, C. E. (2012). Object-based cloud and cloud shadow detection in Landsat imagery. *Remote Sensing of Environment*, 118, 83–94. <https://doi.org/10.1016/j.rse.2011.10.028>.
- Gumma, M. K., Tummala, K., Dixit, S., Collivignarelli, F., Holecz, F., Kolli, R. N., & Whitbread, A. M. (2020). Crop type identification and spatial mapping using Sentinel-2 satellite data with focus on field-level information. *Geocarto International*, 37(7), 1833–1849. <https://doi.org/10.1080/10106049.2020.1805029>.
- Wardlow, B. D., & Egbert, S. L. (2008). Large-area crop mapping using time-series MODIS 250 m NDVI data: An assessment for the U.S. Central Great Plains. *Remote Sensing of Environment*, 112(3), 1096–1116. <https://doi.org/10.1016/j.rse.2007.07.019>.

### 2.1.1 Time Series Analysis

**Time Series Analysis** uses temporal patterns in satellite data to classify crop types, often leveraging phenological stages, with different thresholds that can be determined manually or automatically based on label data. These methods are effective for datasets with distinct seasonal growth patterns (Petitjean et al., 2011; Zhu & Woodcock, 2014). Time-Weighted Dynamic Time Warping (TWDTW) was also used for detecting double cropping crop types in Brazil (section 3.5).

- **Key References:**

- Petitjean, F., Ketterlin, A., & Gançarski, P. (2011). A global averaging method for dynamic time warping, with applications to clustering. *Pattern Recognition*, 44(3), 678–693. <https://doi.org/10.1016/j.patcog.2010.09.013>.
- Zhu, Z., & Woodcock, C. E. (2014). Continuous change detection and classification of land cover using all available Landsat data. *Remote Sensing of Environment*, 144, 152–171. <https://doi.org/10.1016/j.rse.2014.01.011>.
- Bolton, D. K., Gray, J. M., Melaas, E. K., Moon, M., Eklundh, L., & Friedl, M. A. (2020). Continental-scale land surface phenology from harmonized Landsat 8 and Sentinel-2 imagery. *Remote Sensing of Environment*, 240, 111685. <https://doi.org/10.1016/j.rse.2020.111685>.

- Belgiu, M., Bijker, W., Csillik, O., & Stein, A. (2021). Phenology-based sample generation for supervised crop type classification. *International Journal of Applied Earth Observation and Geoinformation*, 95, 102264. <https://doi.org/10.1016/j.jag.2020.102264>.
- Johnson, M. C., Reich, B. J., & Gray, J. M. (2021). Multisensor fusion of remotely sensed vegetation indices using space-time dynamic linear models. *Journal of the Royal Statistical Society: Series C (Applied Statistics)*, 70(3), 793–812. <https://doi.org/10.1111/rssc.12495>.
- Gao, X., McGregor, I. R., Gray, J. M., Friedl, M. A., & Moon, M. (2023). Observations of satellite land surface phenology indicate that maximum leaf greenness is more associated with global vegetation productivity than growing season length. *Global Biogeochemical Cycles*, 37, e2022GB007462. <https://doi.org/10.1029/2022GB007462>.

### 2.1.2 Traditional Machine Learning models

**Random Forest (RF).** RF is an ensemble learning method that builds multiple decision trees and merges their results to improve accuracy and control overfitting. RF models have proven effective for classification tasks due to its ability to handle large datasets and its robustness to noise. They also offer some interpretability such as the identification of the most influential features.

**Support Vector Machines (SVM)** is a supervised learning algorithm that finds an optimal hyperplane to separate different classes. SVM methods are suitable for high-dimensional data and perform well with a clear margin of separation (Cortes & Vapnik, 1995; Mountrakis, Im, & Ogole, 2011).

**k-Nearest Neighbors (k-NN)** methods classify data based on the closest training examples in the feature space. They are simple and effective for small datasets but computationally intensive for large datasets such as EO-data (Cover & Hart, 1967).

#### ● Key References:

- Cortes, C., & Vapnik, V. (1995). Support-vector networks. *Machine Learning*, 20(3), 273–297. <https://doi.org/10.1007/BF00994018>.
- Mountrakis, G., Im, J., & Ogole, C. (2011). Support vector machines in remote sensing: A review. *ISPRS Journal of Photogrammetry and Remote Sensing*, 66(3), 247–259. <https://doi.org/10.1016/j.isprsjprs.2010.11.001>.
- Cover, T., & Hart, P. (1967). Nearest neighbor pattern classification. *IEEE Transactions on Information Theory*, 13(1), 21–27. <https://doi.org/10.1109/TIT.1967.1053964>.

### 2.1.3. Deep Learning models

**Convolutional Neural Networks (CNNs)** are deep learning models designed to process data with grid-like topology, such as images, being rather widely used as they are highly effective for high-resolution satellite images due to their ability to capture spatial hierarchies (LeCun et al., 2015; Ji et al., 2013; Pelletier et al., 2019).

**Recurrent Neural Networks (RNNs)** and Long Short-Term Memory (LSTM) RNNs are designed to handle sequential data, making them suitable for time series analysis in crop classification using e.g. frequent revisits offered by sensors such as Sentinel or MODIS. By construction, these methods are effective for temporal data analysis and capturing temporal dependencies (Hochreiter & Schmidhuber, 1997; Kratzert et al., 2018).

**U-Net convolutional neural networks** excel in agricultural applications by accurately segmenting different crops within agricultural fields and monitoring crop rotation. Its architecture combines a deep context-capturing pathway with precise localization abilities, crucial for distinguishing crop types in densely planted areas. U-Net is particularly effective with limited training datasets, employing data augmentation to leverage satellite imagery for consistent analysis of crop rotation patterns, supporting precise agriculture management.

**Vision Transformers (ViT)** adapt the transformer architecture for image analysis, treating image patches as sequences. This approach is effective for detecting crop types and monitoring crop rotation, as it integrates

detailed local observations with broader field context. ViTs excel when scaled with large datasets, typical in satellite monitoring, providing enhanced accuracy in complex agricultural landscapes. Their robust performance in large-scale data environments helps track crop dynamics and field conditions over time, aiding sustainable farming practices.

#### ● Key References:

- LeCun, Y., Bengio, Y., & Hinton, G. (2015). Deep learning. *Nature*, 521(7553), 436–444.  
<https://doi.org/10.1038/nature14539>.
- Ji, S., Xu, W., Yang, M., & Yu, K. (2013). 3D Convolutional Neural Networks for Human Action Recognition. *IEEE Transactions on Pattern Analysis and Machine Intelligence*, 35(1), 221–231.  
<https://doi.org/10.1109/TPAMI.2012.59>.
- Pelletier, C., Webb, G. I., & Petitjean, F. (2019). Temporal convolutional neural network for the classification of satellite image time series. *Remote Sensing*, 11(5), 523.  
<https://doi.org/10.3390/rs11050523>.
- Hochreiter, S., & Schmidhuber, J. (1997). Long short-term memory. *Neural Computation*, 9(8), 1735–1780. <https://doi.org/10.1162/neco.1997.9.8.1735>.
- Kratzert, F., Klotz, D., Brenner, C., Schulz, K., & Herrnegger, M. (2018). Rainfall–runoff modelling using long short-term memory (LSTM) networks. *Hydrology and Earth System Sciences*, 22(6005–6022).  
<https://doi.org/10.5194/hess-22-6005-2018>.


## 2.2. Review of methods to characterise crop phenology based on EO data.

### 2.2.1 Crop phenology definitions

Different crop types have characteristic seasonal fingerprints that allow us to distinguish between them. Furthermore, different management practices, e.g. double cropping, also show distinct phenological characteristics. Phenology of vegetation can be characterised by different indicators, for example direct measurements of net and gross carbon fluxes at eddy-covariance towers, , using cameras such as the phenocam network unfortunately limited to few sites (<https://phenocam.nau.edu/webcam/>), or by remote-sensing data. In the case of remote-sensing, Leaf area Index and vegetation indices (VIs) based on optical data have been widely used (de Pue et al., 2023), but with the availability of high-resolution SAR data by Sentinel-1 (Khabbazan et al., 2019; Schlund et al., 2020; Xie et al., 2022; Qadir et al., 2023), radar backscatter information has also been used to study crop phenology. This signal is especially appealing to study crop phenology in the tropics, where cloud cover poses a problem for the use of VIs. Most studies have focused on a limited number of commonly used optical vegetation indices, comparing the timing of the relevant phenological metrics obtained by remote-sensing with the timing of the eddy-covariance measurements. Some studies have, however, compared the results using light-use efficiency models to derive gross primary productivity based on remote-sensing, and then compared these with observations.

The definition of crop phenology metrics differs considerably across studies and is strongly dependent on the method applied. Typically, some smoothing filter is applied to extract the seasonal to annual components of vegetation dynamics and reduce the effect of noise. The choice of smoothing filter has a considerable influence on the phenological metrics and their long-term variability. Furthermore, metrics such as the onset or end of growing season often rely on threshold definitions. It has been shown that long-term trends and interannual variability of these phenological metrics are very sensitive to the thresholds applied (Panwar et al. 2023). The threshold methods are further unlikely to be suitable for the characterization of double-cycles, so that other methods, e.g. based on the analysis of the first and second derivatives of the time-series might be more suitable. In addition, the merging of optical data from Sentinel 2 and Landsat provides improved observation for tracking phenological changes of vegetation (Wulder et al., 2021; Chen and Zhang, 2023).



Deliverable no. D1.1 Requirements Baseline (RB) document	ESA Carbon-RO, EO4BK Contract no. 4000144916/24/I-EF	 International Institute for Applied Systems Analysis IIASA www.iiasa.ac.at
--	---	--

Phenology defines characteristic timings relevant to study crop development such as

- Planting date
- Start of growing season (SOS)
- Timing of the peak of growing season (PGS)
- End of growing season (EOS) - precedes or coincides with harvest date
- Number of phenological cycles/peaks within a calendar year (nGS) in the case of double cropping

Phenological stages have been well defined by crop science and the question is how EO data can be used to detect the principal events during the growing cycle of each specific crop type. Ground based data are not abundant although there are networks of citizen science in Europe such as the Pan European Phenological database (PEP725: Templ et al., 2018), PlantNet <https://plantnet.org/>, the phenological observations from Climate Data Center (CDC, available at: [https://opendata.dwd.de/climate\\_environment/CDC/observations\\_germany/phenology/](https://opendata.dwd.de/climate_environment/CDC/observations_germany/phenology/)) of the Deutscher Wetterdienst or Flora Incognita (Mora et al., 2024). Phenological metrics based on remote-sensing generally show better agreement with ground data for croplands and grasslands than for other vegetation types. The start of the growing season tends to be better captured than the end of the growing season (Wu et al., 2017; Balzarolo et al., 2016). No evaluation of SAR-based crop phenology with ground data has been done to the best of our knowledge.

#### ● Key references:

- Khabbazan, S., Vermunt, P., Steele-Dunne, S., Ratering Arntz, L., Marinetti, C., van der Valk, D., Iannini, L., Molijn, R., Westerdijk, K., & van der Sande, C. (2019). Crop Monitoring Using Sentinel-1 Data: A Case Study from The Netherlands. *Remote Sensing*, 11(16), 1887. <https://doi.org/10.3390/rs11161887>.
- Schlund, M., & Erasmi, S. (2020). Sentinel-1 time series data for monitoring the phenology of winter wheat. *Remote Sensing of Environment*, 246, 111814. <https://doi.org/10.1016/j.rse.2020.111814>.
- Xie, G., & Niculescu, S. (2022). Mapping Crop Types Using Sentinel-2 Data Machine Learning and Monitoring Crop Phenology with Sentinel-1 Backscatter Time Series in Pays de Brest, Brittany, France. *Remote Sensing*, 14(18), 4437. <https://doi.org/10.3390/rs14184437>.
- Qadir, A., Skakun, S., Eun, J., Prashnani, M., & Shumilo, L. (2023). Sentinel-1 time series data for sunflower (*Helianthus annuus*) phenology monitoring. *Remote Sensing of Environment*, 295, 113689. <https://doi.org/10.1016/j.rse.2023.113689>.
- Bolton, D. K., Gray, J. M., Melaas, E. K., Moon, M., Eklundh, L., & Friedl, M. A. (2020). Continental-scale land surface phenology from harmonized Landsat 8 and Sentinel-2 imagery. *Remote Sensing of Environment*, 240, 111685. <https://doi.org/10.1016/j.rse.2020.111685>.
- Panwar, A., Migliavacca, M., Nelson, J.A. *et al.* Methodological challenges and new perspectives of shifting vegetation phenology in eddy covariance data. *Sci Rep* **13**, 13885 (2023). <https://doi.org/10.1038/s41598-023-41048-x>.
- Mora, K., Rzanny, M., Wäldchen, J., Feilhauer, H., Kattenborn, T., Kraemer, G., Mäder, P., Svidzinska, D., Wolf, S., & Mahecha, M. D. (2024). Macrophenological dynamics from citizen science plant occurrence data. *Methods in Ecology and Evolution*, 15, 1422–1437. <https://doi.org/10.1111/2041-210X.14365>
- Wu, C., Peng, D., Soudani, K., Siebicke, L., Gough, C. M., Arain, M. A., Bohrer, G., Lafleur, P. M., Peichl, M., Gonsamo, A., Xu, S., Fang, B., & Ge, Q. (2017). Land surface phenology derived from normalized difference vegetation index (NDVI) at global FLUXNET sites. *Agricultural and Forest Meteorology*, 233, 171–182. <https://doi.org/10.1016/j.agrformet.2016.11.193>
- Balzarolo, M., Vicca, S., Nguy-Robertson, A. L., Bonal, D., Elbers, J. A., Fu, Y. H., Grünwald, T., Horemans, J. A., Papale, D., Peñuelas, J., Suyker, A., & Veroustraete, F. (2016). Matching the phenology

of Net Ecosystem Exchange and vegetation indices estimated with MODIS and FLUXNET in-situ observations. *Remote Sensing of Environment*, 174, 290–300.

<https://doi.org/10.1016/j.rse.2015.12.017>.

- De Pue, J., Wieneke, S., Bastos, A., Barrios, J. M., Liu, L., Ciais, P., Arboleda, A., Hamdi, R., Maleki, M., Maignan, F., Gellens-Meulenberghs, F., Janssens, I., & Balzarolo, M. (2023). Temporal variability of observed and simulated gross primary productivity, modulated by vegetation state and hydrometeorological drivers. *Biogeosciences*, 20(23), 4795–4818. <https://doi.org/10.5194/bg-20-4795-2023>.
- Templ, B., Koch, E., Bolmgren, K., Ungersböck, M., Paul, A., Scheifinger, H., Rutishauser, T., Busto, M., Chmielewski, F. M., Hájková, L., Hodzić, S., Kaspar, F., Pietragalla, B., Romero-Fresneda, R., Tolvanen, A., Vučetič, V., Zimmermann, K., & Zust, A. (2018). Pan European Phenological database (PEP725): A single point of access for European data. *International Journal of Biometeorology*, 62(6), 1109–1113. <https://doi.org/10.1007/s00484-018-1512-8>.
- Wulder M. A., Hermosilla, T., White, J. C., Hobart, G., & Masek, J. G. (2021). Augmenting Landsat time series with Harmonized Landsat Sentinel-2 data products: Assessment of spectral correspondence. *Science of Remote Sensing*, 4, 100031. <https://doi.org/10.1016/j.srs.2021.100031>.
- Chen, J., & Zhang, Z (2023). An improved fusion of Landsat-7/8, Sentinel-2, and Sentinel-1 data for monitoring alfalfa: Implications for crop remote sensing. *International Journal of Applied Earth Observation and Geoinformation*, 124, 103533. <https://doi.org/10.1016/j.jag.2023.103533>.

## 2.2.2 Time series analysis and smoothing filters to detect crop phenology events using EO data

- **Description:** Smoothing filters are used to extract sub-annual cycles in time-series (e.g. Savitzky-Golay, Fourier Analysis, Whittaker Smoother, Singular Spectrum Analysis) and subsequent approaches to derive EOS, SOS metrics (10, 20, 30 % of peak thresholds, second derivative analysis, etc.).
- **Performance:** Remote-sensing optical data generally shows a fair agreement with ground data for croplands and grasslands. The start of the growing season tends to be better captured than the end of the growing season and the crop maturity stages. No evaluation of SAR-based crop phenology with ground data has been done to the best of our knowledge. The spatial scale of crop fields is critical for the requirements as moderate resolution imagery (MODIS) can give good results in the US Corn Belt (Zhu et al., 2018) where the field size is large but cannot be used in Europe where fields tend to be smaller and crop rotations more diverse. In addition, cloud coverage prevents the analysis of phenology in Europe during parts of the year in some cloudy years, which calls for higher resolution and high frequency data, such as Sentinel 2 and Sentinel 1. Note that phenology is also the basis for crop types classification methods (see section 3) so that if we have a good classification method, it makes it easier to extract the timing of key phenological events
- **Key references:**
  - Zhu, P., Jin, Z., Zhuang, Q., Ciais, P., Bernacchi, C., Wang, X., Makowski, D., & Lobell, D. (2018). The important but weakening maize yield benefit of grain filling prolongation in the US Midwest. *Global Change Biology*, 24(10), 4718–4730. <https://doi.org/10.1111/gcb.14356>.
  - Panwar, A., Migliavacca, M., Nelson, J. A., Cortés, J., Bastos, A., Forkel, M., & Winkler, A. J. (2023). Methodological challenges and new perspectives of shifting vegetation phenology in eddy covariance data. *Scientific Reports*, 13(1), 13885. <https://doi.org/10.1038/s41598-023-41048-x>
  - Schierbaum, D. (2024). Long-term Trends in Photosynthetic Phenology and their Detection with Remote Sensing: A Case Study of an old German Beech Forest (2000 - 2021). MSc Thesis, Leipzig University, Leipzig, Germany.



### 2.3. Review of methods to map agricultural management practices based on EO data.

Classifying crop cultivation practices using satellite data involves advanced remote sensing techniques and sophisticated algorithms to identify specific agricultural practices such as no-till, harvest date, planting date, irrigation, cover crops, and double cropping. We reviewed the literature about which type of management practices can be detected and quantified using EO data at large scale, including

- No-till / Tillage
- Cover crops
- Harvesting dates
- Irrigation
- Double cropping

Methods to detect these practices are summarised in the following sub-sections

#### 2.3.1 No-till / tillage Practices

##### Spectral Analysis and Vegetation Indices

- **Description:** Uses spectral bands and vegetation indices (e.g. NDVI, EVI) to detect soil disturbance and residue cover.
- **Performance:** Effective in distinguishing no-till from conventional tillage practices, especially in visible and near-infrared bands.
- **Key References:**
  - Daughtry, C. S. T., Hunt, E. R., Jr., Doraiswamy, P. C., & McMurtrey, J. E. (2005). Remote sensing the spatial distribution of crop residues. *Agronomy Journal*, 97(3), 864–871. <https://doi.org/10.2134/agronj2003.0291>.
  - Serbin, G., & Daughtry, C. S. T. (2012). Spatial and temporal evaluation of no-till cropping systems using remote sensing. *Agricultural Systems*, 112, 14-23.
  - Jain, K., John, R., Torbick, N., et al. (2024). Monitoring the spatial distribution of cover crops and tillage practices using machine learning and environmental drivers across eastern South Dakota. *Environmental Management*, 74, 742–756. <https://doi.org/10.1007/s00267-024-02021-0>.

##### Disaggregation of official cover crop statistics


- **Description:** Statistical model to downscale regional-level statistics on tillage adoption to a 100 m spatial resolution using Sentinel-1 time-series.
- **Performance:** Unknown.
- **Key References:**
  - Fendrich, A. N., Matthews, F., Van Eynde, E., Carozzi, M., Li, Z., d'Andrimont, R., Lugato, E., Martin, P., Ciais, P., & Panagos, P. (2023). From regional to parcel scale: A high-resolution map of cover crops across Europe combining satellite data with statistical surveys. *Science of the Total Environment*, 873, 162300. <https://doi.org/10.1016/j.scitotenv.2023.162300>.

#### 2.3.2 Harvest Dates

Harvest dates can be extracted by the analysis of phenological stages, as described in 2.2.

##### Time Series Analysis

- **Description:** Analyses time series of vegetation indices (e.g. NDVI, EVI) to determine key phenological stages and harvest dates

Deliverable no. D1.1 Requirements Baseline (RB) document	ESA Carbon-RO, EO4BK Contract no. 4000144916/24/I-EF	 <b>International Institute for Applied Systems Analysis</b> IIASA www.iiasa.ac.at
--	---	--

- **Performance:** High accuracy in identifying harvest dates by monitoring crop growth cycles. We expect EOS to be a good proxy for harvest dates, although small biases are likely, as shown by Amin et al. (2022)
- **Key References:**
  - Zhang, X., Friedl, M. A., Schaaf, C. B., Strahler, A. H., & Liu, Z. (2005). Monitoring the response of vegetation phenology to precipitation in Africa by coupling MODIS and TRMM instruments. *Journal of Geophysical Research: Atmospheres*, 110(D12). <https://doi.org/10.1029/2004JD005263>. .
  - Sakamoto, T., Yokozawa, M., Toritani, H., Shibayama, M., Ishitsuka, N., & Ohno, H. (2005). A crop phenology detection method using time-series MODIS data. *Remote Sensing of Environment*, 96(3–4), 366–374. <https://doi.org/10.1016/j.rse.2005.03.008>.
  - Amin E, Belda S, Pipia L, Szantoi Z, El Baroudy A, Moreno J, Verrelst J. Multi-Season Phenology Mapping of Nile Delta Croplands Using Time Series of Sentinel-2 and Landsat 8 Green LAI. *Remote Sensing*. 2022; 14(8):1812. <https://doi.org/10.3390/rs14081812>
  - Diao C, Li G. Near-Surface and High-Resolution Satellite Time Series for Detecting Crop Phenology. *Remote Sensing*. 2022; 14(9):1957. <https://doi.org/10.3390/rs14091957>.

### 2.3.4. Irrigation

#### Thermal Infrared Imagery


- **Description:** Uses thermal infrared data to detect variations in soil moisture and identify irrigated areas.
- **Performance:** Effective in mapping irrigation by detecting changes in surface temperature and soil moisture.
- **Key References:**
  - Allan, R., Pereira, L., & Smith, M. (1998). Crop evapotranspiration: Guidelines for computing crop water requirements (FAO Irrigation and Drainage Paper No. 56). FAO. <https://www.fao.org/4/x0490e/x0490e00.htm>.
  - Ozdogan, M., & Gutman, G. (2008). A new methodology to map irrigated areas using multi-temporal MODIS and ancillary data: An application example in the continental US. *Remote Sensing of Environment*, 112(9), 3520–3537. <https://doi.org/10.1016/j.rse.2008.04.010>.

#### Detection with remote sensing and machine learning tools

- **Description:** Uses satellite images from Copernicus program combining with machine learning tools to detect the irrigated areas.
- **Performance:** High spatial and temporal resolution of irrigation mapping with machine learning and remote sensing tools.
- **Key References:**
  - Elwan, E.; Le Page, M.; Jarlan, L.; Baghdadi, N.; Brocca, L.; Modanesi, S.; Dari, J.; Quintana Seguí, P.; Zribi, M. Irrigation Mapping on Two Contrasted Climatic Contexts Using Sentinel-1 and Sentinel-2 Data. *Water* 2022, 14, 804. <https://doi.org/10.3390/w14050804>.
  - Pageot, Y., Baup, F., Inglada, J., Baghdadi, N., & Demarez, V. (2020). Detection of irrigated and rainfed crops in temperate areas using Sentinel-1 and Sentinel-2 time series. *Remote Sensing*, 12(18), Article 3044. <https://doi.org/10.3390/rs12183044>.

#### Detection with remote sensing and deep learning tools

- **Description:** Uses satellite images such as Sentinel 2 or Landsat 8 combining with deep learning tools to detect the irrigated areas.
- **Performance:** High spatial and temporal resolution of irrigation mapping with deep learning and remote sensing tools.

Deliverable no. D1.1 Requirements Baseline (RB) document	ESA Carbon-RO, EO4BK Contract no. 4000144916/24/I-EF	 <b>International Institute for Applied Systems Analysis</b> IIASA www.iiasa.ac.at
--	---	--

#### ● Key References:

- Piedelobo L, Ortega-Terol D, Del Pozo S, Hernández-López D, Ballesteros R, Moreno MA, Molina J-L, González-Aguilera D. HidroMap: A New Tool for Irrigation Monitoring and Management Using Free Satellite Imagery. *ISPRS International Journal of Geo-Information*. 2018; 7(6):220. <https://doi.org/10.3390/ijgi7060220>.
- Agastya, C., Ghebremusse, S., Anderson, I., Vahabi, H., & Todeschini, A. (2021). Self-supervised contrastive learning for irrigation detection in satellite imagery. arXiv. <https://doi.org/10.48550/arXiv.2108.05484>.
- Liu, X., He, W., Liu, W., Yin, G., & Zhang, H. (2023). Mapping annual center-pivot irrigated cropland in Brazil during the 1985–2021 period with cloud platforms and deep learning. *ISPRS Journal of Photogrammetry and Remote Sensing*, 205, 227–245. <https://doi.org/10.1016/j.isprsjprs.2023.10.007>.
- de Bem, P. P., de Carvalho Júnior, O. A., de Carvalho, O. L. F., Gomes, R. A. T., Guimarães, R. F., & Pimentel, C. M. M. (2021). Irrigated rice crop identification in Southern Brazil using convolutional neural networks and Sentinel-1 time series. *Remote Sensing Applications: Society and Environment*, 24, 100627. <https://doi.org/10.1016/j.rsase.2021.100627>.

### 2.3.5 Cover Crops

#### Object-Based Image Analysis (OBIA)


- **Description:** Segments images into meaningful objects and analyses their spectral, spatial, and temporal characteristics.
- **Performance:** High accuracy in detecting cover crops by differentiating them from other land cover types.
- **Key References:**
  - Peña-Barragán, J. M., Ngugi, M. K., Plant, R. E., & Six, J. (2011). Object-based crop identification using multiple vegetation indices, textural features and crop phenology. *Remote Sensing of Environment*, 115(6), 1301–1316. <https://doi.org/10.1016/j.rse.2011.01.009>.
  - Eisfelder, C., Boemke, B., Gessner, U., Sogno, P., Alemu, G., Hailu, R., Mesmer, C., & Huth, J. (2024). Cropland and Crop Type Classification with Sentinel-1 and Sentinel-2 Time Series Using Google Earth Engine for Agricultural Monitoring in Ethiopia. *Remote Sensing*, 16(5), 866. <https://doi.org/10.3390/rs16050866>.

#### Disaggregation of official cover crop statistics

- **Description:** Statistical model to downscale regional-level statistics on cover crop adoption to a 100 m spatial resolution using Sentinel-1 time-series.
- **Performance:** Good performance detecting parcels with cover crops (AUC = 0.74; Area Under Curve defined by the area under the Receptor Oriented Curve which plots the cumulative distributions of true positive vs the false positive events), with regional variations in France (0.65 < AUC < 0.77).
- **Key References:**
  - Fendrich, A. N., Matthews, F., Van Eynde, E., Carozzi, M., Li, Z., d'Andrimont, R., Lugato, E., Martin, P., Ciais, P., & Panagos, P. (2023). From regional to parcel scale: A high-resolution map of cover crops across Europe combining satellite data with statistical surveys. *Science of the Total Environment*, 873, 162300. <https://doi.org/10.1016/j.scitotenv.2023.162300>.

### 2.3.6 Double Cropping

#### Multi-Temporal Analysis

Deliverable no. D1.1 Requirements Baseline (RB) document	ESA Carbon-RO, EO4BK Contract no. 4000144916/24/I-EF	 International Institute for Applied Systems Analysis IIASA www.iiasa.ac.at
--	---	--

- **Description:** Uses multi-temporal satellite imagery to identify double cropping cycles—where multiple crops are cultivated in the same area within a single growing season.
- **Performance:** Effective in identifying double cropping by analysing crop phenology and harvest patterns.
- **Key References:**
  - Zhang, M., Wu, B., Zeng, H., He, G., Liu, C., Tao, S., Zhang, Q., Nabil, M., Tian, F., Bofana, J., Beyene, A. N., Elnashar, A., Yan, N., Wang, Z., & Liu, Y. (2021). GCI30: A global dataset of 30 m cropping intensity using multisource remote sensing imagery. *Earth System Science Data*, 13(4799–4817). <https://doi.org/10.5194/essd-13-4799-2021>.
  - Upcott, E. V., Henrys, P. A., Redhead, J. W., Jarvis, S. G., & Pywell, R. F. (2023). A new approach to characterising and predicting crop rotations using national-scale annual crop maps. *Science of The Total Environment*, 860, 160471. <https://doi.org/10.1016/j.scitotenv.2022.160471>.

### 3. Proposed methodologies to deliver EO-based maps of crop types, phenology, and agricultural cultivation practices for WP3

#### 3.1 Proposed method to classify crop types at 10 m resolution from Sentinel data, Europe and Brazil

In EO4BK, we will focus on two RECCAP2 regions where sufficient data is available to support the work proposed and to benchmark our results in Europe and Brazil. We will test our approach for a period of five year from 2018 to 2022. We propose to compute crop type maps over the period 2018-2022 for the target regions Europe and Brazil **using a pixel-level deep learning time series classification model** to identify the crops, followed by a **semantic classification model to mask the non-agricultural areas** (urban areas, water surfaces, etc.). The resulting product will be annual maps of 18 different annual crop types, 6 permanent crop types plus two grassland categories at the scale of individual fields where a crop type cultivation can be considered as homogeneous (**Table 3.2**).

We propose to use the **temporal convolutional neural network (TempCNN)** to perform the land cover classification (Pelletier et al., 2019). In Europe, the model is fed by pixel-level time series of Sentinel-2 L2A products from March to November, considering the 10 spectral bands at 10 m and 20 m. The preprocessing of the time series includes normalization of the reflectance values, resampling of the 20 m bands to 10 m, masking of the clouds and shadows with the built-in masks, daily interpolation, and resampling with a 3-day step. Currently, the model predicts a crop class following a nomenclature of 22 classes, including wheat, maize, barley, rapeseed, and sunflower classes. The model is trained with a 17 million pixel time series, spatially distributed over Austria, Belgium, France, Italy, Netherlands, Portugal, Slovenia, and Spain between 2018 and 2023. The pixel labels are extracted from the Integrated Administration and Control System Land-parcel Identification System (LPIS) from several countries. For reference, this model has demonstrated an overall accuracy of 86 % and an F1-Score on the wheat class of 89 % on an independent validation dataset covering the same regions and years (approximately 500,000 validation samples per year). This model can be applied for crop classification maps every year. The training over multiple European regions and years ensures the robustness of the model when it is transferred to other regions.

The semantic classification used by KERMAP is currently done using a U-Net model, with an encoder based on a pre-trained VGG16 (Simonyan and Zisserman, 2015). It takes as input the monthly syntheses of Sentinel-2 surface reflectance products from the NIMBO platform, working on 256x256 pixels patches and considering the four spectral bands at 10 m (Blue, Green, Red, NIR). The months of May or June are chosen preferably because they offer good vegetation coverage. This is a binary classification problem, where the model predicts a class (agricultural or non-agricultural) for each pixel of the considered 256x256 patch. The model is calibrated with deep learning techniques on a training dataset of 11,000 256x256 patches distributed all over France in May and June 2020. Data augmentation is used to multiply the number of patches (rotations). The considered ground-truth is the footprint of the French LPIS (RPG) 2020 enhanced with a remote sensing-based classification

map (Inglada et al., 2015). In a previous study, the model reached a global accuracy of 89.9 % on a distinct validation dataset of 800 patches distributed over France for June 2020. After applying this model to the target tiles and years, we are able to finalise the crop maps by masking the non-agricultural areas. KERMAP's current method uses Sentinel-2 time series only. However given important cloud coverage in Brazil, we will try to use both Sentinel-1 and Sentinel-2 data

### ● Key References:

- Pelletier, C., Webb, G. I., & Petitjean, F. (2019). Temporal convolutional neural network for the classification of satellite image time series. Remote Sensing, 11(5), 523.  
<https://doi.org/10.3390/rs11050523>.
- Simonyan, K., & Zisserman, A. (2015). Very deep convolutional networks for large-scale image recognition. 3rd International Conference on Learning Representations (ICLR 2015), 1–14.
- Inglada, J., Arias, M., Tardy, B., Hagolle, O., Valero, S., Morin, D., Dedieu, G., Sepulcre, G., Bontemps, S., Defourny, P., & et al. (2015). Assessment of an operational system for crop type map production using high temporal and spatial resolution satellite optical imagery. Remote Sensing, 7(9), 12356–12379.  
<https://doi.org/10.3390/rs70912356>.

## 3.2. Proposed nomenclature for crop types

We propose a nomenclature for classifying crop types based on a multi-level hierarchical approach. This structured classification system provides a detailed and consistent framework for distinguishing crops types over both Europe and Brazil, as given in **Table 3.1**. The Level-1 (L1) "Non-permanent crops" class includes all annual crops and is subdivided based on cropping practices. The **"single cropping class" gathers crops that complete their life cycle within a single growing season** and includes cereals (e.g. wheat, barley, oats, maize), root crops (e.g., potatoes, sugar beet), oil seeds (e.g. sunflower, rapeseed, soybean), protein crops and other specific crop types. The **"double cropping" class identifies fields where two successive crops are cultivated within a single year**. It mostly concerns Brazilian crops as European datasets do not provide any reference data about double cropping. Each L3 "double cropping" class will be modelled, if the model can not differentiate, some of them could be combined. The L1 **"Permanent crops" includes specific crop types that do not need annual replanting** such as coffee, fruit and nuts orchards, palm oil, grapes, olive groves and other permanent crops. Finally, the L1 **"Grasslands" class is divided into two sub-categories, the fodder crops and all the other grassland classes** (e.g. meadow). The nomenclature below is currently the most accurate and the one we are aiming for, but it may evolve slightly based on the results of the experiments conducted in WP3.

**Table 3.1:** Proposed nomenclature of crop types for Europe and Brazil.

Level 1	Level 2	Level 3	Level 4
1. Non-permanent crops	1.1. Single cropping	1.1.1. Cereals	1.1.1.1. Wheat
			1.1.1.2. Barley
			1.1.1.3. Oats
			1.1.1.4. Maize/Corn
			1.1.1.5. Sorghum
			1.1.1.6. Millet
			1.1.1.7. Rice

			1.1.1.8. Other cereals
		1.1.2. Root crops	1.1.2.1. Potatoes
			1.1.2.2. Sugar beet
			1.1.2.3. Other root crops
		1.1.3. Oil seeds	1.1.3.1. Sunflower
			1.1.3.2. Rapeseed
			1.1.3.3. Soybean
			1.1.3.4. Other oil seeds
		1.1.4. Protein crops	
		1.1.5. Misc crops*	1.1.5.1. Cotton
			1.1.5.2. Sugarcane
			1.1.5.3. Flax
			1.1.5.4 Other single crops
	1.2. Double cropping Europe	1.2.1. Soybean / Maize	
		1.2.2. Soybean / Sorghum	
		1.2.3. Soybean / Millet	
		1.2.4. Soybean / Other Cereals	
		1.2.5. Soybean / Protein crops	
		1.2.6. Soybean / Cotton	
		1.2.7. Soybean / Fodder crops	
		1.2.8. Maize / Fodder crops	
		1.2.9. Other double crops	
1.3 Double cropping Brazil	1.3.1 Soybean / Sorghum		
	1.3.2 Soybean / Fodder		
	1.3.3 Soybean /Cereals		
	1.3.4 Soybean / Protein		
	1.3.5 Maize / Fodder		
	1.3.6 Other double crops		
2. Permanent crops	2.1. Coffee		
	2.2. Fruit and nuts orchards		
	2.3. Palm oil		
	2.4. Grapes		



3. Grasslands	2.5. Olive groves
	2.6. Other permanent crops
	3.1. Fodder crops
	3.2. Other grasslands

**Table 3.1:** Proposed nomenclature of crop types for Europe and Brazil. The ‘Misc crops’ class gathers all crops that does not match any other single crop classes (cereals, root crops, oil seeds, protein crops).

In Brazil, Bendini et al. (2019) used a much larger nomenclature but did not provide the frequency of these land uses. Hence the proportion of each and usefulness to include here is unknown (**Fig 3.1**). We do know “the most cultivated crops [identified in Campo Verde] are soybean (210 100 ha), maize (88 760 ha), cotton (81 996 ha), sorghum (3100 ha), and beans (2400 ha)” (Sanches et al., 2018). With “other temporary crops” representing 14 % of cropped area in 2023 (Figure 3.2a) it is possible that these classes are not negligible, i.e. sorghum and beans are 20 % of soybean production in Campo Verde (Sanches et al., 2018). We will nevertheless be restricted to producing the best possible nomenclature given the available in-situ datasets available and the needs of the BK model, and **will adopt for Brazil in the first phase the one of Table 3.1**.

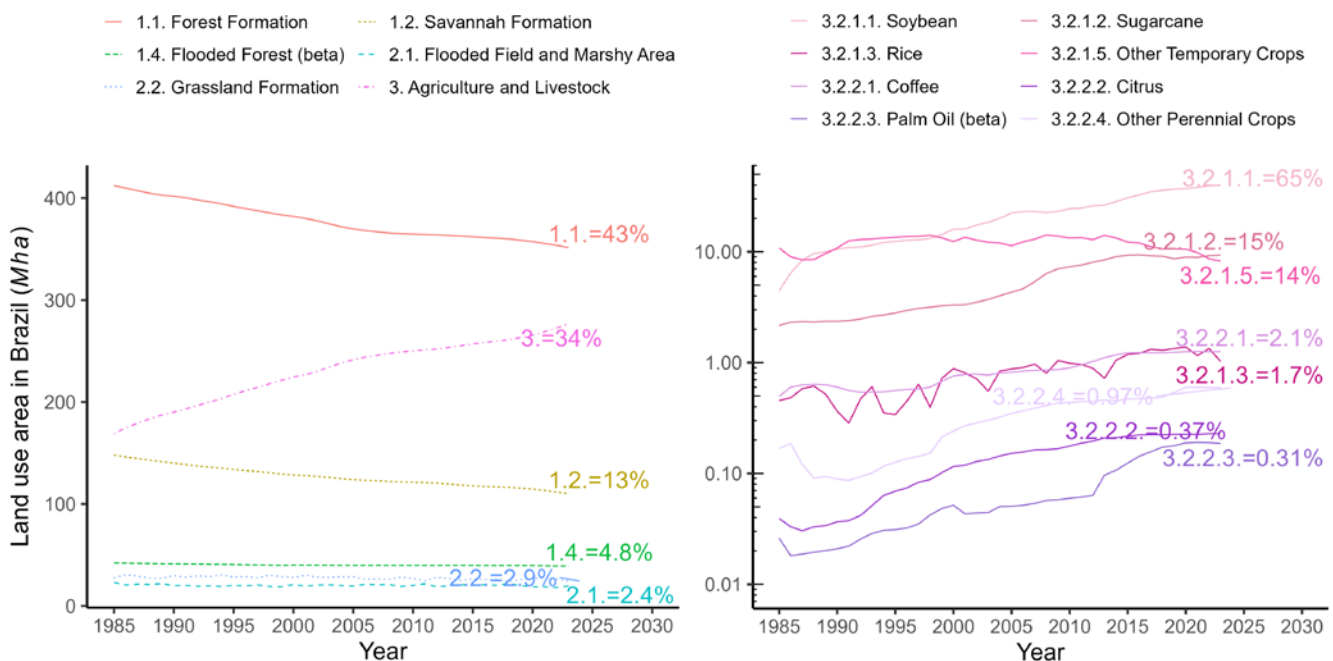


**Figure 3.1.** Natural and anthropogenic land use fraction in Brazil with percentage in 2023 (LHS). Agricultural land covered by each crop type defined in MapBiomass with percentage in 2023. Data from MapBiomass. Note Natural and anthropogenic land uses (LHS) constituting < 1% of total Brazil cover removed and RHS y axis on log10 scale


#### Key References:

- Pitchers, J., Ferrand, N., Pull, M., Minette, S., Abella, M., & Debaeke, P. (2023). Opportunities and risks of double cropping in southwestern France with a focus on soybean and sunflower crops. *OCL*, 30, 16. <https://doi.org/10.1051/ocl/2023016>.
- Fernández-Ortega, J., Álvaro-Fuentes, J., Talukder, R., Lampurlanés, J., & Cantero-Martínez, C. (2023). The use of double-cropping in combination with no-tillage and optimized nitrogen fertilization improve crop yield and water use efficiency under irrigated conditions. *Field Crops Research*, 301, 109017. <https://doi.org/10.1016/j.fcr.2023.109017>.
- Láng, V., Dafnaki, D., Balla, I., Czako, I., Csenki, S., Kovács, G. P., Mutua, K., Szlatenyi, D., Vulcz, L., & Bukombe, B. (2023). Double cropping as an adaptation mechanism to climate change patterns in the Carpathian Basin. *Acta Agriculturae Scandinavica, Section B — Soil & Plant Science*, 73(1), 184–198. <https://doi.org/10.1080/09064710.2023.2257218>.
- do Nascimento Bendini, H., Garcia Fonseca, L. M., Schwieder, M., Sehn Körting, T., Rufin, P., Del Arco Sanches, I., Leitão, P. J., & Hostert, P. (2019). Detailed agricultural land classification in the Brazilian Cerrado based on phenological information from dense satellite image time series. *International Journal of Applied Earth Observation and Geoinformation*, 82, 101872. <https://doi.org/10.1016/j.jag.2019.05.005>.
- Del'Arco Sanches, I., Feitosa, R. Q., Achancaray Diaz, P. M., Dias Soares, M., Barreto Luiz, A. J., Schultz, B., & Pinheiro Maurano, L. E. (2018). Campo Verde Database: Seeking to Improve Agricultural Remote Sensing of Tropical Areas. *IEEE Geoscience and Remote Sensing Letters*, 15(3), 369–373. <https://doi.org/10.1109/LGRS.2017.2789120>.

### 3.3 Reference data on crop types and management practices for training models.

For the analysis of **crop types, cropland phenology and irrigation we will focus primarily on reference data from the Land Use/Cover Area frame Survey (LUCAS) Copernicus database** (d'Andrimont et al., 2021). The new LUCAS module specifically tailored to Earth Observation and was introduced in 2018: the LUCAS Copernicus module, aiming at surveying land cover extent up to 51 m in four cardinal directions around a point of observation. The new dataset is designed to ensure comparability between the surveyed area and remote-sensing observation (e.g. homogeneous land cover) and includes a total of 58,428 polygons with 66 land cover classes, including crop type and including crop type, and 38 land use classes (e.g., agriculture), and surveys on water management (e.g., type of irrigation, water source and delivery system). Given the expected high quality of this data, EO4BK will use LUCAS Copernicus as the reference database for Europe. We may also consider utilising LPIS (Land Parcel Identification System) data for crop types detection. Although not available for all EU countries, it offers significant advantages where it is accessible. LPIS data provides a much larger volume of information and covers a longer time span for those countries, which could enhance the robustness and accuracy of the model. This additional dataset could improve the model's generalizability by incorporating more extensive temporal and spatial variability in crop classification.

Crop type and irrigation practice identification across Brazil will utilise the **combined datasets from Luís Eduardo Magalhães (LEM), the National Supply Company (CONAB), and the National Water and Sanitation Agency (ANA)**. These data sources include monthly in-situ crop sampling, annual in-situ sampling, expert interpretation of phenological signals, and spatial indicators, providing sufficient data for model production and validation over the 5-year EO4BK period and Sentinel-2 operational dates. Major crops and irrigation practices, monitored by CONAB and ANA, also reflect Brazil's environmental gradients, which should enhance prediction accuracy. However, no publicly available reference datasets (i.e. delineation by visual interpretation or in-situ sampling) currently exist for crops like sugarcane in Brazil, which covered 14 % of Brazil's agricultural land in 2023 , only outputs from other TempCNNs including MapBiomass or Zheng et al. (2021). EO4BK may therefore rely on MapBiomass CNN outputs without the need to create new polygons from phenological interpretations of Sentinel-2 images in sugarcane-dominant municipalities. A similar approach may be needed for palm oil and citrus plantations, which combined represent less than 1 % of Brazil's agricultural land in 2023. Double crop

Deliverable no. D1.1 Requirements Baseline (RB) document	ESA Carbon-RO, EO4BK Contract no. 4000144916/24/I-EF	 International Institute for Applied Systems Analysis IIASA www.iiasa.ac.at
--	---	--

identification will solely rely upon the LEM (2017-2018), LEM+ (2019-2020) providing a combined monitored area of 570 and 2510 km<sup>2</sup> in Bahia state respectively, and CONAB for Soybean/Maize in Paraná State.

- **Key References:**

- d'Andrimont, R., Verhegghen, A., Lemoine, G., Kempeneers, P., Meroni, M., & van der Velde, M. (2021). From parcel to continental scale – A first European crop type map based on Sentinel-1 and LUCAS Copernicus in-situ observations. *Remote Sensing of Environment*, 266, 112708. <https://doi.org/10.1016/j.rse.2021.112708>.
- Zheng, Y., dos Santos Luciano, A. C., Dong, J., & Yuan, W. (2022). High-resolution map of sugarcane cultivation in Brazil using a phenology-based method. *Earth System Science Data*, 14(4), 2065–2080. <https://doi.org/10.5194/essd-14-2065-2022>.

### 3.4 Proposed method to derive phenology from Sentinel 1 and Sentinel 2 remote-sensing indices

#### 3.4.1 Selection of Sentinel indices

To derive crop phenology, Sentinel-1 and Sentinel-2 data will be used. Specifically, we will focus on the following Essential Climate Variables (ECVs): GRD (Ground Range Detected) products from Sentinel-1, surface reflectance information from all bands of Sentinel-2, as well as derived indices and products, such as, Enhanced Vegetation Index (EVI), kernel Normalised Difference Vegetation Index (kNDVI), near-infrared of vegetation (NIRv), fraction of absorbed photosynthetically active radiation (fAPAR), leaf area index (LAI) and fraction of vegetation cover. The data will be analysed at 10m spatial resolution over the five-year period considered in the project. The data will be downloaded for the selected polygons in Europe and Brazil based on the reference data as mini-cubes covering the full period available on record. For Sentinel-2 data, we will apply a rigorous pre-processing of the raw dataset by applying the open source **Sentle python package developed by C. Mosig at Leipzig University**. The Sentle pre-processing pipeline allows for integrated cloud detection based on the improved CloudSEN12 (Aybar et al., 2022), snow masking, harmonization, merging, and temporal compositing.

- **Key References:**


- Aybar, C., Ysuhuaylas, L., Loja, J. *et al.* CloudSEN12, a global dataset for semantic understanding of cloud and cloud shadow in Sentinel-2. *Sci Data* **9**, 782 (2022). <https://doi.org/10.1038/s41597-022-01878-2>.
- CMOSig. (n.d.). Sentle. GitHub. Retrieved October 29, 2024, from <https://github.com/cmogig/sentle>.

#### 3.4.2 Time series analysis and smoothing filters to detect crop phenology metrics using Sentinel data

Given the high dependence of phenological metrics on the type of smoothing applied and the different approaches to quantify phenological metrics, in EO4BK we will quantify not only the timing of each phenological phase, but work towards an uncertainty assessment. We will thus apply **different smoothing filters used in the literature to extract sub-annual cycles in time-series, namely Savitzky-Golay, Whittaker Smoother, Harmonic Analysis of Time Series (HANTS) and Generalised Additive Models (GAM)**.

For the analysis of phenology we will consider the following phenological metrics:

- Start of growing season (SOS)
- Timing of the peak of growing season (PGS)
- End of growing season (EOS)
- Number of phenological cycles/peaks within a calendar year (nGS) in the case of double cropping

Deliverable no. D1.1 Requirements Baseline (RB) document	ESA Carbon-RO, EO4BK Contract no. 4000144916/24/I-EF	 International Institute for Applied Systems Analysis IIASA www.iiasa.ac.at
--	---	--

Planting date will not be considered given that it is difficult to detect from remote-sensing data.

For the SOS and EOS metrics, we will evaluate the influence of the choice of different thresholds (10, 20, 30% of peak thresholds) and other methods proposed in the literature (e.g. second derivative analysis) on the mean value, interannual variability and trends of these metrics.

#### ● Key References:


- Jönsson, P., & Eklundh, L. (2004). TIMESAT—a program for analyzing time-series of satellite sensor data. *Computers & Geosciences*, 30(8), 833–845. <https://doi.org/10.1016/j.cageo.2004.05.006>.
- Eklundh, L., Jönsson, P. (2015). TIMESAT: A Software Package for Time-Series Processing and Assessment of Vegetation Dynamics. In: Kuenzer, C., Dech, S., Wagner, W. (eds) *Remote Sensing Time Series. Remote Sensing and Digital Image Processing*, vol 22. Springer, Cham. [https://doi.org/10.1007/978-3-319-15967-6\\_7](https://doi.org/10.1007/978-3-319-15967-6_7).
- Bolton, D. K., Gray, J. M., Melaas, E. K., Moon, M., Eklundh, L., & Friedl, M. A. (2020). Continental-scale land surface phenology from harmonized Landsat 8 and Sentinel-2 imagery. *Remote Sensing of Environment*, 240, 111685. <https://doi.org/10.1016/j.rse.2020.111685>.
- Tian, F., Cai, Z., Jin, H., Hufkens, K., Scheifinger, H., Tagesson, T., Smets, B., Van Hoolst, R., Bonte, K., Ivits, E., Tong, X., Ardö, J., & Eklundh, L. (2021). Calibrating vegetation phenology from Sentinel-2 using eddy covariance, PhenoCam, and PEP725 networks across Europe. *Remote Sensing of Environment*, 260, 112456. <https://doi.org/10.1016/j.rse.2021.112456>.

### 3.5 Proposed methods to classify cropland management practices.

#### 3.5.1 Method to map cover crops at 100 m resolution in Europe

For cover crops (CCs), the difficulty is the lack of site data for training and evaluation of models. **We propose to compute cover crop maps by the statistical downscaling method of Fendrich et al. 2023.** Multi-temporal Sentinel-1 data was used to monitor changes in the landscape surface condition through time. The Sentinel-1 SAR constellation re-visits the EU territory with a minimum 6-day revisit period since 2016 (until the Sentinel-1B defect in December 2021), providing a dense temporal time series for phenological monitoring. Compared to optical sensors (e.g. Sentinel-2), its microwave backscatter retrieval is practically uninfluenced by atmospheric conditions. In the agricultural context, microwave backscattering is sensitive to crop canopy structure, which means it can detect plant growth at the parcel spatial resolution. For these reasons, Sentinel-1 data offers a consistent source of plant phenological data in winter months for mapping CCs in combination with other computational techniques. Spatio-temporally consistent time-series of Sentinel-1 data were generated as follows: i) analysis-ready Sentinel-1 data was accessed in Google Earth Engine (Gorelick et al., 2017) (i.e. COPENICUS/S1\_GRD), already pre-processed to account for thermal-noise removal, radiometric calibration, and terrain correction; ii) a temporal stack of 31 rasters of the VV and VH bands was created, for both ascending and descending orbits, giving 12-day composites from the 10<sup>th</sup> of August 2016 to the same date in 2017; iii) the cross-polarization ratio (CR) was calculated as  $CR = VV / VH$ , giving 31 spatio-temporal layers for the period of study. Finally, the data was resampled using the median statistic to a 100-m spatial resolution, the target resolution adopted for the new spatially explicit CC dataset for reasons of computational trade-offs vs. spatial resolution (data size) in spatial disaggregation models.

The choice of the CR time series as an indicator of the existence of CCs came from recent evidence highlighting the correlation of this index with the more well-known Normalised Difference Vegetation Index (NDVI) in the context of crop phenology (Meroni et al., 2021), crop dynamics (Veloso et al., 2017) and vegetation dynamics (Ma et al., 2022; Vreugdenhil et al., 2020). The choice of the period of analysis (i.e. 10<sup>th</sup> of August 2016–2017) was mainly driven by the need to match the period of most recent the coarse CC data available in Europe. In this case, it corresponds to the 2016 dataset on CCs per NUTS2 region published by the European Commission,

Deliverable no. D1.1 Requirements Baseline (RB) document	ESA Carbon-RO, EO4BK Contract no. 4000144916/24/I-EF	 International Institute for Applied Systems Analysis IIASA www.iiasa.ac.at
--	---	--

which estimates the total CC area in arable lands (European Commission, 2022c). The exact definition of the variable used (i.e. “cover or intermediate crops”) reads: “An area of arable land on which plants are sown specifically to reduce the loss of soil, nutrients and plant protection products during the winter or other periods when the land would otherwise be bare and susceptible to losses. The economic interest of these crops is low, and the main goal is soil and nutrient protection. (...) These crops should not be mistaken for normal winter crops or grassland” (European Commission, 2022e).

In order to filter the location of arable lands, the CORINE Land Cover 2018 at a 100-m spatial resolution and with a minimum mapping unit of 25 ha was used (Copernicus, 2022). By doing so, predictions of CC existence were restricted to a spatial domain where agricultural activity was previously detected in an external dataset. From the complete CORINE database, the class arable land was created by selecting the classes “non-irrigated arable land”, “permanently irrigated land”, and “rice fields”. Additionally, other agricultural classes were included to avoid having an overly restrictive spatial domain. Even though the period of CORINE does not match the period of 2016–2017, it can be accepted as adequate under the assumption that no drastic changes occurred in European arable lands from 2016 to 2017, the year where CORINE Land Cover 2018 images were mainly taken (Büttner and Kosztra, 2022). Then, because the amount of arable land calculated using FSS (European Commission, 2022c) and CORINE are different, the CC area consistent with CORINE was defined by multiplying the original CC area from Farm Structure Survey (FSS) by the ratio of CORINE to FSS arable land area (A), giving  $CC_{Corine} = CCFSS \cdot A_{Corine}/A_{FSS}$ . Such an arable land ratio varies from 0.02 to 3.69, with an average of 1.02.

In order to disaggregate CC information from the (215) NUTS2 regions to the (156 million) pixels at 100 m resolution, the estimation method proposed by Fendrich et al. (2022) was used. As in any other regression modelling approach, the technique consists of first making assumptions about the relationships between explanatory and dependent variables at the fine scale (**Figure 3.2**).

$$y_i = g \left[ \sum_t s(\text{lat}_i, \text{long}_i, t, CR_i(t)) \right] + \varepsilon, \quad \varepsilon \sim N(0, \sigma^2) \quad (1)$$

It was assumed that the fraction of CCs in a pixel varies in three dimensions, namely: space, time, and the observed Sentinel-1 CR. Each of these dimensions are assumed to vary (possibly smoothly) with nonlinear interactions between them. Such an assumption is equivalent to assuming that the interpretation of a given CR time series varies so that it might indicate the existence of CCs in one particular place and its neighbouring areas but not in other more distant regions. In mathematical notation, this can be represented as:

with  $y_i$  being the fraction from 0 to 100 % of CCs within pixel indexed  $i$ ;  $\text{lat}_i$ ,  $\text{long}_i$ ,  $t$ ,  $CR_i(t)$  being latitude, longitude, time and the CR time-series with a timestep of 12 days, respectively. The function  $g(x) = 1/(1 + \exp(x))$  was chosen to be the link function, since  $y_i$  varies from 0 to 100 %. The term  $\varepsilon$  is the residual term, assumed to be normally distributed, and  $s(\cdot)$  is the joint function to be estimated from the data. Penalised smoothers that can be represented using basis expansions and a penalty matrix to control function smoothness are a common choice for the one-dimensional smoothers inside  $s(\cdot)$ , and the interaction is often represented as tensor products (Wood, 2017). Under such a representation, Eq. (1) could be recognised as a nonlinear mixed model (Bates and Watts, 1988; Wolfinger, 1993). In the representation of Eq. (1), the fraction of CC at the pixel level is assumed to be a random variable. Consequently, the sum of the CC fractions in the pixels that belong to a NUTS2 region creates another random variable representing the CC area at the NUTS2 level. It can be shown that, in this case, a second nonlinear mixed model can be derived for the NUTS2 level, and it preserves the original parameters necessary to construct the pixel-level smoothers of Eq. (1). Such a NUTS2-level model allows us to attempt to reconstruct the pixel-level information by performing regression analysis on the coarse data.



During the parameter estimation phase, an optimization procedure handles the tradeoff between i) approximating the reconstructed to the observed values at the NUTS2 level; and ii) enforcing the mathematical assumptions for the function  $s(\cdot)$  described above (i.e. that the one-dimensional smoothers are continuous functions, that the effect of the CR varies in space and time).

Parameter estimation is done through a numerical optimization procedure, which maximises the chance of observing the aggregated data given the assumptions made at the pixel level (i.e. maximum likelihood estimation). In this work, we slightly modified the original method of Fendrich et al. (2022) to use a quadratic instead of a first-order approximation to the log-likelihood in each iteration. Such a modification led to the natural interpretation of each iteration as a Newton-Raphson step of the original guess towards the maximum a posteriori estimates, similar to the scheme proposed by Rossell et al. (2021).

As disaggregation problems are fundamentally undetermined with infinite solutions, choosing proper assumptions is essential for narrowing the possibilities. Therefore,  $s(\cdot)$  was assumed to be a tensor product, and several possibilities for the one-dimensional smoothers of Eq. (1) were tested, including thin-plate, cubic and P-splines, with different basis dimensions and penalty orders. The SM 4 shows the results for the four best models found during model selection according to the area under the curve (AUC) performance metric (see Section 2.4.2 for details about the validation dataset). The final alternative was chosen to be four P-splines (Wood, 2016), with basis dimensions 9 for the longitude and 8 for latitude, time and CR. After the estimation of model parameters, the expected value of  $s(\cdot)$  given the parameters was calculated and plotted to allow the visualisation of the estimated one-dimensional smoothers. The predicted CC fraction and the corresponding uncertainty were calculated as the point estimate of the median and the bounds of the 90 % confidence intervals for the expected value of the response variable of Eq. (1) given the parameters, respectively.

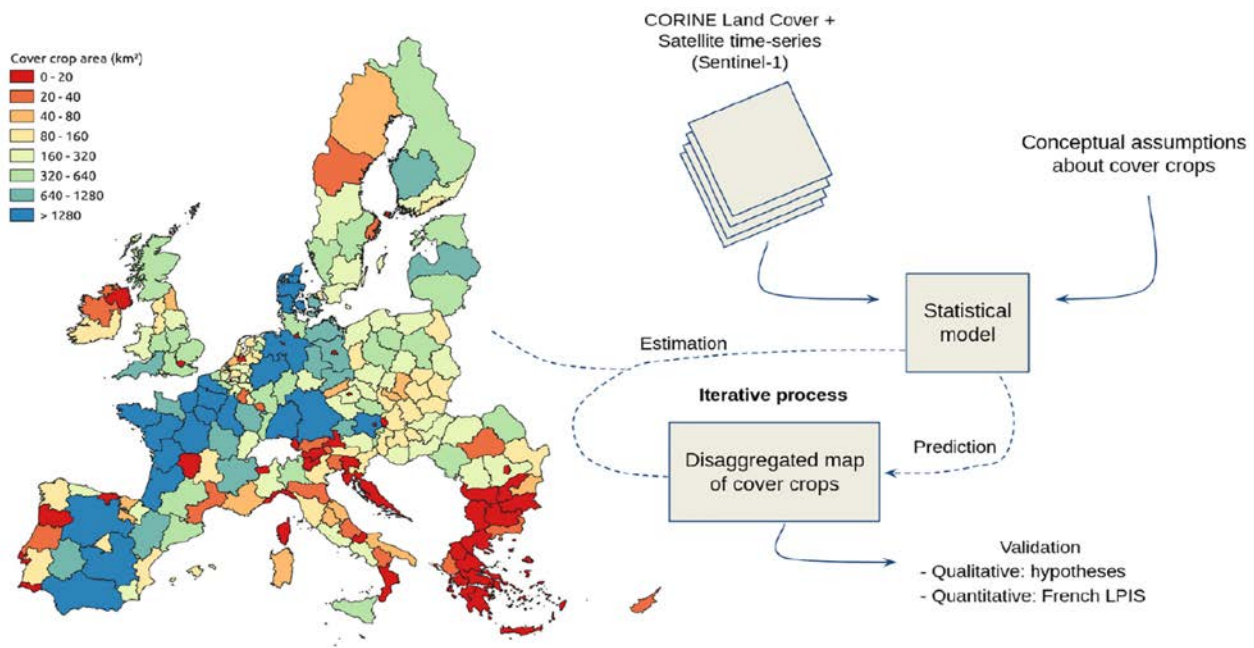


**Figure 3.2:** Summary of the method used for mapping cover crops in 2016-17. Left: area of cover crops in 2016 visualised using the cover crop extent per region from the FSS (European Commission, 2022d).

#### ● Key References:

- Fendrich, A. N., Matthews, F., Van Eynde, E., Carozzi, M., Li, Z., d'Andrimont, R., Lugato, E., Martin, P., Ciais, P., & Panagos, P. (2023). From regional to parcel scale: A high-resolution map of cover crops



- across Europe combining satellite data with statistical surveys. *Science of the Total Environment*, 873, 162300. <https://doi.org/10.1016/j.scitotenv.2023.162300>.
- Gorelick, N., Hancher, M., Dixon, M., Ilyushchenko, S., Thau, D., & Moore, R. (2017). Google Earth Engine: Planetary-scale geospatial analysis for everyone. *Remote Sensing of Environment*, 202, 18–27. <https://doi.org/10.1016/j.rse.2017.06.031>.
  - Meroni, M., d'Andrimont, R., Vrieling, A., Fasbender, D., Lemoine, G., Rembold, F., Seguíni, L., & Verhegghen, A. (2021). Comparing land surface phenology of major European crops as derived from SAR and multispectral data of Sentinel-1 and -2. *Remote Sensing of Environment*, 253, 112232. <https://doi.org/10.1016/j.rse.2020.112232>.
  - Veloso, A., Mermoz, S., Bouvet, A., Le Toan, T., Planells, M., Dejoux, J.-F., & Ceschia, E. (2017). Understanding the temporal behavior of crops using Sentinel-1 and Sentinel-2-like data for agricultural applications. *Remote Sensing of Environment*, 199, 415–426. <https://doi.org/10.1016/j.rse.2017.07.015>.
  - Ma, Y., Hu, Y., Moncrieff, G. R., Slingsby, J. A., Wilson, A. M., Maitner, B., & Zhou, R. Z. (2022). Forecasting vegetation dynamics in an open ecosystem by integrating deep learning and environmental variables. *International Journal of Applied Earth Observation and Geoinformation*, 114, 103060. <https://doi.org/10.1016/j.jag.2022.103060>.
  - Vreugdenhil, M., Navacchi, C., Bauer-Marschallinger, B., Hahn, S., Steele-Dunne, S., Pfeil, I., Dorigo, W., & Wagner, W. (2020). Sentinel-1 cross ratio and vegetation optical depth: A comparison over Europe. *Remote Sensing*, 12(20), 3404. <https://doi.org/10.3390/rs12203404>.
  - European Commission. (2022c). Eurostat: Soil cover by NUTS2 regions. [https://ec.europa.eu/eurostat/databrowser/view/ef\\_mp\\_soil/default/table?lang=en](https://ec.europa.eu/eurostat/databrowser/view/ef_mp_soil/default/table?lang=en).
  - European Commission. (2022e). Glossary: Soil cover. [https://web.archive.org/web/20220119025400/https://ec.europa.eu/eurostat/statistics-explained/index.php?title=Glossary:Soil\\_cover](https://web.archive.org/web/20220119025400/https://ec.europa.eu/eurostat/statistics-explained/index.php?title=Glossary:Soil_cover).
  - Copernicus. (2022). CLC 2018. <https://land.copernicus.eu/pan-european/corine-land-cover/clc2018>. Accessed: 2022-09-20.
  - Büttner, G., & Kosztra, B. (2022). CLC2018 technical guidelines. [https://land.copernicus.eu/usercorner/technical-library/clc2018technicalguidelines\\_final.pdf](https://land.copernicus.eu/usercorner/technical-library/clc2018technicalguidelines_final.pdf).
  - Fendrich, A. N., Ciais, P., Lugato, E., Carozzi, M., Guenet, B., Borrelli, P., Naipal, V., McGrath, M., Martin, P., & Panagos, P. (2022). Matrix representation of lateral soil movements: Scaling and calibrating CE-DYNAM (v2) at a continental level. *Geoscientific Model Development*, 15(20), 7835–7857. <https://doi.org/10.5194/gmd-15-7835-2022>.
  - Wood, S. (2017). *Generalized additive models: An introduction with R* (2nd ed.). Chapman and Hall/CRC.
  - Bates, D. M., & Watts, D. G. (Eds.). (1988). *Nonlinear regression analysis and its applications*. John Wiley & Sons, Inc. <https://doi.org/10.1002/9780470316757>.
  - Wolfinger, R. (1993). Laplace's approximation for nonlinear mixed models. *Biometrika*, 80, 791–795. <https://doi.org/10.1093/biomet/80.4.791>.
  - Rossell, D., Abril, O., & Bhattacharya, A. (2021). Approximate Laplace approximations for scalable model selection. *Journal of the Royal Statistical Society: Series B, Statistical Methodology*, 83, 853–879.
  - Wood, S. N. (2016). P-splines with derivative based penalties and tensor product smoothing of unevenly distributed data. *Statistical Computing*, 27, 985–989. <https://doi.org/10.1007/s11222-016-9666-x>.
  - European Commission. (2022d). Glossary: Farm structure survey (FSS). [https://web.archive.org/web/20220901054908/https://ec.europa.eu/eurostat/statistics-explained/index.php?title=Glossary:Farm\\_structure\\_survey\\_\(FSS\)](https://web.archive.org/web/20220901054908/https://ec.europa.eu/eurostat/statistics-explained/index.php?title=Glossary:Farm_structure_survey_(FSS)).


### 3.5.2. Potential strategy for mapping tillage over Europe

The construction of a disaggregation model for tillage presents similarities with cover crops, with works reporting the successful use of Sentinel 1 and 2 data for tillage detection at ~100 m spatial resolution (Satalino et al., 2018; Liu et al., 2022; Xiang et al., 2022). However, an important additional challenge is the lack of field observations, which is fundamental for validating results at the parcel scale. One possibility to overcome the lack of validation data is using spatially distributed geo-tagged photos with land cover information (d'Andrimont et al., 2022). Such photos span the period 2006-2018 and may contain information about the adoption of tillage practices when taken during the intercropping season. The example of **Figure 3.3** exemplifies how such photos can be used. In the project, **we do not plan to provide tillage maps** but if another related projects is funded (HR on soil erosion) we will contribute a dataset by year 3.



**Figure 3.3::** Patterns of tillage adoption in 2015, as detected by LUCAS photos (source: d'Andrimont et al. (2022)).

Manually labelling tillage adoption in photos taken on the field is an inherently subjective task, and additional measures are needed to reduce the uncertainty of such assessment. For instance, a group of researchers can be set up to classify a set of photos according to their expertise, and only the subset of images with identical classification can be used further in the analysis. Next, such a subset can be used as an input for machine learning algorithms of image recognition, similarly as used for leaf analysis, pest control, and plant growth monitoring (Keyvanpour et al., 2022). Finally, image recognition algorithms could reclassify the whole set of LUCAS photos, providing a reliable way to gather validation data at the parcel scale for tillage disaggregation. This step would allow the application of similar methods as those used for the disaggregation of cover crops by Fendrich et al. (2023) for tillage where official statistics are available. In the EO4BK project, **we will not provide**

Deliverable no. D1.1 Requirements Baseline (RB) document	ESA Carbon-RO, EO4BK Contract no. 4000144916/24/I-EF	 International Institute for Applied Systems Analysis IIASA www.iiasa.ac.at
--	---	--

**maps of tillage across Europe.** If an EU project (soil erosion) submitted Oct 2024 (in the HORIZON-MISS-2024-SOIL-01 call) is accepted, by the year 3 of EO4BK, such maps will be available.

- **Key References:**

- Satalino, G., et al. (2018). Sentinel-1 & Sentinel-2 data for soil tillage change detection. In IGARSS 2018 - 2018 IEEE International Geoscience and Remote Sensing Symposium (pp. 6627–6630). Valencia, Spain. <https://doi.org/10.1109/IGARSS.2018.8519103>.
- Liu, Y., Rao, P., Zhou, W., Singh, B., Srivastava, A. K., & others. (2022). Using Sentinel-1, Sentinel-2, and Planet satellite data to map field-level tillage practices in smallholder systems. PLOS ONE, 17(11), e0277425. <https://doi.org/10.1371/journal.pone.0277425>.
- Xiang, X., Du, J., Jacinthe, P.-A., Zhao, B., Zhou, H., Liu, H., & Song, K. (2022). Integration of tillage indices and textural features of Sentinel-2A multispectral images for maize residue cover estimation. Soil and Tillage Research, 221, 105405. <https://doi.org/10.1016/j.still.2022.105405>.
- d'Andrimont, R., Yordanov, M., Martinez-Sanchez, L., Haub, P., Buck, O., Haub, C., Eiselt, B., & van der Velde, M. (2022). LUCAS cover photos 2006–2018 over the EU: 874,646 spatially distributed geo-tagged close-up photos with land cover and plant species label. Earth System Science Data, 14(10), 4463–4472. <https://doi.org/10.5194/essd-14-4463-2022>.
- Keyvanpour, M. R., & Barani Shirzad, M. (2022). Machine learning techniques for agricultural image recognition. In M. A. Khan, R. Khan, & M. A. Ansari (Eds.), Application of machine learning in agriculture (pp. 283–305). Academic Press. <https://doi.org/10.1016/B978-0-323-90550-3.00011-4>.
- Fendrich, A. N., Matthews, F., Van Eynde, E., Carozzi, M., Li, Z., d'Andrimont, R., Lugato, E., Martin, P., Ciais, P., & Panagos, P. (2023). From regional to parcel scale: A high-resolution map of cover crops across Europe combining satellite data with statistical surveys. Science of the Total Environment, 873, 162300. <https://doi.org/10.1016/j.scitotenv.2023.162300>.

### 3.5.3 Crop harvest dates

In this project, crop **harvest dates will be inferred from the phenological metrics, namely end of season.**

### 3.5.4. Double cropping in Europe

Double cropping is less common in Europe compared to warmer regions of the world. The total area under double cropping in Europe accounts for less than 3 % of the world's double-cropped lands (Waha et al., 2020). The current European regions where double cropping can be practised are mostly located in the mediterranean basin (Su et al., 2023). However, in the context of global warming, it has become important to assess the feasibility of implementing double cropping systems across various regions in Europe. Rising temperatures and extended growing seasons could make double cropping more viable in areas previously unsuitable for such practices. They projected that both western and eastern Europe would have up to 40 % chance to implement double-cropping successfully by the end of 2100, while southern Europe could expect a 27.3 % increase in calorie production from a double-cropping maize-wheat system compared to single cropping. The proposed method for classifying double cropping is to **extend Kermap's current crop identification method (cf 3.1)**, currently predicting only single crop classes, to detect single and double crop classes. It will require training data for all classes, single and double crops. Currently, none of the European reference datasets (LUCAS, LPIS, EuroCrops) provide clear information on double cropping. Here, we will therefore **extend the analysis to the dataset from Su et al. (submitted), who compiled double cropping data** for maize and wheat in Europe.

- **Key References:**

- Waha, K., Dietrich, J. P., Portmann, F. T., Siebert, S., Thornton, P. K., Bondeau, A., & Herrero, M. (2020). Multiple cropping systems of the world and the potential for increasing cropping intensity. Global Environmental Change, 64, 102131. <https://doi.org/10.1016/j.gloenvcha.2020.102131>.



- Su, Y., Lauerwald, R., Makowski, D., Viovy, N., Guilpart, N., Zhu, P., Gabrielle, B., & Ciais, P. (2023). Global warming increases the chance of success of maize-wheat double cropping in Europe. PREPRINT (Version 1). Research Square. <https://doi.org/10.21203/rs.3.rs-3112511/v1>.

### 3.5.5. Double cropping in Brazil

Here we propose deploying a tempCNN model to detect the presence of double cropping, as outlined in Section 3.1 into 5 frequent and unique crop combinations as well as a general double cropping class (Table 3.1). This approach expands the suite of statistical methodologies currently applied across the region, providing the opportunity to enhance the capacity to identify cropping patterns with greater accuracy and detail at the national scale. In the ambition to reach carbon neutral targets by 2050 the establishment of double cropping practises in Brazil has been integral for increasing national agricultural yields whilst simultaneously limiting further deforestation (Brazil NDC, 2022). Additionally, rise in double cropping area has additionally been driven by the increased export value of soybean and farmers incapacity to maintain yield densities (Xu et al., 2021) effects tied to increased climate variability (Reis et al., 2020) and government intervention such as the Soybean moratorium (Gibbs et al., 2015). Uptake in these land management practices has nearly doubled in 10 years estimated to cover 16 Mha primarily through increases in 2<sup>nd</sup> season corn in Mato Grosso and Paraná states (Novaes et al., 2017; Novaes et al., 2022) (Figure 3.4). Due to the increasing presence of double cropping in Brazilian agriculture and the substantial contribution of the nation to global crop markets, new methods to improve the capacity and accuracy of double cropping identification across Brazil annually is vital in improving C exchange estimates of the sector and region.

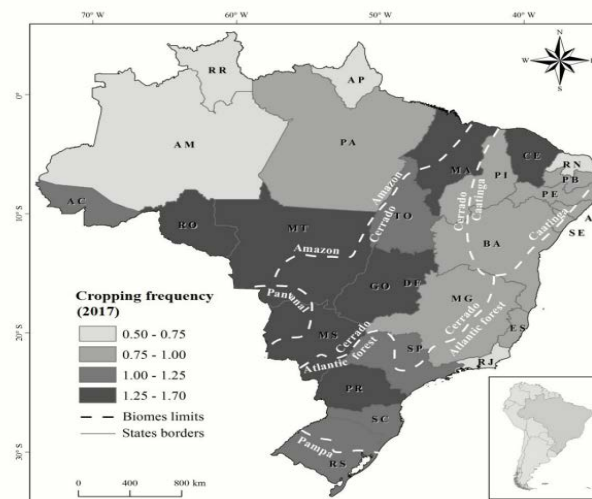


**Figure 3.4:** Cropping frequency variation across Brazilian states, based on IBGE data recorded for 2017 (taken from: Novares et al., 2022)

Mapping of double cropping practises in Brazil has previously been produced at the state and national level, yet currently, no temporally consistent annual databases exist nationally post-2019. Additionally, these datasets are primarily produced at the relatively moderate resolution of 250 m (Picoli et al., 2018; Chaves et al., 2021), except for non-national analysis conducted with PlanetScope imaging at 5 m (Sano et al., 2023), classification of soybean in the Cerrado with Landsat/Sentinel-2 (Parreiras et al., 2022) and double cropping the the Cerrado with Landsat in a Random Forest (RF) model (Bendini et al., 2019). These recent works build upon longer-standing classifications of land use from MODIS vegetation indices (VIs) using RF and other traditional machine

learning (ML) classifiers achieving accuracies between 74-94 % accuracy (Arvor et al., 2011; Brown et al., 2013; Chen et al., 2018; Galford et al., 2008). However, many of these earlier studies remain restricted to Mato Grosso state and did not attempt to classify double cropping. Consequently, there is potential to utilise new earth observation initiatives (Harmonised Landsat and Sentinel-2; HLS) and statistical techniques such as CNNs to increase the resolution of existing benchmark maps to 10-30 m, whilst increasing both the spatiotemporal extent of analysis and land use/practise nomenclature.

Applications of MODIS (250m) for double cropping identification have previously deployed Support Vector Machines (SVMs) (Picoli et al., 2018; Simoes et al., 2020), Time-Weighted Dynamic Time Warping (TWDTW) (Maus et al., 2019; Chaves et al., 2021) and Landsat feed random forest (RF) (Bendini et al., 2019) machine learning techniques. These algorithms have proved effective in classifying reflectance time series data into distinct land uses and practices, yet differ in statistical procedures. SVMs determine optimal hyperplanes to differentiate classes particularly useful in highly dimensional parameter space whilst TWDTWs are most effective at affiliating time series data when alignment of signals in terms of both speed and phase are crucial (see Maus et al., 2019). In contrast, RF techniques utilise a set of decision trees to classify time series data.

These studies were conducted across Mato Grasso and Bahia states, two major agricultural regions, utilising either a single vegetation index (EVI; Bendini et al., 2019) or a set of vegetation indices (EVI, NDVI) and reflectance bands (NIR, MIR supplemented by red and blue bands in Chaves et al., 2021) applied with logistic or smoothing functions prior to image classification. Double crop identification from TWDTW (Chaves et al., 2021), SVMs (Picoli et al., 2018) and RF (Bendini et al., 2019) algorithms generated accuracies between 89-93 %, 87-100 %, 93-99 %, respectively, all above the 85 % threshold deemed desirable (Foody 2002). Hence, through the adoption of deep learning techniques, the accuracy of double crop identification has increased dramatically.

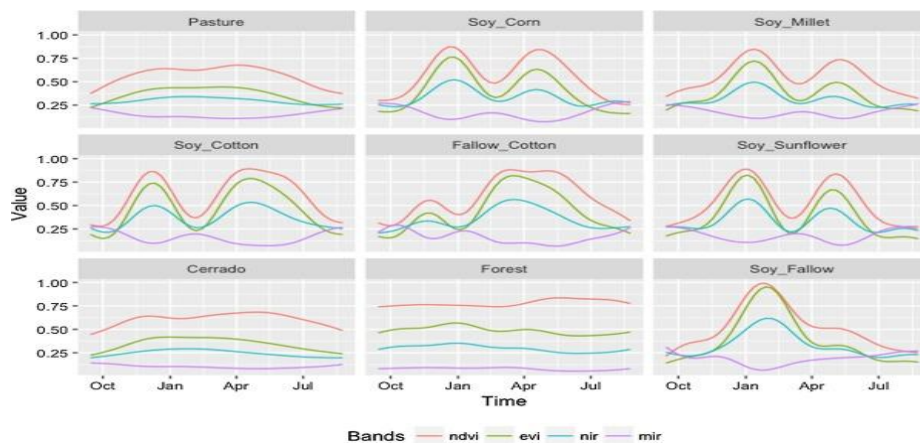


**Figure 3.5:** Estimated temporal patterns of NDVI, EVI, NIR and MIR bands for the selected land cover classes (taken from: Picoli et al., 2018).

With studies forming the basis of their training samples before 2016 through in-situ observations and interviews with local farmers (SVM:  $N_{\text{Total}} = 2115$ ,  $N_{\text{Double}} = 1173$ ; TWDTW:  $N_{\text{Total}} = 603$ ,  $N_{\text{Double}} = 603$ ; RF: currently unknown), this project using Sentinel-2 and its limit in scope to provide new in-situ sources may be required to rely upon the machine learning outputs generated to train the convolutional neural network (CNN) developed by KERMAP unless the LHS dataset is used (Câmara et al., 2020 SVM 2001-2019 outputs available at <https://doi.pangaea.de/10.1594/PANGAEA.911560>; LHS available <https://hls.gsfc.nasa.gov/> -- LP DAAC repository or via SITS R package).

CNN training samples (derived from in-situ observations or ML outputs) in this project covering the whole of Brazil are advised to be derived from a range of environmental backgrounds including climate, topography (test BRDF robustness) and soil genesis as they will impact crop growth patterns i.e., speed and amplitude of reflectance signals that may disrupt classification accuracy over large areas. This additionally may be a crucial validation stage to understand in which environments the CNN algorithm has a reduced capacity to differentiate different crop types and land practices. There may be some utility in also incorporating textural auxiliary information from the Sentinel Application Platform (SNAP) image processing software from ESA, albeit with consideration to not over-parameterise the CNN algorithm with correlated variables at the expense of computational cost (Sano et al., 2023). Nevertheless, the use of high-resolution imagery (10-30 m) here from Sentinel-2 or from HLS will provide greater coverage and temporal consistency due to the effect of increasing imaging resolution upon cloud-free pixels over Brazil in the wet season. Moreover, the higher resolution of the proposed sensor/harmonised sensors (HLS) will further provide unique insights into small-scale farming outside of the agricultural frontier where large farming monoculture practices are increasingly common. The analysis in EO4BK will hence build upon Sano et al., 2023 which deployed very high-resolution imagery over Goiatuba municipality (247 k ha<sup>-1</sup>) only classifying double cropping from bare soil (not double cropping) and Landsat derived double cropping using RF (Bendini et al., 2021). Whilst previous studies have focused on traditional VIs there also exists scope to use newer indices such as the Greenness and Water Content Composite Index (GWCCI) proven to be effective in mapping soybean in China (Chen et al., 2023).

The accuracy in the detection of single cropped land uses is expected to be greater than doubled cropped regions (Picoli et al., 2018) due to the similar biophysical and phenological characteristics of crops such as maize and millet over the 2<sup>nd</sup> season, however, accuracy is yet to be determined using CNNs. Further inaccuracies are introduced due to the variable timings of harvest of 1<sup>st</sup> season crops (soybean) depending on the 2<sup>nd</sup> season crop, impacting both time series duration and amplitude (Chaves et al., 2021). Double cropping databases will be required to be supplemented with the MapBiomas land cover datasets available between 1985-2023 (<https://brasil.mapbiomas.org/>) to provide examples of other single crop land uses such as coffee, palm oil, sugarcane and other crops not identified in Mato Grosso from Picoli et al. (2018) or Chaves et al. (2021). This Landsat derived dataset (30 m) primarily uses a RF algorithm within GEE to classify natural and anthropogenic land uses including the division between perennial/permanent crops, natural grassland/pasture and identification of land with a mosaic of uses proving highly useful in the detection land-use change in Brazil. Other land uses and practices such as aquaculture, irrigation, mining, rice, palm oil and citrus are additionally identified using a U-Net CNN with a 93 % global accuracy (MapBiomas, 2024) (see irrigation section describing U-Net CNN architecture and application in Brazil).

#### ● Key References:

- Federative Republic of Brazil. (2022, March 21). Paris Agreement: Nationally Determined Contribution (NDC). Brasília. Retrieved from <https://faolex.fao.org/docs/pdf/bra217881.pdf>.
- Xu, J., Gao, J., de Holanda, H. V., Rodríguez, L. F., Caixeta-Filho, J. V., Zhong, R., Jiang, H., Li, H., Du, Z., Wang, X., Wang, S., Ting, K. C., Ying, Y., & Lin, T. (2021). Double cropping and cropland expansion boost grain production in Brazil. *Nature Food*, 2(4), 264–273. <https://doi.org/10.1038/s43016-021-00255-3>.
- Reis, L., Santos e Silva, C. M., Bezerra, B., Mutti, P., Spyrides, M. H., Silva, P., Magalhães, T., Ferreira, R., Rodrigues, D., & Andrade, L. (2020). Influence of climate variability on soybean yield in MATOPIBA, Brazil. *Atmosphere*, 11(10), 1130. <https://doi.org/10.3390/atmos11101130>.
- Gibbs, H. K., Rausch, L., Munger, J., Schelly, I., Morton, D. C., Noojipady, P., Soares-Filho, B., Barreto, P., Micol, L., & Walker, N. F. (2015). Brazil's Soy Moratorium. *Science*, 347(6220), 377–378. <https://doi.org/10.1126/science.aaa0181>.
- Novaes, R. M. L., Pazianotto, R. A. A., Brandão, M., Alves, B. J. R., May, A., & Folegatti-Matsuura, M. I. S. (2017). Estimating 20-year land-use change and derived CO<sub>2</sub> emissions associated with crops,



pasture and forestry in Brazil and each of its 27 states. *Global Change Biology*, 23(9), 3716–3728.  
<https://doi.org/10.1111/gcb.13708>.

- Novaes, R. M. L., Tubiello, F. N., Garofalo, D. F. T., De Santis, G., Pazianotto, R. A. A., & Matsuura, M. D. S. (2022). Brazil's agricultural land, cropping frequency and second crop area: FAOSTAT statistics and new estimates. Embrapa. <http://www.infoteca.cnptia.embrapa.br/infoteca/handle/doc/1140492>.
- Picoli, M. C. A., Camara, G., Sanches, I., Simões, R., Carvalho, A., Maciel, A., Coutinho, A., Esquerdo, J., Antunes, J., Begotti, R. A., Arvor, D., & Almeida, C. (2018). Big earth observation time series analysis for monitoring Brazilian agriculture. *ISPRS Journal of Photogrammetry and Remote Sensing*, 145, 328–339. <https://doi.org/10.1016/j.isprsjprs.2018.08.007>.
- Câmara, G., Simoes, R., Picoli, M., Andrade, P. R., Rorato, A., Santos, L., Maciel, A., Sanches, I., Coutinho, A., Esquerdo, J., Antunes, J., Arvor, D., Begotti, R., Sanchez, A., Queiroz, G., & Ferreira, K. (2020). Land use and land cover maps for Amazon biome in Brazil for 2001-2019 derived from MODIS time series [dataset]. PANGAEA. <https://doi.org/10.1594/PANGAEA.911560>.
- Chaves, M. E. D., Alves, M. de C., Sáfyadi, T., de Oliveira, M. S., Picoli, M. C. A., Simoes, R. E. O., & Mataveli, G. A. V. (2021). Time-weighted dynamic time warping analysis for mapping interannual cropping practices changes in large-scale agro-industrial farms in Brazilian Cerrado. *Science of Remote Sensing*, 3, 100021. <https://doi.org/10.1016/j.srs.2021.100021>.
- Sano, E. E., Bolfe, É. L., Parreiras, T. C., Bettiol, G. M., Vicente, L. E., Sanches, I. D. A., & Victoria, D. C. (2023). Estimating double cropping plantations in the Brazilian Cerrado through PlanetScope monthly mosaics. *Land*, 12(3), 581. <https://doi.org/10.3390/land12030581>.
- Parreiras, T. C., Bolfe, É. L., Chaves, M. E. D., Del'Arco Sanches, I., Sano, E. E., Victoria, D. C., Bettiol, G. M., & Vicente, L. E. (2022). Hierarchical classification of soybean in the Brazilian savanna based on harmonized Landsat Sentinel data. *Remote Sensing*, 14(15), Article 3736. <https://doi.org/10.3390/rs14153736>.
- do Nascimento Bendini, H., Garcia Fonseca, L. M., Schwieder, M., Sehn Körting, T., Rufin, P., Del Arco Sanches, I., Leitão, P. J., & Hostert, P. (2019). Detailed agricultural land classification in the Brazilian Cerrado based on phenological information from dense satellite image time series. *International Journal of Applied Earth Observation and Geoinformation*, 82, 101872. <https://doi.org/10.1016/j.jag.2019.05.005>.
- Arvor, D., Jonathan, M., Meirelles, M. S. P., Dubreuil, V., & Durieux, L. (2011). Classification of MODIS EVI time series for crop mapping in the state of Mato Grosso, Brazil. *International Journal of Remote Sensing*, 32(22), 7847–7871. <https://doi.org/10.1080/01431161.2010.531783>.
- Brown, J. C., Kastens, J. H., Coutinho, A. C., Victoria, D. de C., & Bishop, C. R. (2013). Classifying multiyear agricultural land use data from Mato Grosso using time-series MODIS vegetation index data. *Remote Sensing of Environment*, 130, 39-50. <https://doi.org/10.1016/j.rse.2012.11.009>.
- Chen, Y., Lu, D., Moran, E., Batistella, M., Dutra, L. V., Sanches, I. D'A., da Silva, R. F. B., Huang, J., Luiz, A. J. B., & de Oliveira, M. A. F. (2018). Mapping croplands, cropping patterns, and crop types using MODIS time-series data. *International Journal of Applied Earth Observation and Geoinformation*, 69, 133–147. <https://doi.org/10.1016/j.jag.2018.03.005>.
- Chen, H., Li, H., Liu, Z., Zhang, C., Zhang, S., & Atkinson, P. M. (2023). A novel Greenness and Water Content Composite Index (GWCCI) for soybean mapping from single remotely sensed multispectral images. *Remote Sensing of Environment*, 295, Article 113679. <https://doi.org/10.1016/j.rse.2023.113679>.
- Galford, G. L., Mustard, J. F., Melillo, J., Gendrin, A., Cerri, C. C., & Cerri, C. E. P. (2008). Wavelet analysis of MODIS time series to detect expansion and intensification of row-crop agriculture in Brazil. *Remote Sensing of Environment*, 112(2), 576–587. <https://doi.org/10.1016/j.rse.2007.05.017>.

- Simoes, R., Picoli, M. C. A., Camara, G., Almeida, C. A., Esquerdo, J. C. D. M., Marris, G., & Adami, M. (2020). Land use and cover maps for Mato Grosso State in Brazil from 2001 to 2017. Scientific Data, 7, 34. <https://doi.org/10.1038/s41597-020-0371-4>.
- Maus, V., Câmara, G., Appel, M., & Pebesma, E. (2019). dtwSat: Time-Weighted Dynamic Time Warping for Satellite Image Time Series Analysis in R. Journal of Statistical Software, 88(5), 1–31. <https://doi.org/10.18637/jss.v088.i05>.
- Foody, G. M. (2002). Status of land cover classification accuracy assessment. Remote Sensing of Environment, 80(1), 185-201. [https://doi.org/10.1016/S0034-4257\(01\)00295-4](https://doi.org/10.1016/S0034-4257(01)00295-4).
- MapBiomass. (2024). MapBiomass General “Handbook” Algorithm Theoretical Basis Document (ATBD) Collection 9 Version 1. Retrieved from <https://brasil.mapbiomas.org/en/atbd-entenda-cada-etapa/>.

### 3.5.6. Irrigation in Europe

For this project, **we propose to explore a methodology based on the work of Pageot et al. (2020). It will rely on the use of S1, S2 and rainfall data, compared to LUCAS 2022 reference dataset, to detect irrigation in Europe.**

Irrigation is an important component of agriculture in Europe. With 40 % of total water used per year, the agricultural sector is the largest consumer of freshwater in Europe (**Figure 3.6**). The repartition of the water consumption for irrigation varies, depending on factors such as climate, water availability and traditional cropping systems. In central and northern Europe, rainfalls generally provide an adequate quantity of water for crop growth and irrigation is used to improve yield, especially for crops that require a lot of water to grow synch as maize. In southern Europe, with a Mediterranean climate characterised by hot and warm dry summers (Chen et al., 2013), an irrigation process is needed to maintain agricultural productivity. Spain has the largest irrigated area in Europe with a total of 29.9 % of the total irrigated surfaces (**Figure 3.7**), followed by Italy (24.6 %), France (13.3 %), Greece (10.4 %), Portugal (4.6 %) and Germany (4.4 %). The other European countries share 13 % of remaining global irrigated areas. Irrigation systems also differ between countries, mostly due to variation in crop type and cultivation practices. Generally speaking, sprinkler irrigation is the most commonly used system in northern Europe, but ground irrigation is also employed for orchard cultivation in the south of France for instance. Climate change is posing a serious threat to the agricultural sector. According to the water exploitation index plus (WEI+) developed by the European Environment Agency (EEA), water consumption has exceeded the resource’s renewal capacity, in more than 20 % of the areas of Europe since the early 2000s, reaching 29 % during the most recent survey in 2019 (**Figure 3.8**). It is expected that drought events will be more frequent and intense, making irrigation a major challenge for the agricultural sector in the coming years.

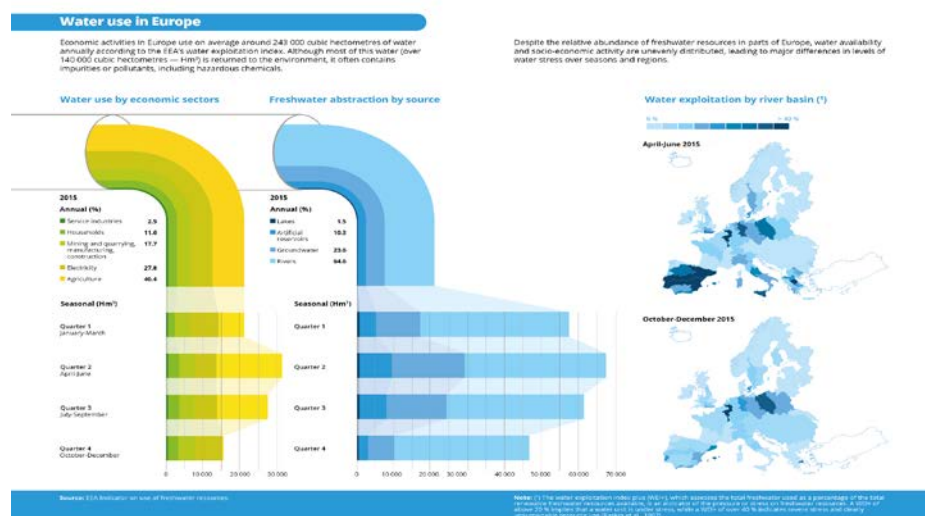


**Figure 3.6:** Repartition of freshwater use in Europe per economic sector and sources in Europe (Source : EEA).

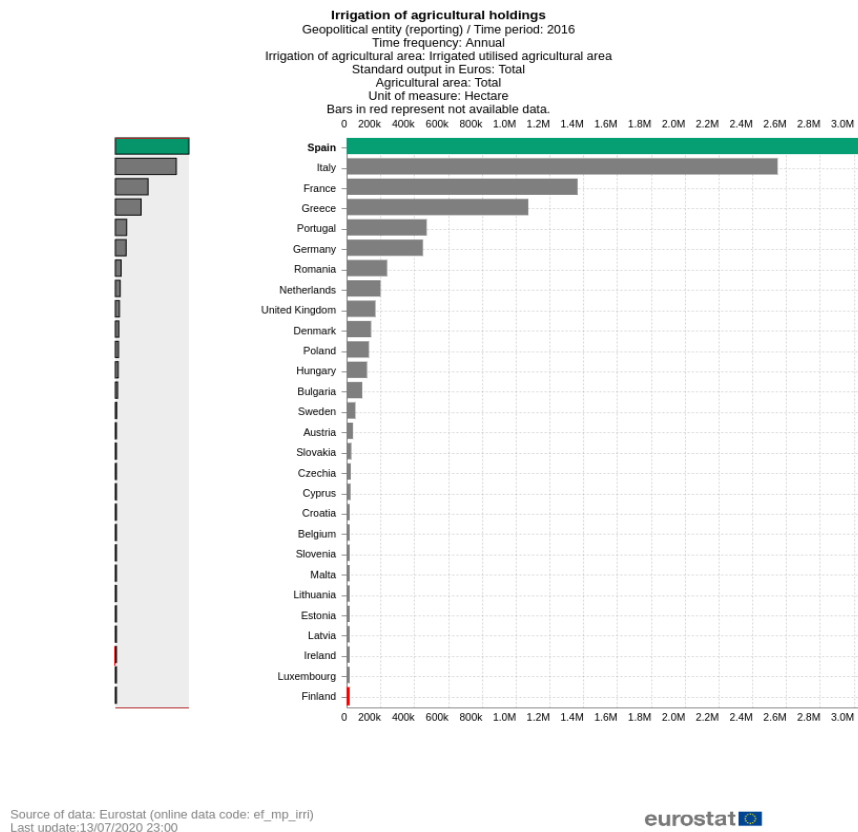


**Figure 3.7:** Graphic representation of the total surface of irrigated areas per country in 2016.

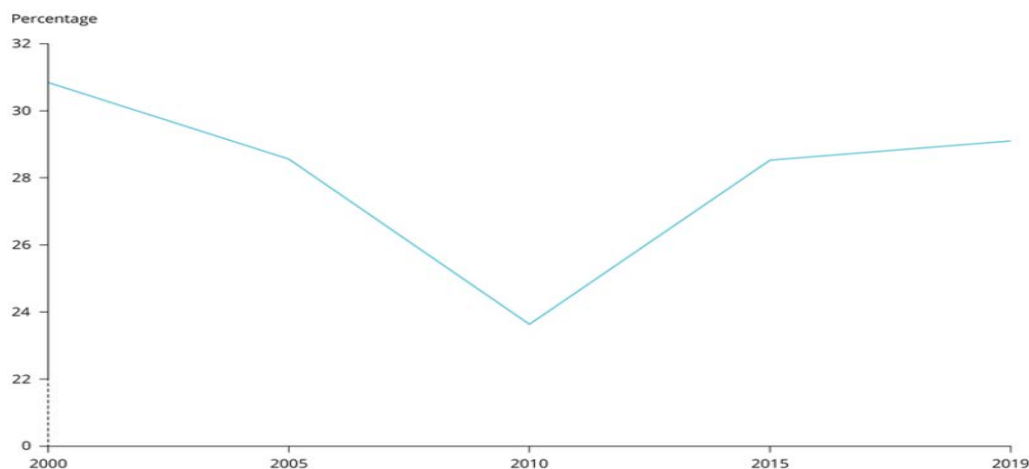


**Figure 3.8:** Evolution of percentage of European countries where the water consumption exceeded the resource's renewal capacity from 2000 to 2019.

The **LUCAS 2022** dataset used in the project provides in-situ information about water management ('survey\_wm') in agricultural parcels all over the European Union (Figure 3.9). Data for water management has been collected for places where land use is identified as agriculture or fallow land or if the grassland module has been assessed. This data typically includes whether irrigation was present at the time of collection, and if so, details on the type of irrigation, its source, and the delivery system. Out of 78,473 parcels where irrigation data was gathered, 62,458 parcels (80 %) showed no visible water management during the survey (Table 3.2). However, as the data was collected on a single date, it cannot definitively confirm whether irrigation occurred at other times or not. Another 1,587 field plots were collected with no certainty that the crop was actually irrigated. Finally, 2,546 field plots (3 %) were recorded as irrigated with proof of irrigation such as ground photos. These points are mostly located in Spain, Italy and Greece, but also in France and Portugal (Figure 3.10).

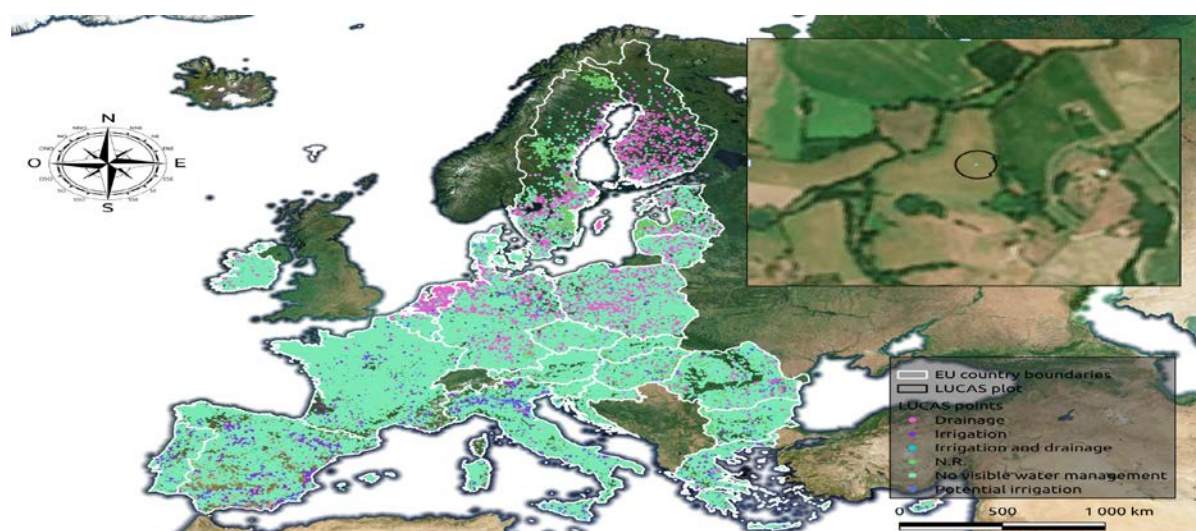


**Figure 3.9:** Repartition of LUCAS 2022 ground data over the European Union and spatialisation of a ground plot.

survey_wm	counts
Drainage	8 541
Irrigation	2 546
Irrigation and drainage	146
N.R.	3 192
No visible water management	62 458
Potential irrigation	1 587

**Table 3.2:** Total count of water management types over the European Union.



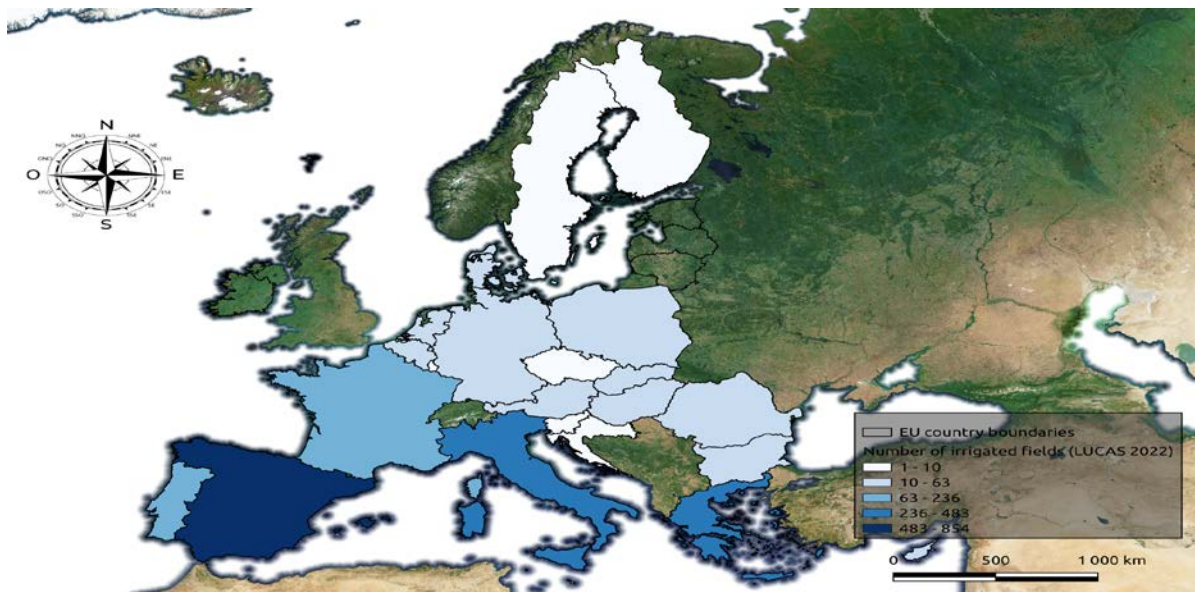


**Figure 3.10:** Total count of irrigated parcels by country in the European Union (source : LUCAS 2022)

In France, for instance, research work has demonstrated the interest of EO to monitor irrigation practices. The French centre of spatial studies for biosphere (CESBIO) developed a classification method based on machine learning combining Sentinel-1 and Sentinel-2 data (Pageot et al., 2020). The research unit TETIS proposes a method combining radar data and rainfall information, which does not require ground observations (Bazzi et al., 2019). The research unit EMMAH developed methods based on the use of points characterising the temporal profiles of crops and achieved high performance on irrigated grasslands to distinguish orchards from vineyards (Abubakar et al., 2022, Abubakar et al., 2023). However, there is no relevant open-source data on irrigation at the parcel level due to the sensitivity of the information. The BNPE (Base Nationale des Prélèvements en Eau) in France collects and reports water abstractions at the municipality level by various users, including agriculture.

#### ● Key References:

- Pageot, Y., Baup, F., Inglada, J., Baghdadi, N., & Demarez, V. (2020). Detection of irrigated and rainfed crops in temperate areas using Sentinel-1 and Sentinel-2 time series. *Remote Sensing*, 12(18), Article 3044. <https://doi.org/10.3390/rs12183044>.
- Bazzi, H., Baghdadi, N., Ienco, D., El Hajj, M., Zribi, M., Belhouchette, H., Escorihuela, M. J., & Demarez, V. (2019). Mapping irrigated areas using Sentinel-1 time series in Catalonia, Spain. *Remote Sensing*, 11(15), Article 1836. <https://doi.org/10.3390/rs11151836>.
- Abubakar, S., Mukhtar, M., Chanzy, A., Pouget, G., Flamain, F., & Courault, D. (2022). Detection of irrigated permanent grasslands with Sentinel-2 based on temporal patterns of the leaf area index (LAI). *Remote Sensing*, 14(13), Article 3056. <https://doi.org/10.3390/rs14133056>.
- Abubakar, S., Mukhtar Adamu, M., Chanzy, A., Flamain, F., Pouget, G., & Courault, D. (2023). Delineation of orchard, vineyard, and olive trees based on phenology metrics derived from time series of Sentinel-2. *Remote Sensing*, 15(9), Article 2420. <https://doi.org/10.3390/rs15092420>.

#### 3.5.7. Irrigation in Brazil

To quantify irrigation in Brazil, namely CPICs and irrigation farming, **we propose to use a U-Net CNN procedure similar to Lui et al., 2023 outlined in Section 3.1 with Sentinel-1 and -2 imagery.** Despite the phenological signals from rice identifiable through tempCNN's, the specialised use of CNNs to increase spatial information

extraction which should prove to be more accurate. Strict quality control will need to be in place to limit the misclassification of other land use formations of a similar shape (**Figure 3.13**) such as cross validation with agricultural land uses or identification of phenological signals (single or double cropped).

From 1985 to 2021 the area of centre pivot irrigated cropland (CPIC) has quadrupled in Brazil reaching  $1.8 \times 10^6$  ha (2021) (Lui et al., 2023) in order to preserve water security and crop yields due to increased pressure from climate variability (MapBiomias, 2024). Estimates suggest that 76 % of these centre pivot farms situated primarily in Minas Gerais, Goiás and Bahia states are used to produce soybeans and have the secondary advantage of being able to produce double cropping cycles in the Cerrado region where precipitation cycles are shorter. Flooding irrigation, associated with rice farming, now represents only 44 % (2021) of total irrigated agricultural land located mainly in southern Brazil whilst some states such as Tocantins have experienced increasing flood irrigation practices since 1985. Despite CPIC proving useful in increasing crop yields to support growing a global population, concerns have been raised about its possible interference with the reduction of deforestation in public policy (Gibbs et al., 2010) and groundwater supply mismanagement (Spera et al., 2016).

CPICs and flood irrigated land for rice cropping across Brazil is currently being monitored at 30m resolution by Landsat with data distributed by MapBiomias (available at: <https://mapbiomas.org/>) using U-Net convolutional neural networks (CNNs). CNNs are deployed in the detection over random forest (RF) as used for other land use identification due to their performance in regional analysis of tropical tree type (Braga et al., 2020, Wagner et al., 2019; Wagner et al., 2020), large scale mapping works (Brandt et al., 2020; Sirko et al., 2021) and previous CPIC delineation (de Albuquerque et al. 2020). The U-net architecture of this deep learning (DL) method allows for a good ability to predict new data using skipped connections. It is also highly robust to noise in input data with an asymmetric structure, provides better performances than ML due to its capacity to identify textures and shapes in multi-dimensional data (Kussul et al., 2017; Zhong et al., 2019), and can learn both high-level semantic information and low-level detail in a very memory-efficient way (Bem et al., 2021) (**Figure 3.11**).

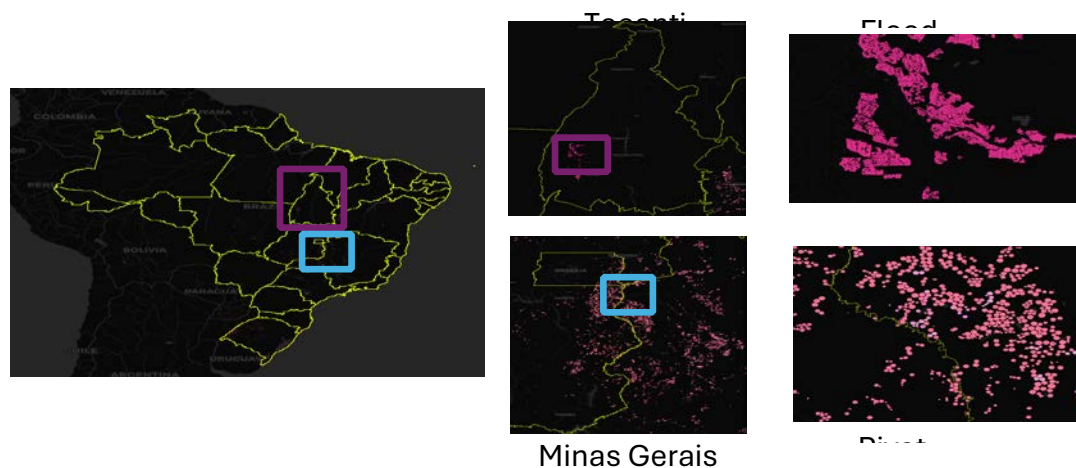


**Figure 3.11:** Flood and pivot irrigation practises across 2 Brazilian states. Maps at different scales. Images/screenshots taken from MapBiomias interactive maps (<https://plataforma.brasil.mapbiomas.org/>).

U-Net training samples for CPICs are collected from bi-decadal censuses distributed by Brazilian ANA in 1985, 1990, 2000, 2005, 2010, 2014, 2017, and 2019 (available at: <https://www.gov.br/ana/en/monitoring>) with issues from unbalanced data between CPIC and non-CPIC land cover resolved via Tversky loss functions. To reduce the computational cost of the CNN, initial tests indicated that 3 parameters derived from Landsat ( $EVI_{max}$ ,  $BSI_{max}$  and  $Green_{median}$ ) were the most important indicators of CPICs. Post U-Net training final temporal filtering (Li et al., 2015) was then necessitated to ensure a consistent identification of CPICs loss and gain distribution



using a probability of consistency function and a lower threshold of 0.5. This methodology yielded an average precision of CPIC detection between 1985-2021 of  $0.996 (\pm 0.005)$  and the final production of a model that can be applied to future years without retaining (Figure 3.12). However, MapBiomass delineations of CPIC remain affected by misclassification, albeit rare, where natural vegetation and anthropogenic modified landscapes such as pasture are in a circular pattern (**Figures 3.12 and 3.13**) (Sano et al., 2024). Hence, temporal CNNs may be better equipped to limit these misclassifications as temporal signals from crops are different from these vegetation types.

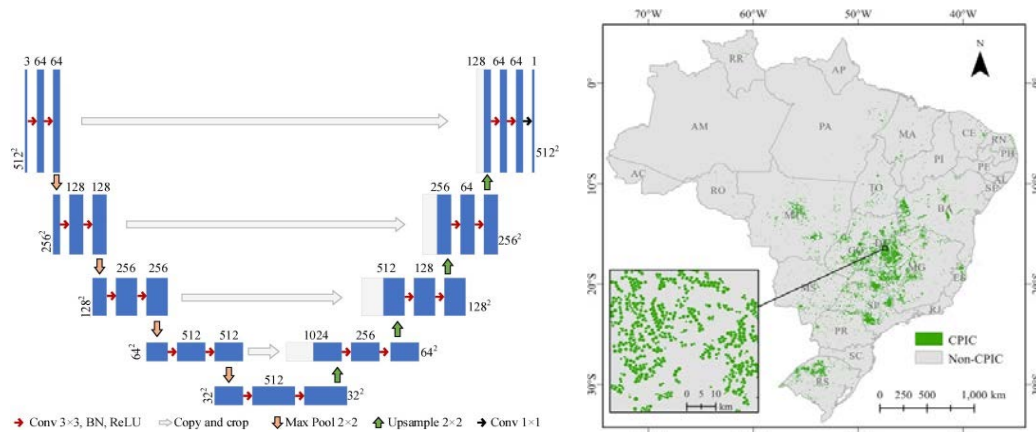


**Figure 3.12:** Architecture of U-Net Convolutional Neural Network (CNN) on LHS and distribution of CPICs in Brazil during 2021 on RHS (taken from Lui et al., 2023)

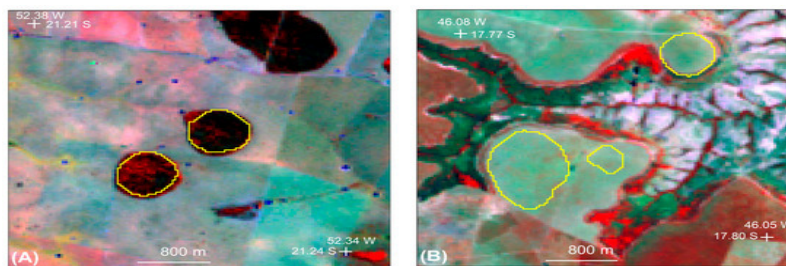


**Figure 3.13:** Misclassification of CPIC by MapBiomass. LHS natural vegetation and RHS Pasture (taken from Sano et al., 2024)

Identification of rice farming in Brazil is additionally feasible through the deployment of CNNs (Bem et al., 2021) whilst also evidenced as possible through decision tree (DT) classifiers (Nguyen et al., 2016), rule-based classifiers (Nelson et al., 2014), Random Forest (RF) (Lasko et al., 2018), and Support Vector Machines (SVM) techniques (Minh et al., 2019). The DL techniques in CNNs should, however, provide better results than other ML methods due to their textural and spatial pattern identification of homogeneous morphology of rice fields and irrigation channels of the terraces. However, with some agronomic farming only lasting 1-2 months detection using optical sensors remains difficult in the tropics.

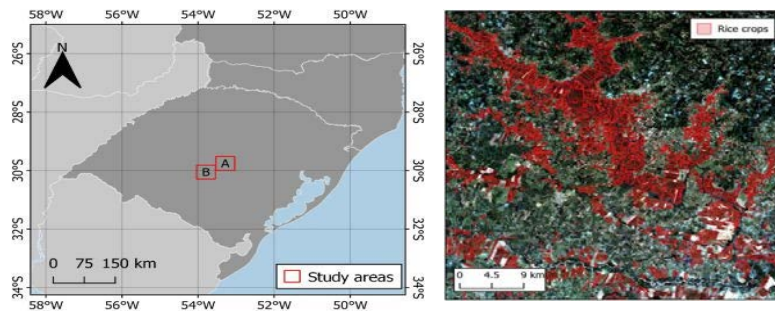


**Figure 3.14:** Location of the (A) training and (B) test sites in the state of Rio Grande do Sul (LHS) and round truth map for the training area over a true colour SENTINEL-2 image (RHS) (taken from Ben et al., 2021)

Training data for irrigated rice crops can be obtained from the Brazilian National Supply Company (available at <https://www.conab.gov.br/info-agro/safras>) which is produced through visual interpretation by experts using the distinctive spectral and spatial patterns of rice farms between August 2019 and May 2020 (**Figure 3.13**). Multiple U-Net models were subsequently produced using different band combinations (VV-only, VH-only, and VV + VH). and U-Net backbones resulting in 24 combinations in which images were applied with random horizontal and vertical flip augmentation to increase sample numbers and reduce overfitting. The best-performing model was using the LinkNet architecture and ResNeXt modules trained with the VH + VV dataset yielded accuracy, values of 0.98 and 0.93, respectively, in line with other studies globally using such methodologies with Sentinel2 datasets (**Figures 3.14 and 3.15**). U-Net CNNs, as used by KERMAP, are hence proven tools to identify both CPICs and rice agriculture in Brazil and will be well adapted for use in this project.

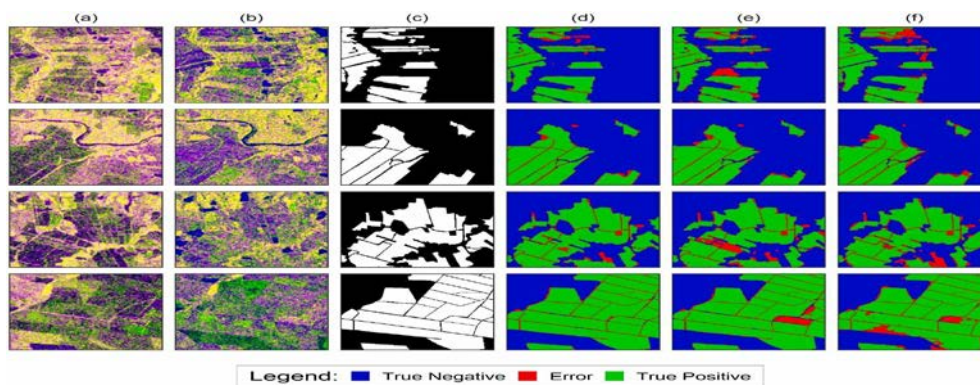


**Figure 3.15:** Spatial distribution of rice crop identification using a U-Net CNN (taken from Bem et al., 2021).

#### ● Key References:

- Liu, X., He, W., Liu, W., Yin, G., & Zhang, H. (2023). Mapping annual center-pivot irrigated cropland in Brazil during the 1985–2021 period with cloud platforms and deep learning. *ISPRS Journal of Photogrammetry and Remote Sensing*, 205, 227–245. <https://doi.org/10.1016/j.isprsjprs.2023.10.007>.
- MapBiomass. (2024). MapBiomass General “Handbook” Algorithm Theoretical Basis Document (ATBD) Collection 9 Version 1. Retrieved from <https://brasil.mapbiomas.org/en/atbd-entenda-cada-etapa/>.
- Gibbs, H. K., Ruesch, A. S., Achard, F., Clayton, M. K., Holmgren, P., Ramankutty, N., & Foley, J. A. (2010). Tropical forests were the primary sources of new agricultural land in the 1980s and 1990s. *Proceedings of the National Academy of Sciences*, 107(38), 16732–16737. <https://doi.org/10.1073/pnas.0910275107>.

- Spera, S. A., Galford, G. L., Coe, M. T., Macedo, M. N., & Mustard, J. F. (2016). Land-use change affects water recycling in Brazil's last agricultural frontier. *Global Change Biology*, 22(10), 3405–3413. <https://doi.org/10.1111/gcb.13298>.
- Braga, J. R., Peripato, V., Dalagnol, R., Ferreira, M. P., Tarabalka, Y., Aragão, L. E. O. C., Velho, H. F. de C., Shiguemori, E. H., & Wagner, F. H. (2020). Tree crown delineation algorithm based on a convolutional neural network. *Remote Sensing*, 12(8), 1288. <https://doi.org/10.3390/rs12081288>.
- Wagner, F. H., Sanchez, A., Tarabalka, Y., Lotte, R. G., Ferreira, M. P., Aidar, M. P. M., Gloor, E., Phillips, O. L., & Aragão, L. E. O. C. (2019). Using the U-net convolutional network to map forest types and disturbance in the Atlantic rainforest with very high resolution images. *Remote Sensing in Ecology and Conservation*, 5(4), 360–375. <https://doi.org/10.1002/rse2.111>.
- Wagner, F. H., Dalagnol, R., Tagle Casapia, X., Streher, A. S., Phillips, O. L., Gloor, E., & Aragão, L. E. O. C. (2020). Regional mapping and spatial distribution analysis of canopy palms in an Amazon forest using deep learning and VHR images. *Remote Sensing*, 12(14), 2225. <https://doi.org/10.3390/rs12142225>.
- Brandt, M., Tucker, C. J., Kariryaa, A., Rasmussen, K., Abel, C., Small, J., Chave, J., Rasmussen, L. V., Hiernaux, P., Diouf, A. A., Kergoat, L., Mertz, O., Igel, C., Gieseke, F., Schöning, J., Li, S., Melocik, K., Meyer, J., Sinno, S., Romero, E., Glennie, E., Montagu, A., Dendoncker, M., & Fensholt, R. (2020). An unexpectedly large count of trees in the West African Sahara and Sahel. *Nature*, 587(7832), 78–82. <https://doi.org/10.1038/s41586-020-2824-5>.
- Sirko, W., Kashubin, S., Ritter, M., Annkah, A., Bouchareb, Y. S. E., Dauphin, Y. N., Keysers, D., Neumann, M., Cissé, M., & Quinn, J. (2021). Continental-scale building detection from high resolution satellite imagery. *arXiv*. <https://doi.org/10.48550/arXiv.2107.12283>.
- de Albuquerque, A. O., de Carvalho Júnior, O. A., Ferreira de Carvalho, O. L., Pozzobon de Bem, P., Guimarães Ferreira, P. H., dos Santos de Moura, R., Rosa Silva, C., Trancoso Gomes, R. A., & Guimarães, R. F. (2020). Deep semantic segmentation of center pivot irrigation systems from remotely sensed data. *Remote Sensing*, 12(13), 2159. <https://doi.org/10.3390/rs12132159>.
- Kussul, N., Lavreniuk, M., Skakun, S., & Shelestov, A. (2017). Deep learning classification of land cover and crop types using remote sensing data. *IEEE Geoscience and Remote Sensing Letters*, 14(5), 778–782. <https://doi.org/10.1109/LGRS.2017.2681128>.
- Zhong, L., Hu, L., & Zhou, H. (2019). Deep learning based multi-temporal crop classification. *Remote Sensing of Environment*, 221, 430–443. <https://doi.org/10.1016/j.rse.2018.11.032>.
- Pozzobon de Bem, P., de Carvalho Júnior, O. A., de Carvalho, O. L. F., Gomes, R. A. T., Guimarães, R. F., & Pimentel, C. M. M. (2021). Irrigated rice crop identification in Southern Brazil using convolutional neural networks and Sentinel-1 time series. *Remote Sensing Applications: Society and Environment*, 24, 100627. <https://doi.org/10.1016/j.rsase.2021.100627>.
- Sano, E. E., Magalhães, I. A. L., Rodrigues, L. N., & Bolfe, É. L. (2024). Spatio-temporal dynamics of center pivot irrigation systems in the Brazilian tropical savanna (1985–2020). *Water*, 16(13), 1897. <https://doi.org/10.3390/w16131897>.
- Nguyen, D. B., Gruber, A., & Wagner, W. (2016). Mapping rice extent and cropping scheme in the Mekong Delta using Sentinel-1A data. *Remote Sensing Letters*, 7(12), 1209–1218. <https://doi.org/10.1080/2150704x.2016.1225172>.
- Nelson, A., Setiyono, T., Rala, A. B., Quicho, E. D., Raviz, J. V., Abonete, P. J., Maunahan, A. A., Garcia, C. A., Bhatti, H. Z. M., Villano, L. S., & et al. (2014). Towards an operational SAR-based rice monitoring system in Asia: Examples from 13 demonstration sites across Asia in the RIICE project. *Remote Sensing*, 6(11), 10773–10812. <https://doi.org/10.3390/rs61110773>.
- Lasko, K., Vadrevu, K. P., Tran, V. T., & Justice, C. (2018). Mapping double and single crop paddy rice with Sentinel-1A at varying spatial scales and polarizations in Hanoi, Vietnam. *IEEE Journal of Selected*

Topics in Applied Earth Observations and Remote Sensing, 11(2), 498-512.

<https://doi.org/10.1109/JSTARS.2017.2784784>.

- o Minh, H. V. T., Avtar, R., Mohan, G., Misra, P., & Kurasaki, M. (2019). Monitoring and mapping of rice cropping pattern in flooding area in the Vietnamese Mekong Delta using Sentinel-1A data: A case of An Giang Province. ISPRS International Journal of Geo-Information, 8(5), 211.  
<https://doi.org/10.3390/ijgi8050211>.

## 4. Definition of performances metrics for crop types and cultivation practices maps & existing reference maps as input to WP3

### 4.1. Performance metrics upon which the proposed methods and EO datasets produced in the project will be benchmarked.

Typical benchmark metrics involve the knowledge of site data or the use of another reference map of crop types and management practices. Classical metrics are listed below. Computational Efficiency should also be considered as an overall algorithm performance metrics and depends on algorithm complexity and dataset size. We propose to use the following metrics in the EO4BK project (**Table 4.1**).

<b>Accuracy</b>	Overall correctness of classification
<b>Precision and Recall</b>	Specific to individual crop types, important for imbalance in crop area distributions.
<b>F1-Score</b>	Harmonic means of precision and recall.

**Table 4.1.** Metrics used to evaluate EO4BK datasets against reference data


### 4.2 Reference crop types maps / datasets upon which the results of the methods proposed in section 3 can be benchmarked.

As EO based crop types and cultivation practices classification methods are expected to provide spatially and temporally explicit estimates of crop types and cultivation practices, evaluation of those maps against independent datasets is challenging, as independent data are not available at field scale. We identified the **following datasets to benchmark the maps that will be produced in the project**: reference EO-based maps of crop types, national agricultural statistics at the scale of specific administrative units based on surveys

#### 4.2.1 Reference EO and in-situ crop type maps in Europe planned for validation

In EO4BK, we will focus primarily for Europe on reference validation data from the Land Use/Cover Area frame Survey (LUCAS) Copernicus database (d'Andrimont et al., 2021). The new LUCAS module specifically tailored to Earth Observation and was introduced in 2018: the LUCAS Copernicus module, aiming at surveying land cover extent up to 51 meters in four cardinal directions around a point of observation. The new dataset is designed to ensure comparability between the surveyed area and remote-sensing observation (e.g. homogeneous land cover) and includes a total of 58,428 polygons with 66 land cover classes, including crop type and including crop type, and 38 land use classes (e.g., agriculture), and surveys on water management (e.g., type of irrigation, water source and delivery system). Given the expected high quality of this data, EO4BK will use LUCAS Copernicus as the reference database for Europe. For the project, we will use in priority the LUCAS Copernicus module and ICOS data and in the second phase we will extend to additional data from national statistics (EuroCrop) and datasets published in the literature, such as those of Su et al., Belgiu et al. (2018), Inglada et al. (2017) and Van Tricht et al. (2023). In some countries of the EU, field level data with farmers



Deliverable no. D1.1 Requirements Baseline (RB) document	ESA Carbon-RO, EO4BK Contract no. 4000144916/24/I-EF	 International Institute for Applied Systems Analysis IIASA www.iiasa.ac.at
--	---	--

report on practices and cultivation types used for the evaluation of the Common Agricultural Policy. Although all countries maintain such information systems based on self-reported data by each farm, the data are usually not available. One exception is France where the RPG (<https://www.data.gouv.fr/fr/datasets/registre-parcellaire-graphique-rpg-contours-des-parcelles-et-ilots-cultureaux-et-leur-groupe-de-cultures-majoritaire/>) is a field based GIS register of farmers reports at the level of individual fields which can be accessed for research purposes with some restrictions such as data anonymization. This data could be supplemented with other datasets e.g. from NL with support of the EO4CSM project. Such Land Parcel Identification System (LPIS) data with parcel-level detailed crop type information is available for several EU countries as listed below. Below is a list of practice datasets that can be used for model evaluation in Europe.

### 1. WorldCereal

- Description : Global maps of temporary crops, crop type (maize, winter cereals and spring cereals) and irrigation for the year 2021, at 10 m resolution. The globe is stratified into agro-ecological zones to handle the various agricultural seasons. The map of the temporary crops does not propose a distinction of the crops.
- Reference : Van Tricht, K., Degerickx, J., Gilliams, S., Zanaga, D., Battude, M., Grosu, A., Brombacher, J., Lesiv, M., Bayas, J. C. L., Karanam, S., Fritz, S., Becker-Reshef, I., Franch, B., Mollà-Bononad, B., Boogaard, H., Pratihast, A. K., and Szantoi, Z. (2023). WorldCereal: a dynamic open-source system for global-scale, seasonal, and reproducible crop and irrigation mapping, *Earth Syst. Sci. Data Discuss.* <https://doi.org/10.5194/essd-2023-184>.

### 2. Theia OSO Land Cover Map

- Description : Land cover maps for France produced automatically from Sentinel-2 data with a Random Forest-based method, at 10m resolution. The annual maps since 2018 follow a 23-classes nomenclature, including 10 crop types : Straw cereals, Winter oilseeds, Spring oilseeds, Soy, Sunflower, Corn, Rice, Tubers and roots, Grasslands, Orchards and Vineyards.
- Reference : Inglada, J., Vincent, A., Arias, M., Tardy, B., Morin, D., & Rodes, I., Operational high resolution land cover map production at the country scale using satellite image time series, *Remote Sensing*, 9(1), 95 (2017). <http://dx.doi.org/10.3390/rs9010095>

### 3. EuroCrops

- Reference: <https://ec.europa.eu/eurostat/data/database>, <https://agri4cast.jrc.ec.europa.eu/DataPortal/>.

### 4. Sentinel-2 cropland mapping


- Description : Pixel-based and object-based time-weighted dynamic time warping analysis for cropland mapping with Sentinel-2 data.
- Reference: Belgiu, M., & Csillik, O. (2018). Sentinel-2 cropland mapping using pixel-based and object-based time-weighted dynamic time warping analysis. *Remote sensing of environment*, 204, 509-523. <https://doi.org/10.1016/j.rse.2017.10.005>.
- Produced maps : not found
- Training/validation data : LUCAS data in Romania and Italy (see LUCAS section below)  
CropScape Cropland Data Layer (CDL) 2016 in California (only for USA)

### 5. Crop field boundaries Waldner et al.

- Description: The data apply deep learning and convolutional neural networks for extracting field boundaries in Europe using Sentinel-2 imagery.
- Reference: Waldner, F., & Diakogiannis, F. I. (2020). Deep learning on edge: Extracting field boundaries from satellite images with a convolutional neural network. *Remote Sensing of Environment*, 245, 111741. <https://doi.org/10.1016/j.rse.2020.111741>.
- About field delimitation only, no crop type identification
- Training/validation data : manually digitised fields, no crop type information
- Produced maps : not found

### 6. Crop field boundaries: AI4Boundaries



Deliverable no. D1.1 Requirements Baseline (RB) document	ESA Carbon-RO, EO4BK Contract no. 4000144916/24/I-EF	 International Institute for Applied Systems Analysis IIASA www.iiasa.ac.at
--	---	--

- Description: The AI4Boundaries data set provides a statistical sampling of agricultural parcel boundaries over key regions of Europe along with 10 m Sentinel-2 satellite time series and 1 m aerial orthophoto imagery. This unique data set allows to benchmark and compare parcel delineation methodologies in a transparent and reproducible way.
- Field delimitation only, no crop type information
- <https://github.com/waldnerf/ai4boundaries>

#### 7. LPIS - Austria

- Available from 2018 to 2023 as geopackage format for all Austria : <https://data.europa.eu/data/datasets?locale=en>

#### 8. LPIS - Belgium

- Available from 2018 to 2022 as geopackage format for all Belgium : <https://data.europa.eu/data/datasets?locale=en>

#### 9. LPIS - France

- Available from 2007 to 2023 as geopackage format for all France : <https://geoservices.ign.fr/-RPG>

#### 10. LPIS - Netherlands

- Available from 2018 to 2022 as geopackage format for all Netherlands : <https://www.nationaalgeoregister.nl/geonetwork/srv/dut/catalog.search#/home>

#### 11. LPIS - Portugal

- Available from 2018 to 2022 as geopackage format for all Portugal : <https://www.ifap.pt/portal/isip>

#### 12. LPIS - Slovenia

- Available from 2019 to 2023 as geopackage format for all Slovenia : <https://rkg.gov.si/vstop/>

#### 13. EuroCrops

- Available for several years, according to the country:
- <https://www.eurocrops.tum.de/index.html>

#### ● Key References:


- d'Andrimont, R., Verhegghen, A., Lemoine, G., Kempeneers, P., Meroni, M., & van der Velde, M. (2021). From parcel to continental scale – A first European crop type map based on Sentinel-1 and LUCAS Copernicus in-situ observations. *Remote Sensing of Environment*, 266, 112708. <https://doi.org/10.1016/j.rse.2021.112708>.

### 4.2.2. Reference EO and in-situ crop types maps in Brazil

Among all the datasets listed below, for the project, we will use in priority for crop types evaluation Dataset from **MapBiomias** and in the second phase Datasets from **CONAB** and **USDA**

#### 1. MapBiomias

- Single cropping area and irrigation practises between 1985-2023
- Description: Derived from in-situ observations which are currently unidentified but 75,000 are used between 1985-2022. In-situ data for model training is from an unknown source (possibly available via <https://github.com/mapbiomas/.github/blob/main/assets/brazil.md>)
- Derived from 75,000 in-situ observations which are currently not distributed
- Produced maps <https://plataforma.brasil.mapbiomas.orghttps://brasil.mapbiomas.org/en>.

Deliverable no. D1.1 Requirements Baseline (RB) document	ESA Carbon-RO, EO4BK Contract no. 4000144916/24/I-EF	 International Institute for Applied Systems Analysis IIASA www.iiasa.ac.at
--	---	--

## 2. CONAB

- Description: Field borders derived from in-situ observations and interpretation of phenological signals from expert technicians of crop type.
- Majority of crop type data available between 2015 and 2023.
- Available at: <https://www.conab.gov.br/>

## 3. USDA

- Crop production per municipality
- [https://ipad.fas.usda.gov/cropeplorer/cropview/comm\\_chartview.aspx?ftypeid=47&fattributionid=1&fctyid=47&fcattributionid=1&regionid=br&cntryid=BRA&cropid=0422110&nationalgraph=False&sel\\_year=2021&startrow=1#](https://ipad.fas.usda.gov/cropeplorer/cropview/comm_chartview.aspx?ftypeid=47&fattributionid=1&fctyid=47&fcattributionid=1&regionid=br&cntryid=BRA&cropid=0422110&nationalgraph=False&sel_year=2021&startrow=1#)

## 4. Double cropping from Campo verde database

- Description: Double cropping maps produced by Bendini et al., 2019.
- Produced maps :<https://iee-dataport.org/documents/campo-verde-database> SITS R package. In this package there are in-situ observations used in Picoli et al., 2019. <https://github.com/e-sensing/sits>. More information on: <https://github.com/e-sensing/sitsdata/blob/main/README.md>. All rds available at <https://github.com/e-sensing/sitsdata/tree/main/data>.
- Reference: do Nascimento Bendini, H., Garcia Fonseca, L. M., Schwieder, M., Sehn Körting, T., Rufin, P., Del Arco Sanches, I., Leitão, P. J., & Hostert, P. (2019). Detailed agricultural land classification in the Brazilian Cerrado based on phenological information from dense satellite image time series. International Journal of Applied Earth Observation and Geoinformation, 82, 101872. <https://doi.org/10.1016/j.jag.2019.05.005>.

## 5. Sugarcane TempCNN

- Description: While this study primarily uses MODIS data, it provides foundational methods and context for subsequent Sentinel-based research in Brazil.
- Reference: Xavier, A. C., Ruddofo, B. F. T., Shimabukuro, Y. E., Berka, L. M. S., & Moreira, M. A. (2006). Multi-temporal analysis of MODIS data to classify sugarcane crop. International Journal of Remote Sensing, 27(4), 755-768. <https://doi.org/10.1080/01431160500296735>.
- Training/validation data: sugarcane and non-sugarcane samples from visual interpretation and in-situ observation
- Produced maps: not found

## 6. Double cropping in Brazil from 2001-2019 using MODIS

- Description: Dataset extension from Câmara et al., 2020. Both in-situ data (rds) and application of model Description: DI (raster)
- Produced maps : <https://doi.pangaea.de/10.1594/PANGAEA.911560>.
- Reference: Câmara, G., Simoes, R., Picoli, M., Andrade, P. R., Rorato, A., Santos, L., Maciel, A., Sanches, I., Coutinho, A., Esquerdo, J., Antunes, J., Arvor, D., Begotti, R., Sanchez, A., Queiroz, G., & Ferreira, K. (2020). Land use and land cover maps for Amazon biome in Brazil for 2001-2019 derived from MODIS time series [dataset]. PANGAEA. <https://doi.org/10.1594/PANGAEA.911560>.

## 7. Maps of soybean areas from field campaigns

- <https://www.nature.com/articles/s41893-021-00729-z#data-availability>

## 8. WorldCereal

- Description: Global maps of temporary crops, crop type (maize, winter cereals and spring cereals) and irrigation for the year 2021, at 10 m resolution. The globe is stratified into agro-ecological zones to handle the various agricultural seasons. The map of the temporary crops does not propose a distinction of the crops.
- Reference: Van Tricht, K., Degerickx, J., Gilliams, S., Zanaga, D., Battude, M., Grosu, A., Brombacher, J., Lesiv, M., Bayas, J. C. L., Karanam, S., Fritz, S., Becker-Reshef, I., Franch, B., Mollà-Bononad, B., Boogaard, H., Pratihast, A. K., and Szantoi, Z. (2023). WorldCereal: a dynamic open-source system for global-scale, seasonal, and reproducible crop and irrigation mapping, Earth Syst. Sci. Data Discuss. <https://doi.org/10.5194/essd-2023-184>.

### 4.2.3. National agricultural statistics in Europe

For the project, we propose to **use EUROSTAT for evaluating the area cultivated in each crop type at administrative unit scale** as these data are available across most of Europe in a consistent manner. Where more spatial detail is needed, the national databases and datasets listed above may be useful. These data are available for administrative units such as NUTS, the “Nomenclature of Territorial Units for Statistics” of EUROSTAT, and allow an aggregated evaluation of maps of crop types in regions where those data are available. Usually, national statistics do not give detailed information on cultivation practices but only on crop yields and harvested area at NUTS3 level (county/district level). However, those data are not available for all countries. The EUROSTAT database gives information on yields and harvested area for most countries at the coarser NUTS2 level (regions/provinces level). However, none of these datasets includes information about crop varieties.

**EUROSTAT** is the statistical service of the European Union. It provides datasets on yearly agricultural production at **NUTS2** level. This includes yearly yields and harvested areas for a large selection of crop types. The dataset covers the 27 member states of the EU, and in addition the UK, Iceland, Norway, Switzerland, Liechtenstein, Serbia, Albania, Kosovo, Bosnia-Herzegovina, Montenegro, North Macedonia, and Turkey. Data is available from the online portal: <https://ec.europa.eu/eurostat/data/database>

Other datasets that can be used for evaluation at administrative unit levels are:

**AGRESTE** is the statistical service of the French Ministry of Agriculture and Food, providing comprehensive and detailed data on agriculture in France. This includes yearly data at department level (**NUTS3** level) on harvested areas and yields for a large variety of crop types, and management practices such as tillage (conventional, reduced, and no-till), cover crops, irrigation, fertiliser and pesticide application. Data is available from the online portal: [www.agreste.agriculture.gouv.fr](http://www.agreste.agriculture.gouv.fr)

**Schauberger et al. (2022)** give an inventory of yearly crop areas and yields of ten major crop types (barley, maize, oats, potatoes, rapeseed, sugarbeet, sunflower, durum wheat, soft wheat and wine) for the 96 **French** departments (**NUTS3** level) covering the years 1900 to 2018. Data until 1988 digitised from statistical yearbooks, can be downloaded from <https://dataservices.gfz-potsdam.de/pik/showshort.php?id=9fed9402-ceaf-11eb-9603-497c92695674>.

**Duden et al. (2024)** give an inventory of yearly crop areas and yields of eleven major crop types (spring barley, winter barley, grain maize, silage maize, oats, potatoes, winter rape, rye, sugarbeet, triticale and winter wheat) for the 391 **German** districts (**NUTS3** level) covering the years 1979 to 2021. The dataset was established by collecting and digitizing statistical data from different sources and is available at [https://www.openagrar.de/receive/openagrar\\_mods\\_00092044](https://www.openagrar.de/receive/openagrar_mods_00092044).

The **I.Stat** data portal offers annual statistics for **Italy** at provincial level (**NUTS3**), including yearly cropland areas and production of a large variety of crops, starting from the year 2006. Data can be retrieved from the online portal: <http://dati.istat.it/?lang=en>

The **ESYRCE** platform of the Spanish Ministry of Agriculture, Fisheries and Food (MAPA) offers annual statistics for **Spain** at provincial level (**NUTS3**), including yearly cropland areas and production of a large variety of crops, starting from the year 2010. Data can be retrieved from the online portal: <https://www.mapa.gob.es/es/estadistica/temas/estadisticas-agrarias/agricultura/esyrce/>

The online platform of the Centraal Bureau voor de Statistiek (**CBS**) offers annual statistics for **the Netherlands** at provincial level (**NUTS3**), including yearly cropland areas and production of a large variety of crops, starting from the year 1994. Data can be retrieved here: <https://opendata.cbs.nl/statline/#/CBS/nl/>

The **Agri4Cast** data portal of the Joint Research Centre (JRC) of the EU offers different gridded datasets. For instance, they offer a dataset on yearly, modelled crop area within the EU from 1980 to 2022, covering 19 perennial crop types. Further, they offer a gridded map of phenological stages of winter soft wheat. This dataset includes usual sowing dates, the number of degree days until flowering and maturity are reached, and the required duration of exposure to vernalisation temperatures. Both datasets are at a 25 km spatial resolution. In addition, they offer an irrigation map for the year 2010 at 10 km spatial resolution. This latter datasets distinguishes about 15 crop types/classes, incl. cereals, maize, pulses, rapeseed, and sunflowers, but also perennial crops such as vines, orchards, and olive groves. Data is available from the online portal: <https://agri4cast.jrc.ec.europa.eu/DataPortal/Index.aspx>

#### ● Key References:

- Schauburger, B., Kato, H., Kato, T., et al. (2022). French crop yield, area and production data for ten staple crops from 1900 to 2018 at county resolution. *Scientific Data*, 9, 38.  
<https://doi.org/10.1038/s41597-022-01145-4>.
- Duden, C., Nacke, C., & Offermann, F. (2024). German yield and area data for 11 crops from 1979 to 2021 at a harmonized spatial resolution of 397 districts. *Scientific Data*, 11, 95.  
<https://doi.org/10.1038/s41597-024-02951-8>.

#### 4.2.4 National agricultural statistics in Brazil

Below is a list of agricultural datasets that can be used for aggregated model evaluation for crop types. For the project, we propose **USDA**, **CONAB**, and **MapBiomass** data which are available across all Brazil in a consistent manner. Where more spatial detail is needed, the national databases and datasets listed above may be useful. These datasets are briefly described below

##### 1. MapBiomass

- Annual crop type in agricultural land between 1985-2023. Provided in broader categories than EO4BK nomenclature
- <http://mapbiomas.org/>

##### 2. CONAB

- Description: annual area planted and weight harvested for multiple crop types including soybean, sugarcane, grains and coffee at the regional and municipality scale.

##### 3. USDA

- Major crop type harvested area per state
- [https://ipad.fas.usda.gov/cropeexplorer/cropview/comm\\_chartview.aspx?ftypeid=47&fattributeid=1&ctypeid=47&fcattributeid=1&regionid=br&cntryid=BRA&cropid=0422110&nationalgraph=False&sel\\_year=2021&startrow=1#](https://ipad.fas.usda.gov/cropeexplorer/cropview/comm_chartview.aspx?ftypeid=47&fattributeid=1&ctypeid=47&fcattributeid=1&regionid=br&cntryid=BRA&cropid=0422110&nationalgraph=False&sel_year=2021&startrow=1#)

#### 4.2.5 Field trials with reported cultivars types

These trials are measuring crop performances for yields and other useful traits expected from crops, but data are generally not publicly available and consist of very small plots with different cultivars and management practices < 10 m in size. So this **source of data will not be used in the project.**

### 4.3 Reference maps / datasets upon which the results of the methods proposed in section 3 can be benchmarked for management practices.

#### 4.3.1 Reference EO and in-situ datasets for irrigation mapping in Brazil

Below is a list of irrigation datasets that can be used for model evaluation for irrigation in Brazil. **For the project, we propose to use the ANA data which are available across all Brazil in a consistent manner.**

##### 1. Brazilian ANA dataset for CPIC irrigation.

- Available for years 1985, 1990, 2000, 2005, 2020, 2014, 2017, 2019, 2022 as shapefiles for all of Brazil.
- Available at: <https://metadados.snirh.gov.br/geonetwork/srv/api/records/e2d38e3f-5e62-41ad-87ab-990490841073>
- For interactive graphics-  
<https://app.powerbi.com/view?r=eyJrJoiZmNmMmU0ZTYtYmZiYS00ZTk3LWFiMTMtZjQwMzU1MGQ1Y2E4IiwidCI6ImUwYmIOMDEyLTgxMGItNDY5YS04YjRkLTU2N2ZjZDFiYWY4OCJ9>

##### 2. Brazilian ANA dataset for flood irrigation

- Agência Nacional de Águas (ANA). Mapeamento do arroz irrigado no Brasil/Agência Nacional de Águas, Companhia Nacional de Abastecimento. Brasília: ANA, 2021b.

Where more spatial detail is needed, the national databases and datasets listed below may be useful:

##### 3. Brazilian National Supply Company for flooded irrigation (rice).

- Available in many states between 2018-2024. <https://www.conab.gov.br/info-agro/safras>. Download at: <https://portaldeinformacoes.conab.gov.br/mapeamentos-agricolas-downloads.html> as shapefile. Normally per state and per year. Will require amalgamation.

##### 4. Mapbiomas 1985-2021 annual CPICs and rice.

- Derived from CNN outputs applied to Landsat data
- <https://brasil.mapbiomas.org/>. In-situ data for model training is from an unknown source (possibly available via <https://github.com/orgs/mapbiomas/repositories>)

#### 4.3.2 Reference maps of double cropping practices in Brazil


For the project, we propose **CONAB and LEM (+)** data which are available across all Brazil in a consistent manner. Where more spatial detail is needed, the national databases and datasets listed above may be useful.

Below is a list of irrigation datasets that can be used for model evaluation for double cropping in Brazil. **Brazilian National Supply Company (CONAB)**

- This is mostly between 2010-2014 and hence may need to deploy extrapolation. Data also include sugar cane, coffee and cotton shapefiles from 2010-2013 and in 2023 and soy across many states and time periods.
- <https://www.conab.gov.br/info-agro/safras>.
- As shapefile at <https://portaldeinformacoes.conab.gov.br/mapeamentos-agricolas-downloads.html>.

##### 1. Luís Eduardo Magalhães (LEM)



Deliverable no. D1.1 Requirements Baseline (RB) document	ESA Carbon-RO, EO4BK Contract no. 4000144916/24/I-EF	 International Institute for Applied Systems Analysis IIASA www.iiasa.ac.at
--	---	--

- LEM (+) datasets are our primary source of double cropping data in smaller frequency nomenclature, i.e., soybean/protein. All data is available within Sentinel-2 operational dates but across limited climatic variability.

### 4.3.3. Reference maps of agricultural practices in Europe

For the project, **we propose to use in priority LUCAS Copernicus data which are available across all Europe in a consistent manner.**

### 4.3.4. ICOS Eddy covariance flux towers with reported crop types and management information

**ICOS data are too sparse to be used for systematic evaluation of practices across Europe but they will be used for evaluating the phenology products** because of their very high temporal resolution. These sites are measuring CO<sub>2</sub> and energy fluxes with a footprint of about 150 m around each tower. The European network coordinated by ICOS in Europe covers different crop types generally operated under common management practices. These sites provide local climate and flux data with ancillary variables such as soil moisture and temperature (from in situ or satellite observations) but they usually do not report systematically the practices and cultivars. In Europe, we worked within the CROP2021 initiative of ICOS to collect management practices and cultivars at 14 crop sites and 163 crop site-years, 26 crop species, from 2001 to 2021. They are listed in the following Table 4.3a. Crop types change from year to year as the sites are managed under typical rotations in their region. These data are valuable for evaluating GPP from EO-data.

Plot_name	Full name	Country	Latitude	Longitude	Elevation m
BE-Lon	Lonzee	Belgium	50°33'06" N	4°44'46" E	167
CH-Oe2	Oensingen	Switzerland	47°17'11.1" N	7°44'1.5" E	452
FR-EM2	Estrees-Mons A28	France	49°52'19.59" N	3°1'14.339" E	84
FR-Lam	Lamasquere	France	43°29'47" N	1°14'16" E	180
FR-Gri	Grignon	France	48°50'39.192"N	1°57'6.876"E	123
FR-Aur	Aurade	France	43°32'58.7364"N	1°6'21.9708"E	245
DE-Geb	Gebesee	Germany	51°5'59.028"N	10°54'52.668"E	161.5
DE-Kli	Klingenberg	Germany	50°53'35.016"N	13°31'20.568"E	478
DE-RuS	Selhausen Juelich	Germany	50°51'57.4"N	6°26'50.1"E	103
IE-Gwr	Gowran	Ireland	52°38'11.4"N	7°0'40.65696"W	51
FI-Qvd	Qvidja	Finland	60°29'55'0 N	22°39'28'1 E	8
PL-Brd	Brody	Poland	52°26'3.0516"N	16°17'58.2828"E	93
IT-Bci	Borgo Cioffi	Italy	40°31'25.500"N	14°57'26.79998"E	15
CZ-KrP	Kresin u Pacova	Czech Republic	49°34'23.727"N	15°04'43.583"E	545

**Table 4.2:** The 14 ICOS eddy covariance crop sites in Europe

## 5. Definition of modelling protocols that will be used in WP5 to estimate the impact of EO information on the BK approach

### 5.1. Protocol for simulations with the land surface model ORCHIDEE to provide additional data to the BK model, as a backstop or extend the model's parameterizations.

**We will use the land surface model ORCHIDEE to simulate land use change impacts on biomass carbon and soil organic carbon (SOC) stocks. We will run simulations for idealised land use change scenarios to quantify the effect of different land use transitions on biomass and soil carbon (incl. litter) stocks and the main fluxes involved in the changes of these carbon stocks: net primary production, litter production, heterotrophic respiration, crop harvest and wood harvest. These simulation results will be used to parameterise and**

benchmark the BK models. For the two study regions, Europe and Brazil, we run simulations at a resolution of ~50 km. The forcing data used for these simulations, which had previously been used by the Global Carbon Budget (Friedlingstein et al., 2023), are listed in **Table 5.1**. The forcing data sets include meteorology data given at 6 hourly time-steps. The other forcing data on land cover, wood harvest rates, and atmospheric CO<sub>2</sub> concentrations are given at a yearly time-step. The land cover data is given as areal proportions of plant functional types (PFTs). The 15 PFTs distinguished for our simulations are listed in **Table 5.2**. Note that ORCHIDEE simulates SOC stock dynamics separately for each PFT that is present in one grid cell of the modelling grid. Despite the coarse spatial resolution, the model is thus able to keep track of the differences in SOC dynamics under different types of land cover.

Data set	Parameters	Spatial resolution	Period covered and temporal resolution
CRU-JRAv2.3	Meteorology	0.5° (~50 km)	1901-2022, 6-hourly
LUHv2.2-GCB2023	Land cover (area proportions of 15 PFTS Table 5.2)	0.5° (~50 km)	1700-2022, yearly
LUHv2.2-GCB2023	Wood harvest rates	0.5° (~50 km)	1700-2022, yearly
CO <sub>2</sub> -GCB2023	Atmospheric CO <sub>2</sub> concentrations	Global average	1700-2022, yearly

**Table 5.1:** Datasets used as model inputs.

#	Name
1	Bare soil
2	Tropical broadleaf evergreen forest
3	Tropical broadleaf rain green forest
4	Temperate needleleaf evergreen forest
5	Temperate broadleaf evergreen forest
6	Temperate broadleaf summergreen forest
7	Boreal needleleaf evergreen forest
8	Boreal broadleaf summergreen forest
9	Boreal needleleaf summergreen forest
10	Natural C3 grass, temperate
14	Natural C3 grass, tropical
15	Natural C3 grass, boreal
11	Natural C4 grass
12	C3 crop
13	C4 crop

**Table 5.2:** Plant functional types (PFTs) used as land cover classes in ORCHIDEE

First, we run simulations of idealised land use change transitions and their impact on biospheric carbon stocks and fluxes. The results of these simulations will help to parameterise the book keeping models. Then, we run simulations of historical land use change and its impacts on biospheric carbon stocks and fluxes. The results of this simulation will be used for benchmarking the simulations of the bookkeeping model.

### 5.1.1 Idealised land use change transitions for parametrization of BK models

The idealised land use changes comprise possible transitions from one PFT (PFT<sub>old</sub>) to any other PFT (PFT<sub>new</sub>) that can occur in the study region. For the simulations, we follow the simulation protocol established by Dinh et al. (2024). This simulation protocol is repeated for each PFT, which is then used as PFT<sub>old</sub>, with the exception of PFT1 (bare soil) and PFTs that do not occur in the study region (like PFTs 2,3 and 14 for Europe, and PFTs 7,8,9 and 15 for Brazil, see **Table 5.2**).

**First, we run a 340 year spin-up** with fixed land cover of 100 % of PFT<sub>old</sub>, using the wood harvest rates of the year 1900, fixing atmospheric CO<sub>2</sub> levels at the value of 1900, and looping over the first 10 years of the meteorological forcing data (1901-1910).

Then, we will run a **transient simulation from 1901 to 1950** with the same fixed land cover (**100 % PFT<sub>old</sub>**) and continuously changing meteorology, wood harvest rates and atmospheric CO<sub>2</sub> levels.

Then, we change the land cover to equal proportions of all other PFTs that may occur in the study region, including the PFT corresponding to PFT<sub>old</sub> that we keep as control without land use change. With that **new land cover composition**, we continue the **transient simulation from 1951 to 2022** with continuously changing meteorology, wood harvest rates and atmospheric CO<sub>2</sub> levels.

Finally, to obtain a longer time-series from which we can cover time horizons up to 100 years, we **continue the simulation for another 30 years**, with the same land cover composition, atmospheric CO<sub>2</sub> levels and wood harvest rates fixed to the values of the year 2022, and looping over the last ten years of the meteorological forcing data (2013-2022).

### 5.1.2. Simulation of historical land use change impacts for benchmarking of BK models

For these simulations, we use the land cover information from the LUHv2.2-GCB2023 data set (see **Table 5.1**).

**First, we run a 340-year spin-up** using the land cover, wood harvest rates, and atmospheric CO<sub>2</sub> levels of the year 1900, and looping over the first 10 years of the meteorological forcing data (1901-1910). Then, we run a **transient simulation from 1901 to 2022**, with continuously changing forcing information on meteorology, land cover, wood harvest rates and atmospheric CO<sub>2</sub> levels. In addition, as **control simulation**, we repeat the transient simulation with land cover and wood harvest rates fixed to the year 1900, while meteorology and atmospheric CO<sub>2</sub> concentrations still change yearly.

### 5.1.3 Model outputs

From both simulations, we will provide the following model outputs as yearly average values at 0.5° (~50 km) spatial resolution:

- Biomass carbon stocks in kg C m<sup>-2</sup>
- Soil (incl. litter) organic carbon stocks in kg C m<sup>-2</sup>
- Net primary production in kg C m<sup>-2</sup>yr<sup>-1</sup>
- Harvest (crop and wood products) in kg C m<sup>-2</sup>yr<sup>-1</sup>
- Litter production in kg C m<sup>-2</sup>yr<sup>-1</sup>
- Heterotrophic respiration in kg C m<sup>-2</sup>yr<sup>-1</sup>

Note that both the idealised land use change simulations and the simulation of historical land use change include control simulations without land use change (see above). The results for these control simulations will help to isolate the land use change impacts on the biospheric carbon stocks and exchange fluxes listed above.

### ● Key References:

- Dinh, T. L. A., Goll, D., Ciais, P., & Lauerwald, R. (2024). Impacts of land-use change on biospheric carbon: An oriented benchmark using the ORCHIDEE land surface model. *Geoscientific Model Development*, 17, 6725–6744. <https://doi.org/10.5194/gmd-17-6725-2024>.
- Friedlingstein, P., O'Sullivan, M., Jones, M. W., Andrew, R. M., Bakker, D. C. E., Hauck, J., Landschützer, P., Le Quéré, C., Luijckx, I. T., Peters, G. P., Peters, W., Pongratz, J., Schwingshackl, C., Sitch, S., Canadell, J. G., Ciais, P., Jackson, R. B., Alin, S. R., Anthoni, P., Barbero, L., Bates, N. R., Becker, M., Bellouin, N., Decharme, B., Bopp, L., Brasika, I. B. M., Cadule, P., Chamberlain, M. A., Chandra, N., Chau, T.-T.-T., Chevallier, F., Chini, L. P., Cronin, M., Dou, X., Enyo, K., Evans, W., Falk, S., Feely, R. A., Feng, L., Ford, D. J., Gasser, T., Ghattas, J., Gkritzalis, T., Grassi, G., Gregor, L., Gruber, N., Gürses, Ö., Harris, I., Hefner, M., Heinke, J., Houghton, R. A., Hurtt, G. C., Iida, Y., Ilyina, T., Jacobson, A. R., Jain, A., Jarníková, T., Jersild, A., Jiang, F., Jin, Z., Joos, F., Kato, E., Keeling, R. F., Kennedy, D., Klein Goldewijk, K., Knauer, J., Korsbakken, J. I., Körtzinger, A., Lan, X., Lefèvre, N., Li, H., Liu, J., Liu, Z., Ma, L., Marland, G., Mayot, N., McGuire, P. C., McKinley, G. A., Meyer, G., Morgan, E. J., Munro, D. R., Nakaoka, S.-I., Niwa, Y., O'Brien, K. M., Olsen, A., Omar, A. M., Ono, T., Paulsen, M., Pierrot, D., Pocock, K., Poulter, B., Powis, C. M., Rehder, G., Resplandy, L., Robertson, E., Rödenbeck, C., Rosan, T. M., Schwinger, J., Séférian, R., Smallman, T. L., Smith, S. M., Sospedra-Alfonso, R., Sun, Q., Sutton, A. J., Sweeney, C., Takao, S., Tans, P. P., Tian, H., Tilbrook, B., Tsujino, H., Tubiello, F., van der Werf, G. R., van Ooijen, E., Wanninkhof, R., Watanabe, M., Wimart-Rousseau, C., Yang, D., Yang, X., Yuan, W., Yue, X., Zaehle, S., Zeng, J., and Zheng, B. (2023). Global Carbon Budget 2023. *Earth System Science Data*, 15, 5301–5369. <https://doi.org/10.5194/essd-15-5301-2023>.

## 5.2. Synthesis of knowledge on the effects of cropland management on soil carbon stocks changes

We will conduct a synthesis of current knowledge on how to quantify the impacts of different land management practices on cropland soil carbon stocks. These practices include:

- Cover crops
- No tillage vs. tillage
- Irrigation
- Double cropping

For this synthesis, **we identified large-scale crop modelling studies as a major source of information.** For instance, model simulations of the effects of cover crops on soil carbon stocks exist at European (Fendrich et al., 2024) and global scale (Porwollik et al., 2022). Similarly, global model studies exist for the effect of tillage vs. no tillage (Lutz et al., 2019). With regard to irrigation and double cropping, no large-scale studies that directly quantified the effects on soil organic carbon stocks are known to the consortium members. However, studies exist that have quantified the effects of these practices on yield and biomass production (Su et al., preprint; Wang et al., 2021), which allows for an estimate of changed litter inputs to the soil organic carbon pools. Note, however, that irrigation not only increases biomass production and litter inputs, but may also decrease soil organic carbon turnover times. For this, information is available from meta-analyses (e.g. Yao et al., 2024).

### ● Key References:

- Fendrich, A. N., Ciais, P., Panagos, P., Martin, P., Carozzi, M., Guenet, B., & Lugato, E. (2024). Including land management in a European carbon model with lateral transfer to the oceans. *Environmental Research*, 245, 118014. <https://doi.org/10.1016/j.envres.2023.118014>.
- Porwollik, V., Rolinski, S., Heinke, J., von Bloh, W., Schaphoff, S., & Müller, C. (2022). The role of cover crops for cropland soil carbon, nitrogen leaching, and agricultural yields – a global simulation study with LPJmL (V. 5.0-tillage-cc). *Biogeosciences*, 19, 957–977. <https://doi.org/10.5194/bg-19-957-2022>.

- Lutz, F., Herzfeld, T., Heinke, J., Rolinski, S., Schaphoff, S., von Bloh, W., Stoorvogel, J. J., & Müller, C. (2019). Simulating the effect of tillage practices with the global ecosystem model LPJmL (version 5.0-tillage). *Geoscientific Model Development*, 12, 2419–2440. <https://doi.org/10.5194/gmd-12-2419-2019>.
- Su, Y., Lauerwald, R., Makowski, D., Viovy, N., Guilpart, N., Zhu, P., Gabrielle, B., & Ciais, P. (2023). Global warming increases the chance of success of maize-wheat double cropping in Europe. PREPRINT (Version 1). Research Square. <https://doi.org/10.21203/rs.3.rs-3112511/v1>.
- Wang, X., Müller, C., Elliot, J. et al. Global irrigation contribution to wheat and maize yield. *Nat Commun* 12, 1235 (2021). <https://doi.org/10.1038/s41467-021-21498-5>.
- Yao, X., Zhang, Z., Yuan, F., & Song, C. (2024). The impact of global cropland irrigation on soil carbon dynamics. *Agricultural Water Management*, 296, 108806. <https://doi.org/10.1016/j.agwat.2024.108806>.

### 5.3. Transient carbon densities and turnover times calibration for the bookkeeping model

The simplest description of the land carbon cycle used for BK modelling in the project is shown in Figure 5.3a. Two pools are represented, the living biomass and soil organic carbon, to which a third must be added to account for harvested wood products (not shown). The calibration of the BK model requires parameters that describe the carbon densities and turnover times for each pool. The proposed protocol to derive these parameters follows the approach used to calibrate the OSCAR BK model (Gasser et al., 2020). It is assumed that knowing the input flux of the pool (e.g. NPP for the biomass pool) and estimating its turnover time as the ratio of the pool's size over its output fluxes (e.g. fire emissions and litterfall) allows to reconstruct the hypothetical steady-state carbon density of the pool. Therefore, only these three aggregate variables are necessary to calibrate the BK model, and a DGVM like ORCHIDEE need only provide these over each of its PFTs to allow parameterisation of the BK model (which corresponds to the variables listed in section 1). However, a key assumption of this calibration approach is that the turnover time of full-grown ecosystems is assumed to be the same as the recovery time (timescale of biomass regrowth and reequilibration of soils) after a land use or land cover change. This assumption has not been tested, and we will investigate it during the benchmarking with existing observations or model simulations described below.

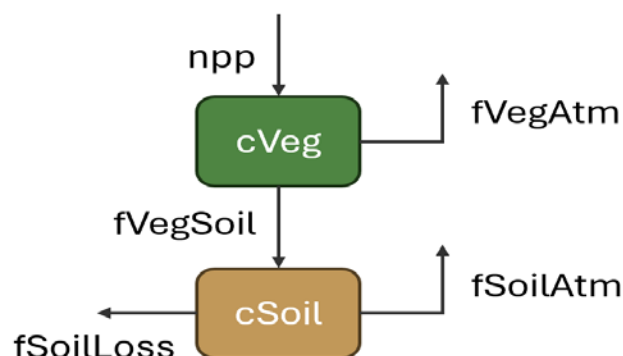


**Figure 5.1:** Illustration of the simplest model structure for bookkeeping, with two pools and input/output fluxes that dictate their turnover time.

#### ● Key References:

- Gasser, T., Crepin, L., Quilcaille, Y., Houghton, R. A., Ciais, P., & Obersteiner, M. (2020). Historical CO<sub>2</sub> emissions from land use and land cover change and their uncertainty. *Biogeosciences*, 17(15), 4075–4101. <https://doi.org/10.5194/bg-17-4075-2020>.



#### 5.4. Protocol for BK simulations, including comparison to parameterizations of established BK models (OSCAR), to other land use and land cover datasets (LUH2 and HILDA+), and to idealised cases in which the C3/C4 and/or crop management distinctions are absent.

The benchmarking of the newly obtained BK model and of its parameters and input datasets against existing data is expected to take place in two steps (both as part of Task 5.3 of WP5).

**Step 1** will quantify the impact of the additional information provided by some of the new EO data, and notably the carbon-cycle relevance of the distinction between C3- and C4-crops and between crop management practices.

To this aim, we will use idealised experiments. Starting from the land cover state of the latest year of the selected land cover dataset, we will prescribe unit transitions that replace:

- a *generic crop type* by a mix of C3- and C4-crops following different proportions (4 sub-experiments: 0 %, 25 %, 50 %, 100 % of C4),
- pasture by a mix of C3- and C4-crops following identical proportions,
- forest by a mix of C3- and C4-crops following identical proportions,
- *current agricultural practices* by a uniform practice (no irrigation, no tillage, single cropping)

This is a total of 16 idealised experiments to quantify the impact of distinguishing between C3- and C4-crops. This will provide a first estimate of the effect early on in the project. The generic crop type in the first set of experiments will be calculated as a mix of C3 and C4 using the land cover dataset chosen as baseline for the experiment. The definition of current agricultural practices will depend on the origin of the BK parameters: taken as the parameters derived from observation of the recent past if EO-based, taken as the default parameters if DGVM-based.


Simulations for this first steps will be carried out twice, for different purposes:

- **Step 1a** will be a test for the new BK modelling platform and will happen as soon as it is available. It is a preliminary step meant to serve as a baseline for the rest of the study. It will use only the parameters derived from ORCHIDEE and literature review (sections 5.1 and 5.2), and it will be run at the models' native resolution (expected: 0.5° globally). The results will inform a first order estimate of the magnitude of the C3/C4 crop distinction, to be available by Milestone 3 of the project.
- **Step 1b** will contribute to the final results of the project and will be run using as many EO-derived parameters at the highest possible resolution, although it will be spatially limited to the two regions of focus (Europe and Brazil). It is furthermore envisaged that not all experiments will be carried out, as the results of phase 1a will indicate which benchmarking simulations are more appropriate.

**Step 2** will deliver the final benchmarking of the modelling platform, as it will quantify and illustrate the value-added of the EO information on the new BK model behaviour by comparing its results across resolution scales as well as against existing land cover datasets and BK parameterisations.

To this aim, we will run the BK model with the time series of land use and land cover change produced by WP4 (and covering the two focus regions and at least 5 years). We will repeat the experiment and introduce variations across several of the model's inputs:

- Using the same dataset, we will vary the model's resolution with at least one input in the range of:
  - 10-30 m (the resolution of the EO4BK WP4 product),
  - 0.3-1 km (the resolution of the HILDA+ dataset (Winkler et al., 2021)),
  - 0.25-0.5° (the resolution of the LUH2 dataset (Hurtt et al., 2020) and the BLUE bookkeeping model (Hansis et al., 2015)).
  - national level (the current resolution of the OSCAR (Gasser et al., 2020) and H&C bookkeeping models (Houghton et al., 2023)).

Deliverable no. D1.1 Requirements Baseline (RB) document	ESA Carbon-RO, EO4BK Contract no. 4000144916/24/I-EF	 International Institute for Applied Systems Analysis IIASA www.iiasa.ac.at
--	---	--

- Under a set resolution (likely that of the lowest resolution dataset), we will vary the input land use and land cover change dataset, using the latest version of:
  - EO4BK WP4 product,
  - HILDA+ dataset,
  - LUH2 dataset.
- Under the newly produced dataset, we will vary the carbon cycle parameters of the model (i.e. carbon densities and timescales), following:
  - the newly derived EO-based parameters (biome-specific and spatially explicit),
  - the best-guess parameters from OSCAR (fewer biomes but defined at national level),
  - the parameters from BLUE (more biomes but defined globally).

This is a total of 8 experiments (as the first of each sub-category is the same baseline experiment).

While these short experiments will not provide a realistic carbon flux (because they will lack a long-term history of input data and thus will not include the legacy fluxes from past land use and land cover changes), they will allow quantification of the uncertainty stemming from each of these factors: resolution, input land use data, parameters. They will also benchmark the EO-based model against existing BK models used in the Global Carbon Budget.

#### • Key References:

- Winkler, K., Fuchs, R., Rounsevell, M. et al. Global land use changes are four times greater than previously estimated. *Nat Commun* 12, 2501 (2021). <https://doi.org/10.1038/s41467-021-22702-2>.
- Hurtt, G. C., Chini, L., Sahajpal, R., Frolking, S., Bodirsky, B. L., Calvin, K., Doelman, J. C., Fisk, J., Fujimori, S., Klein Goldewijk, K., Hasegawa, T., Havlik, P., Heinemann, A., Humpenöder, F., Jungclaus, J., Kaplan, J. O., Kennedy, J., Krisztin, T., Lawrence, D., Lawrence, P., Ma, L., Mertz, O., Pongratz, J., Popp, A., Poulter, B., Riahi, K., Shevliakova, E., Stehfest, E., Thornton, P., Tubiello, F. N., van Vuuren, D. P., & Zhang, X. (2020). Harmonization of global land use change and management for the period 850–2100 (LUH2) for CMIP6. *Geoscientific Model Development*, 13(13), 5425–5464. <https://doi.org/10.5194/gmd-13-5425-2020>.
- Hansis, E., S. J. Davis, and J. Pongratz (2015), Relevance of methodological choices for accounting of land use change carbon fluxes, *Global Biogeochemical Cycles*, 29(9), 1230–1246. <https://doi.org/10.1002/2014GB004997>.
- Gasser, T., Crepin, L., Quilcaille, Y., Houghton, R. A., Ciais, P., & Obersteiner, M. (2020). Historical CO<sub>2</sub> emissions from land use and land cover change and their uncertainty. *Biogeosciences*, 17(15), 4075–4101. <https://doi.org/10.5194/bg-17-4075-2020>.
- Houghton, R. A., & Castanho, A. (2023). Annual emissions of carbon from land use, land-use change, and forestry from 1850 to 2020. *Earth System Science Data*, 15, 2025–2054. <https://doi.org/10.5194/essd-15-2025-2023>.

### 5.5. Protocol for benchmarking LULCC fluxes from BK model against response functions of SOC and biomass C stocks for land use change transitions

As discussed during the KOM and agreed with ESA, **we do not expect to generate fully comparably LULCC fluxes, mostly because the simulations will be limited in length (5 years). This requirement is reframed as a benchmarking of our response functions against others available in the literature and in other projects.** For benchmarking of estimated SOC response functions due to land cover change from cropland to either grassland or forest, or from forest or grassland to cropland, **we will make use of the meta-analysis compiled by Dinh et al. (2024).** Dinh et al. (2024) compiled data from 102 study sites sourced from 34 peer-reviewed publications (see Table S5 in this reference for details) that investigate LUC impacts on SOC stocks across Europe. This meta-

analysis includes studies with paired plots, chronosequences, or repeated sampling designs. They focused on five specific LUC transitions: cropland to grassland (C to G), grassland to cropland (G to C), cropland to forest (C to F), grassland to forest (G to F), and forest to cropland (F to C). They further distinguish cases where the forest floor (i.e. the above-ground litter organic layer) was included in the sampling process for forest sites ( $F_{\text{wFF}}$ ) or not ( $F_{\text{woFF}}$ ). The collected data are categorised into seven conversion types, as detailed in **Table 5.3**. **We will also include simulated response functions for biomass change following land use transitions involving woody land cover types.** Figure 5.2 shows an example of benchmarking simulations of response functions here with the ORCHIDEE model data collected in the study of Dinh et al. (2024). These simulations followed a simulation protocol that is similar to the one described here in section 5.2. To guarantee the comparability of simulations and observations, only the simulation results from model grid cells coinciding with the sites of observation data were selected. We suggest following the same strategy for the model benchmarking of response functions in this project.

<i>LUC</i>	<i>ID</i>	<i>sites</i>	<i>N samples</i>	<i>Depth (cm)</i>	<i>Age (years)</i>
Cropland to grassland	C to G	33	49	$33.71 \pm 22.25$	28.55
Grassland to cropland	G to C	17	49	$42.12 \pm 14.58$	49.86
Grassland to forest (mineral soil or without forest floor)	G to $F_{\text{woFF}}$	34	49	$34.90 \pm 14.59$	40.24
Grassland to forest (with forest floor)	G to $F_{\text{wFF}}$	25	38	$30.53 \pm 2.26$	38.71
Cropland to forest (mineral soil)	C to $F_{\text{woFF}}$	15	65	$34.25 \pm 17.17$	37.43
Cropland to forest (with forest floor)	C to $F_{\text{wFF}}$	8	63	$27.86 \pm 3.33$	30.25
Forest to cropland (mineral soil)	$F_{\text{woFF}}$ to C	7	33	$33.33 \pm 14.77$	17.45

**Table 5.3:** Number of study sites and samples, mean sampling depths with standard deviation, and mean current land-use age for the local-scale observations in the meta-analyses. (taken from Dinh et al., 2024)

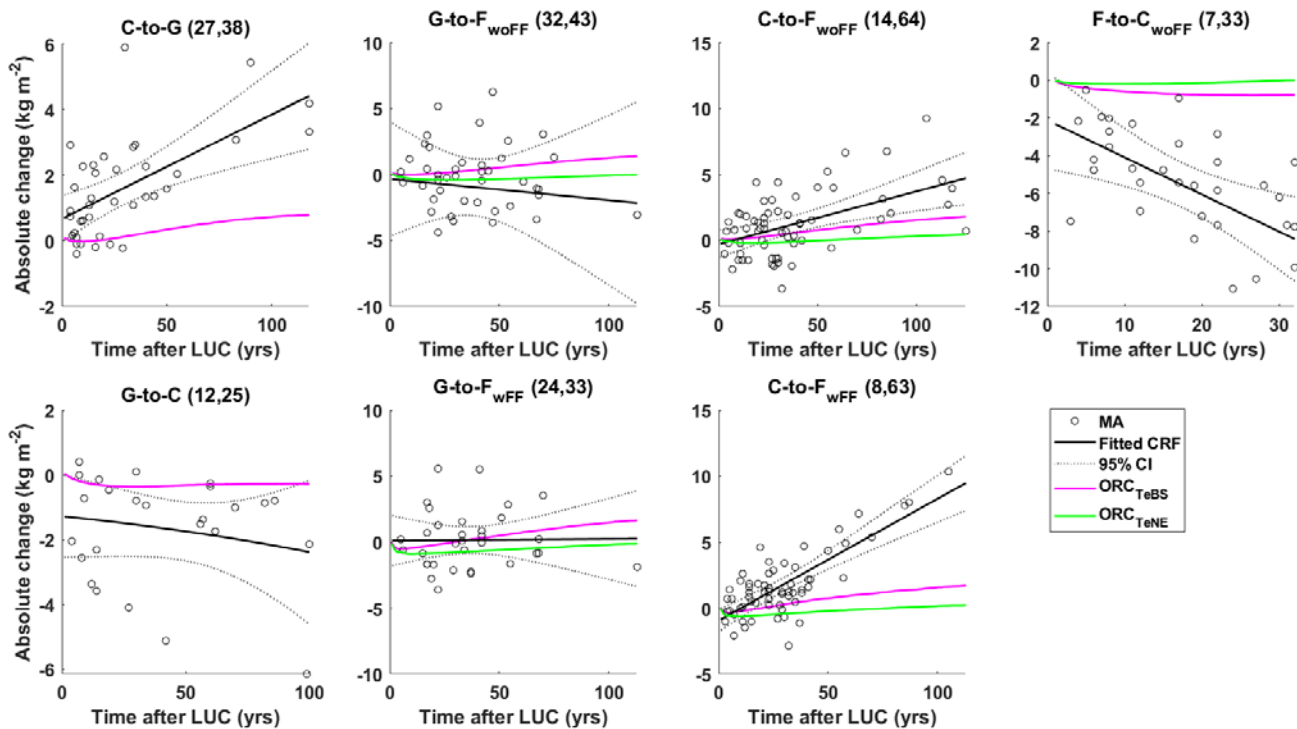


**Figure 5.2:** The absolute soil organic carbon changes (in  $\text{kg m}^{-2}$ ) from site observations in meta-analyses (black circles) and the fitted carbon response function (CRF; black lines)  $\pm 95\%$  confidence interval (dotted black lines) compared to simulated CRFs (magenta and green lines) for different land-use changes (LUCs): cropland to grassland (C to G), grassland to cropland (G to C), grassland to forest (without and with forest floor G to  $F_{\text{woFF}}$ , G to  $F_{\text{wFF}}$ ), cropland to forest (C to  $F_{\text{woFF}}$  and C to  $F_{\text{wFF}}$ ), and forest to cropland (F to  $C_{\text{woFF}}$ ). The first number in the parentheses indicates the number of study sites, and the second is the number of samples in the meta-analyses. Two distinct forest types, namely temperate broadleaf summergreen and temperate needleleaf evergreen, are considered for the forest sites in ORCHIDEE simulations ( $\text{ORC}_{\text{TeBS}}$ ,  $\text{ORC}_{\text{TeNE}}$ ). (taken from Dinh et al., 2024).

Note finally that Dinh et al. (2024) have used an exhaustive meta-analysis of tree age and above ground biomass (Besnard et al., 2021) for forest biomass growth benchmarking simulations, following again a simulation protocol that is similar to the one described here in section 5.2. We suggest using the same dataset from this meta-analysis for benchmarking also in this project.

#### ● Key References:

- Dinh, T. L. A., Goll, D., Ciais, P., & Lauerwald, R. (2024). Impacts of land-use change on biospheric carbon: An oriented benchmark using the ORCHIDEE land surface model. *Geoscientific Model Development*, 17, 6725–6744. <https://doi.org/10.5194/gmd-17-6725-2024>.
- Besnard, S., Koirala, S., Santoro, M., Weber, U., Nelson, J., Gütter, J., Herault, B., Kassi, J., N'Guessan, A., Neigh, C., Poulter, B., Zhang, T., & Carvalhais, N. (2021). Mapping global forest age from forest inventories, biomass and climate data. *Earth System Science Data*, 13, 4881–4896. <https://doi.org/10.5194/essd-13-4881-2021>.

## 5.6. Benchmarking against existing estimates of cropland C budgets including land use change

For Europe, we will use as benchmark evaluation data for the BK model results additional datasets based on meta-analysis that have already collected and harmonised large datasets from the literature about SOC and spatially explicit SOC changes in response to a range of land use change and agricultural practices. In particular the LUCAS three campaigns revisiting > 18000 sites (Figure 6.1) and the model by de Rosa et al. (2023) based on these data. For instance, the site [https://cropdiversification.shinyapps.io/Crop\\_divers/](https://cropdiversification.shinyapps.io/Crop_divers/) provides data and visualisation of cropping system outcomes ( GHG emissions, soil quality, yield, water use ) for the diversification of cropland practices, including cultivation of associated plants, mixed crops types, mixed varieties, intercropping, agroforestry, rotation (Figure 6.2). The results are presented as an effect size, the log ratios of a measurement in a diversified treatment to its value in a less diversified control). Each point corresponds to one effect size from one meta-analysis for one single category of outcome (note that several effect sizes may be affiliated to one single meta-analysis). Vertical bars correspond to 95 % confidence intervals. The number of data used to calculate each effect size are indicated at the bottom of each graph, when available. In some meta-analyses, the effect sizes were computed for a fraction of its total data sample (e.g. per covariate), but only global effect sizes are presented here. Effect sizes that were informed as relative distances were converted to log ratios and integrated in the figure whereas absolute differences and hedge's distances were not. Few other references on the topic of SOC sequestration and agricultural practices on SOC are available, such as Beillouin et al. (2023), Guillaume et al. (2022a), Guillaume et al. (2022b), Garnier et al. (2022).

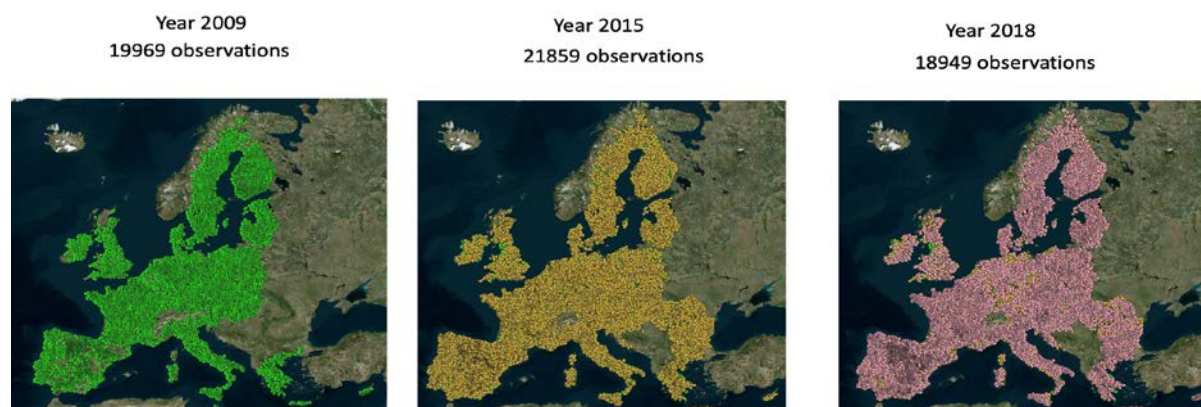


**Figure 6.1** The 3 LUCAS campaigns where the same sites were re-measured in 2009, 2015 and 2018 for SOC changes (0-30 cm)

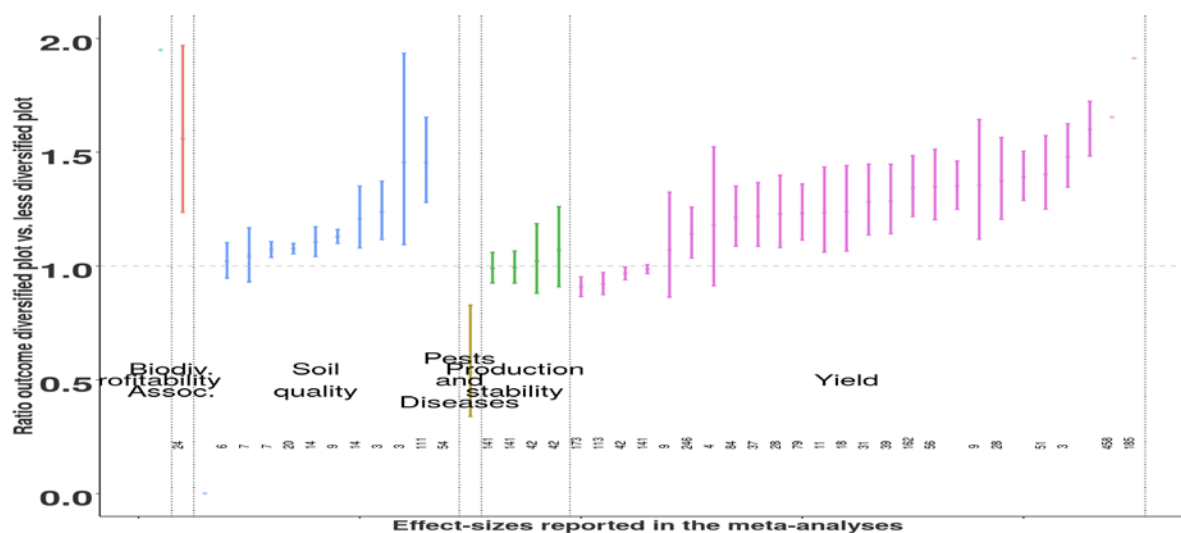
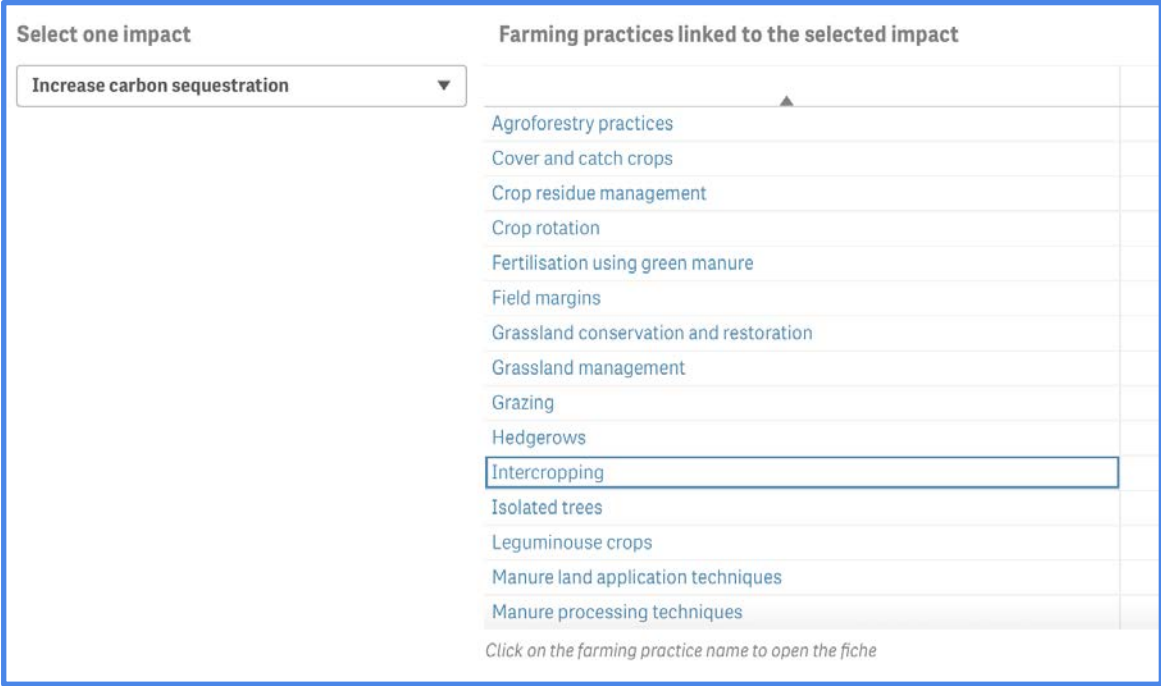




**Figure 6.2** Meta-analysis effect size on different variables of diversified agriculture

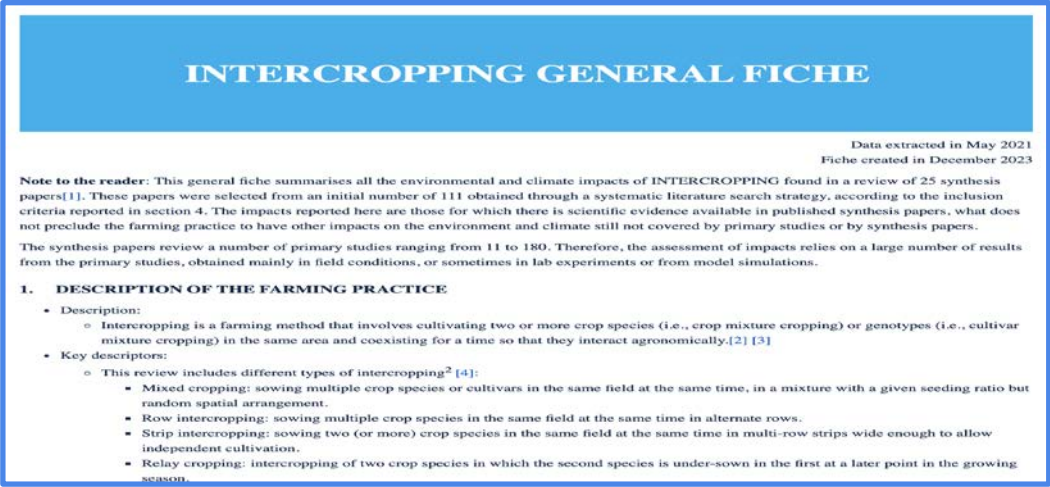
This site from the European Commission <https://wikis.ec.europa.eu/pages/viewpage.action?pageId=44167087> is a register of published meta-analysis results quantifying the impacts of agricultural practices. Several impacted variables are considered, including SOC. In the example below (**Figure 6.3**), we chose for impact “increase carbon sequestration” and selected “intercropping” among different practices as in the following screenshot.



The screenshot shows a web interface with two main sections. On the left, under the heading "Select one impact", there is a dropdown menu with "Increase carbon sequestration" selected. On the right, under the heading "Farming practices linked to the selected impact", there is a list of practices. The practices listed are: Agroforestry practices, Cover and catch crops, Crop residue management, Crop rotation, Fertilisation using green manure, Field margins, Grassland conservation and restoration, Grassland management, Grazing, Hedgerows, Intercropping (which is highlighted with a blue border), Isolated trees, Leguminouse crops, Manure land application techniques, and Manure processing techniques. At the bottom of the list, there is a note: "Click on the farming practice name to open the fiche".

**Figure 6.3** Choices for impact of “increase carbon sequestration” and selected “intercropping” among different practices from EC web site mentioned in the text

This access to a general fiche describing the impact of the chosen practice. However, the site reports qualitative effects but no quantitative data, e.g. SOC changes (see **Figure 6.4**).



The screenshot shows a document titled "INTERCROPPING GENERAL FICHE". At the top right, it says "Data extracted in May 2021" and "Fiche created in December 2023". Below this, there is a "Note to the reader" stating that the fiche summarises environmental and climate impacts of intercropping from 25 synthesis papers. It also mentions that the synthesis papers review a number of primary studies ranging from 11 to 180. The main body of the document is titled "1. DESCRIPTION OF THE FARMING PRACTICE" and contains two bullet points: "Description:" and "Key descriptors:". Under "Description:", it defines intercropping as a farming method involving two or more crop species or genotypes. Under "Key descriptors:", it lists different types of intercropping: Mixed cropping, Row intercropping, Strip intercropping, and Relay cropping.

**Figure 6.4** Impact of the chosen practice, here intercropping, on different variables from EC web site mentioned in the text


In Brazil we propose the MapBiomass SOC dataset (<https://brasil.mapbiomas.org/>) provided annually at 30m between 1985 and 2021. SOC between 0-30 cm depth is derived from 9649 sample points (Figure 6.5) from the SoilData Repository input into a random forest together with environmental covariates that represent the formation factors and transformation drivers of Brazilian soil including age and type of current land use. Other factors include such as climate, organisms, relief, and parent material. Raw soil data is available through institutions such as EMBRAPA, IBGE and Brazilian universities (<https://soildata.mapbiomas.org/dataset.xhtml?persistentId=doi:10.60502/SoilData/XDBQ4U>). Note that the distribution of samples is heterogeneous with the highest densities in the Amazon and Atlantic forests and temporally pre-2000. With this dataset lacking land-use history and multi-year revisits, SOC change may need to be derived using a subset of observations during 1985-2023 to align with LandSat missions and MapBiomass land use products.

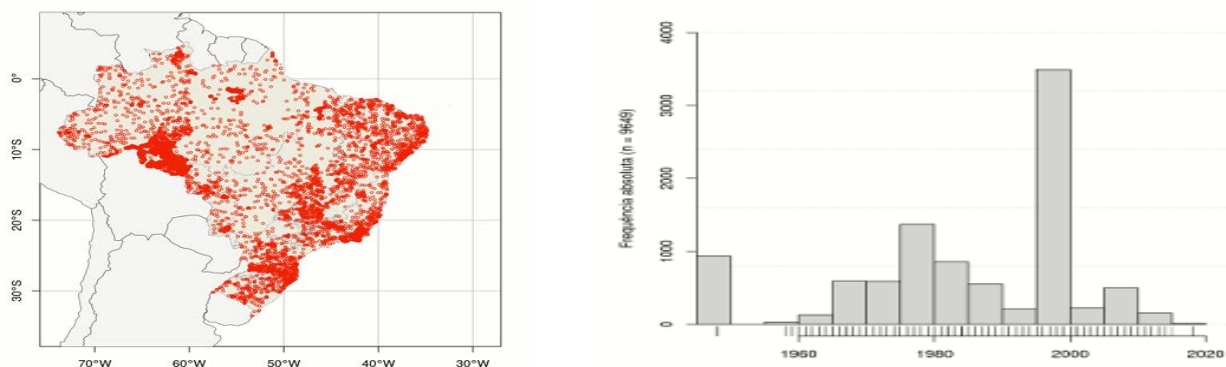


**Figure 6.5** Distribution of 20,000 SOC observations across Brazil (LHS) and temporal frequency of observations (RHS). Taken from [www.MapBiomass.org](http://www.MapBiomass.org)

#### ● Key References:

- De Rosa, D., Ballabio, C., Lugato, E., Fasiolo, M., Jones, A., & Panagos, P. (2024). Soil organic carbon stocks in European croplands and grasslands: How much have we lost in the past decade? *Global Change Biology*, 30, e16992. <https://doi.org/10.1111/gcb.16992>.
- Ciais, P., Gervois, S., Vuichard, N., Piao, S. L., & Viovy, N. (2011). Effects of land use change and management on the European cropland carbon balance. *Global Change Biology*, 17(1), 320–338. <https://doi.org/10.1111/j.1365-2486.2010.02341.x>.
- Beillouin, D., Corbeels, M., Demenois, J. et al. A global meta-analysis of soil organic carbon in the Anthropocene. *Nat Commun* 14, 3700 (2023). <https://doi.org/10.1038/s41467-023-39338-z>.
- Guillaume, T., Makowski, D., Libohova, Z., Elfouki, S., Fontana, M., Leifeld, J., Bragazza, L., & Sinaj, S. (2022a). Carbon storage in agricultural topsoils and subsoils is promoted by including temporary grasslands into the crop rotation. *Geoderma*, 422, 115937. <https://doi.org/10.1016/j.geoderma.2022.115937>.
- Guillaume, T., Makowski, D., Libohova, Z., Bragazza, L., Sallaku, F., & Sinaj, S. (2022b). Soil organic carbon saturation in cropland-grassland systems: Storage potential and soil quality. *Geoderma*, 406, 115529. <https://doi.org/10.1016/j.geoderma.2021.115529>.
- Garnier, P., Makowski, D., Hedde, M. et al. Changes in soil carbon mineralization related to earthworm activity depend on the time since inoculation and their density in soil. *Sci Rep* 12, 13616 (2022). <https://doi.org/10.1038/s41598-022-17855-z>.

Deliverable no. D1.1 Requirements Baseline (RB) document	ESA Carbon-RO, EO4BK Contract no. 4000144916/24/I-EF	 International Institute for Applied Systems Analysis IIASA www.iiasa.ac.at
--	---	--

- MapBiomass. (2023). Annual mapping of soil organic carbon stocks in Brazil 1985–2021 (beta collection) [Data set]. MapBiomass Data (Version 1). <https://doi.org/10.58053/MapBiomass/DHAYLZ>.
- Zinn, Y. L., Lal, R., & Resck, D. V. S. (2005). Changes in soil organic carbon stocks under agriculture in Brazil. Soil and Tillage Research, 84(1), 28–40. <https://doi.org/10.1016/j.still.2004.08.007>.

## 7. First elements on threshold and target scientific and technical requirements to include EO data in carbon budgets that will inform the roadmap in WP6.

Variable	Period covered	EO input data	Ancillary data (e.g. training data)	Evaluation reference data	Method	scientific requirement	threshold	target	technical requirement
<b>Crop types</b>									
<b>Crop types Europe</b>	2018-2022	S1 and S2 data	LUCAS, LPIS	LUCAS, LPIS	Time series classification with TempCNN model (section 3.1)	Transparent and scalable method to classify crop types	Intermediate levels of the nomenclature (table 3.1), Annual, 10m resolution	Most detailed level of the nomenclature (table 3.1), Annual, 10m resolution	F1 score >0.80 on major crops, >0.70 on minor crops
<b>Crop types Brazil</b>	2018-2022	S1 and S2 data	LEM, LEM+, CONAB, ANA	LEM, LEM+, CONAB, ANA	Time series classification with TempCNN model (section 3.1)	Transparent and scalable method to classify crop types	Intermediate levels of the nomenclature (table 3.1), Annual, 10m resolution	Most detailed level of the nomenclature (table 3.1), Annual, 10m resolution	F1 score >0.70 on major crops, >0.60 on minor crops

Crop phenology									
<b>Crop phenology Europe (UL)</b>	2018-2022	S1 and S2 data	Quality flags, cloud cover	ICOS data 14 sites (Table 4.1)	Time series decomposition (section 3.4.2)	Transparent and scalable method to detect main pheno-stages (Start of Season SOS, Peak GS, End of Season EOS)	SOS, peak GS, EOS for single cycles  10m spatial resolution, maximum gap filling < 30%.	SOS, EOS including double cropping (more challenging to detect)  10m spatial resolution, maximum gap filling < 30%.	Accuracy <+-10 days and R <sup>2</sup> of interannual variability >0.90. Based on results from Schierbaum et al. 2024.
<b>Crop phenology Brazil (UL)</b>	2018-2022	S1 and S2 data	Quality flags, cloud cover	Camara et al., 2019 : <a href="https://doi.org/10.1594/PANGAEA.911560">https://doi.org/10.1594/PANGAEA.911560</a>	Time series decomposition (section 3.4.2)	Transparent and scalable method to detect main pheno-stages (Start of Season SOS, Peak GS, End of Season EOS)	SOS, peak GS, EOS for single cycles  10m spatial resolution, maximum gap filling < 30%.	SOS, EOS including double cropping (more challenging to detect)  10m spatial resolution, maximum gap filling < 30%.	Accuracy <+-10 days and R <sup>2</sup> of interannual variability >0.90. Based on results from Schierbaum et al. 2024.



Crop management practices									
<b>Harvest date (UL)</b>	2018-2022	S1 and S2 data	Quality flags, cloud cover	ICOS ancillary management data	Time series decomposition (section 3.4.2)	10m spatial resolution, maximum gap filling < 30%.	Assume EOS as a proxy harvest date	Phenological metric better suited for matching harvest dates.	Accuracy <+-10 days and R <sup>2</sup> of interannual variability >0.90. Based on results from Schierbaum et al. 2024.
<b>Cover crops (LSCE)</b>	Around 2020	S1 cross ratio	EUROSTAT regional statistics of annual cover crops at NUTS2 level	National GIS data of presence / absence at field level where available (RPG in France)	Non parametric downscaling (section 3.5.1)	Transparent and scalable method to classify cover crops at 100 m resolution	classification at 100 m resolution over EU average around ≈ 2020	Annual Classification at 100 m resolution over EU	Accuracy F1 score > 0.6 at NUTS 2 scale in Europe
<b>Tillage (LSCE)</b>	Around 2020	S1 cross ratio	EUROSTAT regional statistics of annual cover crops at NUTS2 level	National GIS data of presence / absence at field level where available (RPG in France)	Non parametric downscaling (section 3.5.2)	Transparent and scalable method to classify tillage crops at 100 m resolution	Not planned	Annual at 100 m resolution over EU if external HE project submitted is funded.	Accuracy F1 score > 0.6 at NUTS 2 scale in Europe
<b>Irrigation Europe</b>	2018-2022	S1 and S2 data, Weather data	LUCAS,	LUCAS	Machine learning approach (section 3.5.6)	Transparent and scalable method to detect irrigation	Irrigation detection (yes/no) in France	Irrigation detection (yes/no) in Europe	F1 score >0.6
<b>Irrigation Brazil</b>	2018-2022	S1 and S2 data	ANA	ANA	U-Net CNN (section 3.5.7)	Transparent and scalable method to detect irrigation	Irrigation detection in Brazil	Irrigation detection in Brazil	F1 score >0.6
<b>Double cropping</b>	2018-2022	S1 and S2 data	BR: LEM, LEM+, CONAB, ANA	BR: LEM, LEM+, CONAB, ANA	Time series classification with TempCNN model (section 3.1)	Transparent and scalable method to classify crop types	Double crop detection without type classification, Annual, 10m resolution, In Brazil	Double crop types (table 3.1), Annual, 10m resolution, In Brazil and Europe	F1 score >0.7

Deliverable no. D1.1  
Requirements Baseline (RB)  
document

ESA Carbon-RO, EO4BK  
Contract no. 4000144916/24/I-EF

Cropland SOC changes from BK model									
<b>Cropland carbon stock (soil carbon)</b>	≈2010s BR: 1985-2021	Not an output of the project	EU: LUCAS and maps derived Brazil: MapBiomass, Global SoilGrid	Used as input of the BK model. No evaluation needed	Existing gridded SOC data products	Existing data	N/A	N/A	N/A
<b>Cropland carbon stock change</b>	2018-2022	Products from WP2 and WP4	ORCHIDEE derived parameters	Listed in section 5.5  LUCAS change at sites (3 campaigns) + De Rosa et al. SOC change model based on LUCAS data  Meta-analysis from multiple studies (5.5)	Bookkeeping (BK) modelling	Extensible platform for VHR BK computing	Resolution: 1km Crop types: generic C3 and C4 EO-based parameters: biomass	Resolution: 10m Crop types: distinct C3 and C4 (as many as in other WPs) EO-based parameters: biomass, soil, turnover times	Computation time of <1 day  Response curves 90% within spread of ref.  Code documentation